Unraveling the metabolic networks involved in the utilization of L-glutamine in *Pseudomonas fluorescens* exposed to nutritional stress

by

Félix Legendre

A thesis submitted in partial fulfillment
of the requirements for the degree of
Doctor of Philosophy (PhD) in Biomolecular Sciences

The Faculty of Graduate Studies
Laurentian University
Sudbury, Ontario, Canada

© Félix Legendre, 2022

THESIS DEFENCE COMMITTEE/COMITÉ DE SOUTENANCE DE THÈSE
Laurentian Université/Université Laurentienne
Office of Graduate Studies/Bureau des études supérieures

Title of Thesis
Titre de la thèse: Unraveling the metabolic networks involved in the utilization of L-glutamine in Pseudomonas fluorescens exposed to nutritional stress

Name of Candidate
Nom du candidat: Legendre, Félix

Degree
Diplôme: Doctor of Philosophy

Department/Program
Département/Programme: PhD Biomolecular Sciences

Date of Defence
Date de la soutenance June 28, 2022

APPROVED/APPROUVÉ

Thesis Examiners/Examinateurs de thèse:

Dr. V. Appanna
(Supervisor/Directeur(trice) de thèse)

Dr. A. Omri
(Co-supervisor/Co-directeur(trice) de thèse)

Dr. A. Omri
(Committee member/Membre du comité)

Dr. S. Tharmalingam
(Committee member/Membre du comité)

Dr. Surajit Das
(External Examiner/Examinateur externe)

Dr. Ramesh Subramanian
(Internal Examiner/Examinateur interne)

Approved for the Office of Graduate Studies
Approuvé pour le Bureau des études supérieures
Tammy Eger, PhD
Vice-President Research (Office of Graduate Studies)
Vice-rectrice à la recherche (Bureau des études upérieures)
Laurentian University / Université Laurentienne

ACCESSIBILITY CLAUSE AND PERMISSION TO USE

I, **Félix Legendre**, hereby grant to Laurentian University and/or its agents the non-exclusive license to archive and make accessible my thesis, dissertation, or project report in whole or in part in all forms of media, now or for the duration of my copyright ownership. I retain all other ownership rights to the copyright of the thesis, dissertation or project report. I also reserve the right to use in future works (such as articles or books) all or part of this thesis, dissertation, or project report. I further agree that permission for copying of this thesis in any manner, in whole or in part, for scholarly purposes may be granted by the professor or professors who supervised my thesis work or, in their absence, by the Head of the Department in which my thesis work was done. It is understood that any copying or publication or use of this thesis or parts thereof for financial gain shall not be allowed without my written permission. It is also understood that this copy is being made available in this form by the authority of the copyright owner solely for the purpose of private study and research and may not be copied or reproduced except as permitted by the copyright laws without written authority from the copyright owner.

Abstract

Sulfur plays an essential role in oxidative homeostasis due to its participation in sulfhydryl groups (SH). A disruption of this vital nutrient is known to promote oxidative stress and activates a plethora of anti-oxidative strategies. Phosphate, a micronutrient that is part of adenosine triphosphate (ATP), the main molecule used as energy and other macromolecules in living cells. The stress response to sulfur and phosphate deficiency in *Pseudomonas fluorescens* was investigated with emphasis on ROS detoxification, and energy production. Metabolite profiling was performed by High Performance Liquid Chromatography (HPLC), enzymatic analysis was done using Blue Native Polyacrylamide Gel Electrophoresis (BN-PAGE) and gene expression assessment of targeted genes was performed with SYBR-Green real-time PCR (qPCR). When cultured in a sulfur-deficient medium with glutamine as the sole carbon and nitrogen source, the microbe reconfigures its metabolism aimed at the enhanced synthesis of NADPH, an antioxidant and the limited production of NADH, a pro-oxidant. The up-regulation of isocitrate dehydrogenase (ICDH)-$NADP^+$ dependent in the soluble fraction of the cells obtained from the S-deficient media results in enhanced NADPH synthesis. This reaction is aided by the concomitant increase in NAD kinase (NADK) activity. The latter converts NAD^+ into $NADP^+$ in the presence of ATP. Additionally, the microbe reprograms its metabolic pathways to produce KG and regenerate this keto-acid from succinate, a by-product of ROS detoxification. Succinate semialdehyde dehydrogenase (SSADH) and KG decarboxylase (KDC) work in partnership to synthesize KG. This process is further aided by the increased activity of the enzymes glutamate decarboxylase (GDC) and γ-amino-butyrate transaminases (GABA-T). Taken together, the data point to a metabolic network involving isocitrate, KG, and ICDH that converts NADH into NADPH in *P. fluorescens* subjected to a S-deprived environment. Finally, when cultured in low phosphate environments, the microbe can produce ATP via substrate level phosphorylation (SLP), in a mechanism involving the reductive isocitrate dehydrogenase (ICDH-NADH), isocitrate lyase (ICL), malate synthase (MS) as well as phosphoenol pyruvate carboxylase (PEPC), phosphoenol pyruvate synthase (PEPS) and pyruvate phosphate dikinase (PPDK). This metabolic reprogramming ensures the survival of the microbe and reveals the central role metabolism plays in cellular adaptation to abiotic stress.

Keywords

Biochemistry, Microbiology, Metabolism, TCA cycle, Abiotic stress, Cellular stress, Sulfur starvation, Phosphate starvation, Glutamine, Energy, ATP, Oxidative stress, Succinate, α-ketoglutarate, NADPH

Acknowledgments

I would like to express my sincere thanks to my thesis supervisor, Dr. Vasu Appanna. Thank you for giving me the amazing opportunity to conduct a PhD in a world-renowned laboratory. Your expertise and guidance really made me a better scientist and allowed me to improve my critical thinking skills. I thank you for believing in me during this long journey during the ups and downs, even in tougher moments. This thesis would not have been possible without all the brainstorming and discussions we had along the way, during which I learned a lot.

I would like to thank the members of my thesis committee, Dr Abdelwahab Omri and Dr Sujeenthar Tharmalingam as well as the internal examiner, Dr Ramesh Subramanian and the external examiner Dr Surajit Das from the National Institute of Technology Rourkela, Odisha, India for their assistance on writing this research thesis.

I would like to acknowledge my fellow lab colleagues that have worked with me during my time at Laurentian University. Thank you to Azhar Alhasawi for training me and showing me the basic techniques used in the Appanna lab and to Alex MacLean for his constant support. Alex and I make a good team and I will miss working in the lab with him. I hope we can collaborate in the future on some other projects.

Finally, a very special thank you to my family. First, to my mother Suzanne Tardif for her ongoing moral support and trust, but also to my father Michel Legendre, my stepfather Réjean Gaivin, my stepmother Céline Gemme and my brother Vincent Legendre. Lastly, I would like to thank my wonderful girlfriend Émilie Racicot for her unconditional love and support.

Table of Contents

List of Tables

List of Figures

1 Introduction

Metabolism is described as the chemical processes that happen within organisms to maintain life. The first thing that comes to mind when studying metabolism in living cells is the production of energy. Many metabolic networks are geared towards ATP production, but there is also a lot more facets of life that require a metabolic response. In this chapter, current knowledge on metabolism are reviewed, with a focus on energy production, antioxidative defense mechanisms as well as the metabolism of glutamine.

1.1 Metabolic pathways

Metabolism can be categorized into two main parts: catabolism and anabolism. Catabolism is defined as the breakdown of bigger and more complex molecules into smaller molecules whereas anabolism is the opposite. Anabolism is the biosynthesis of larger molecules from smaller molecules (Figure 1.1). The end goal of catabolism is energy production whereas the objective of anabolism is energy storage. This section focuses on the energy metabolism as well as amino acid metabolism.

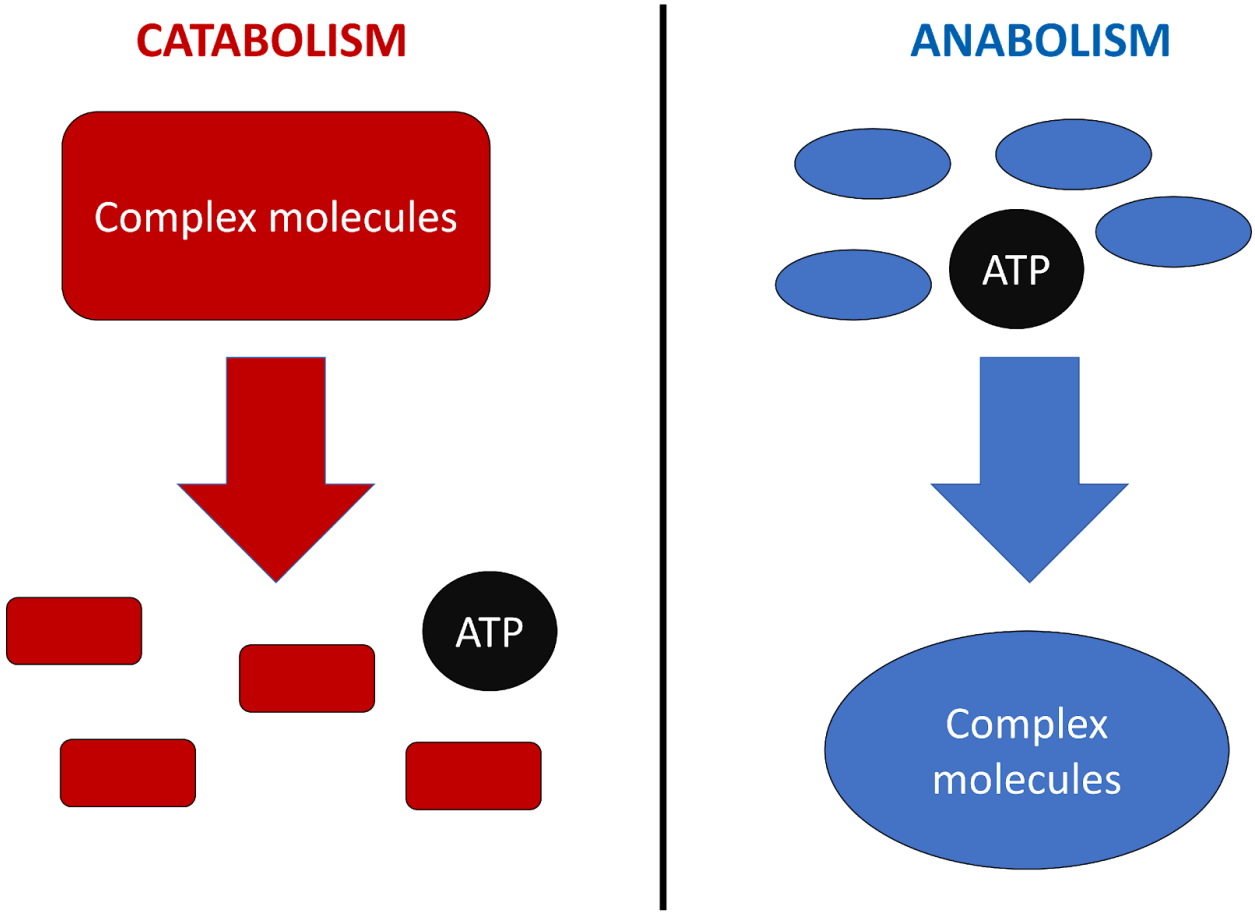

Figure 1.1. Differences between catabolism and anabolism. Catabolism is the breakdown of complex molecules into smaller molecules to generate energy, whereas anabolism is the synthesis of larger molecules for energy storage.

1.1.1 Energy production pathways

There are a lot of possibilities as to how living cells can produce energy, but there are three core pathways aimed at energy production: glycolysis, the tricarboxylic acid cycle and oxidative phosphorylation. The glycolysis is a pathway that break down glucose molecules into ATP, the TCA cycle is a metabolic module that converts acetyl-CoA – a metabolite derived from carbohydrates, lipids and proteins – into ATP, $FADH_2$ and NADH molecules. The NADH and $FADH_2$ can then be used in the oxidative phosphorylation pathway to generate ATP. These pathways are highly conserved from bacteria to human.

1.1.1.1 Glycolysis

The glycolysis pathway allows the generation of energy from glucose. It consists of a series of chemical reactions in which glucose is broken down into two molecules of pyruvate. This also generates two molecules of ATP, two molecules of NADH as well as two molecules of water. The pathway is functional with or without oxygen being present. Energy is required for certain steps of the pathway, but the overall yield in energy is positive.

The first step of glycolysis is the phosphorylation of glucose into glucose-6-phosphate. This chemical reaction is done by the enzyme hexokinase. In this reaction, a mole of ATP is consumed per mole of glucose. The gluocose-6-phosphate produced then undergoes an isomerisation reaction and becomes fructose-6-phosphate. This reaction is catalyzed by glucose-6-phosphate isomerase. The third step is the phosphorylation of fructose-6-phosphate into fructose-1,6-biphosphate via the enzyme phosphofructokinase. This is another step of glycolysis that requires ATP. Following this reaction, the fructose-1,6-biphosphate is cleave into two trioses by the enzyme aldolase. Those sugars are dihydroacetone phosphate and D-glyceraldehyde-3-phosphate. Those two trioses are isomers of each other, and they are interconverted back and forth by triosephosphate isomerase. This is important since D-glyceraldehyde-3-phosphate is the required molecule to proceed in the glycolysis pathway and because the next reactions in the pathway are the ones that will lead to a positive energy yield. The triose D-glyceraldehyde-3-phosphate is converted into 1,3-bisphosphoglycerate by glyceraldehyde phosphate dehydrogenase. This reaction is a redox reaction. The D-glyceraldehyde-3-phosphate is oxydized and phosphorylated. A molecule of NADH is formed from NAD^+ in this reaction. The NADH produced can then be used by the electron transport chain system and undergo oxidative phosphorylation to make ATP for the cell. The next step is catalyzed by phosphoglycerate kinase. The 1,3-bisphosphoglycerate loses a phosphate group, and this phosphate group is added to a molecule of ADP to generate ATP as well as 3-phosphoglycerate. After this, 2-phosphoglycerate is formed from 3-phosphoglycerate following an isomerisation by phosphoglycerate mutase. The enzyme enolase then catalyzes an elimination reaction in which a molecule of water is removed from 2-phosphoglycerate, forming phosphoenolpyruvate (PEP). Finally, the enzyme pyruvate kinase allows the formation of pyruvate from PEP. This reaction produces ATP as well.

The glycolysis pathway is fairly linear. However, there is a good number of pathways that connect to glycolysis. In higher organisms, glucose-6-phosphate, the product of the very first step of glycolysis, can be transformed in a series of anabolic reactions into macromolecules aimed at energy storage, such as glycogen or starch, which are essentially glucose polymers. When glycogen is broken down, it releases glucose-6-phosphate. The molecule glucose-6-phosphate can then also serve as an entry point for glycolysis as well.

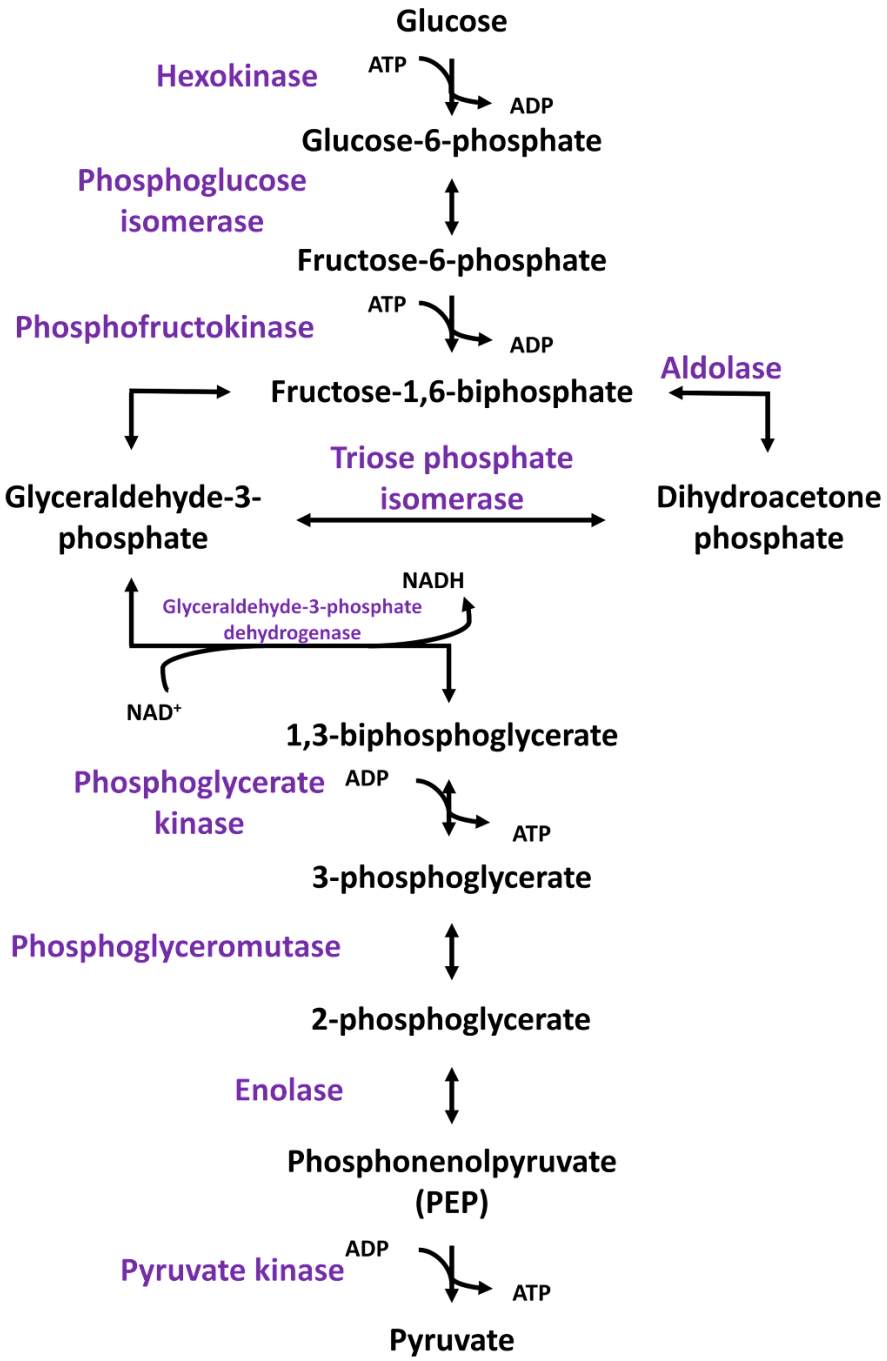

Figure 1.2. Illustration of the glycolysis pathway. Metabolites are represented in black whereas enzymes involved in the pathway are in purple. (Adapted from (1))

1.1.1.2 Tricarboxylic Acid Cycle

The tricarboxylic acid (TCA) cycle is a primordial metabolic pathway essential in all oxidative organisms and is highly conserved throughout evolution. In higher organisms, this pathway occurs in the mitochondrion. This pathway as the name implies is circular, with acetyl-CoA being the starting metabolite. Although some molecules can enter the TCA cycle at different points, degradation of carbohydrates and lipids, the nutrients that are the most concentrated in energy, enter the TCA cycle through acetyl-CoA. Although the TCA cycle is often viewed solely as an energy producing metabolic pathway due to its ability to produce NADH and $FADH_2$, there is more and more evidence that shows that this network participates in a wide variety of other biological processes in many organisms. Other than its very well characterized role of producing NADH and $FADH_2$ in order to shuttle it to the oxidative phosphorylation, the TCA cycle is involved in combatting cellular stress by maintaining NADH/NADPH homeostasis, scavenging ROS, producing ATP by substrate-level phosphorylation and supplying metabolites to cope with different stressors. There is a growing body of evidence showing that the TCA cycle is a very dynamic and flexible pathway that can be adapted and modified, especially in microorganisms, in order to survive under some stress conditions. (2-4)

The TCA cycle is often seen as the second phase of the energy metabolism. A phase that follows glycolysis. In fact, acetyl-CoA can be produced from pyruvate with the enzyme pyruvate dehydrogenase, making this a very common entry point to the TCA cycle for the metabolism of carbohydrates. In the cycle, oxaloacetate and acetyl-CoA are used as substrates to generate citrate and coenzyme A, a reaction catalyzed by citrate synthase. Citrate is a molecule that contain six carbons, whereas oxaloacetate and acetyl-CoA had four and two respectively. Citrate is isomerised by aconitase to generate *cis*-aconitate. The latter is hydrated into isocitrate by the same enzyme. Isocitrate can be converted into α-ketoglutarate (KG) by isocitrate dehydrogenase. Then, KG can lose a molecule of CO_2 and undergo oxidation to produce succinyl-CoA, a process aided by α-ketoglutarate dehydrogenase (KGDH). Following this, the enzyme succinyl-CoA synthetase converts succinyl-CoA to succinate. Succinate dehydrogenase acts to convert succinate into fumarate as the next step of the cycle. Following the reaction, fumarate is hydrated to form malate, a reaction catalyzed by fumarase. Malate is then oxidized into oxaloacetate by malate dehydrogenase, producing a NADH molecule than can be used in the

oxidative phosphorylation process. This is the traditional TCA cycle pathway, represented in figure 1.3.

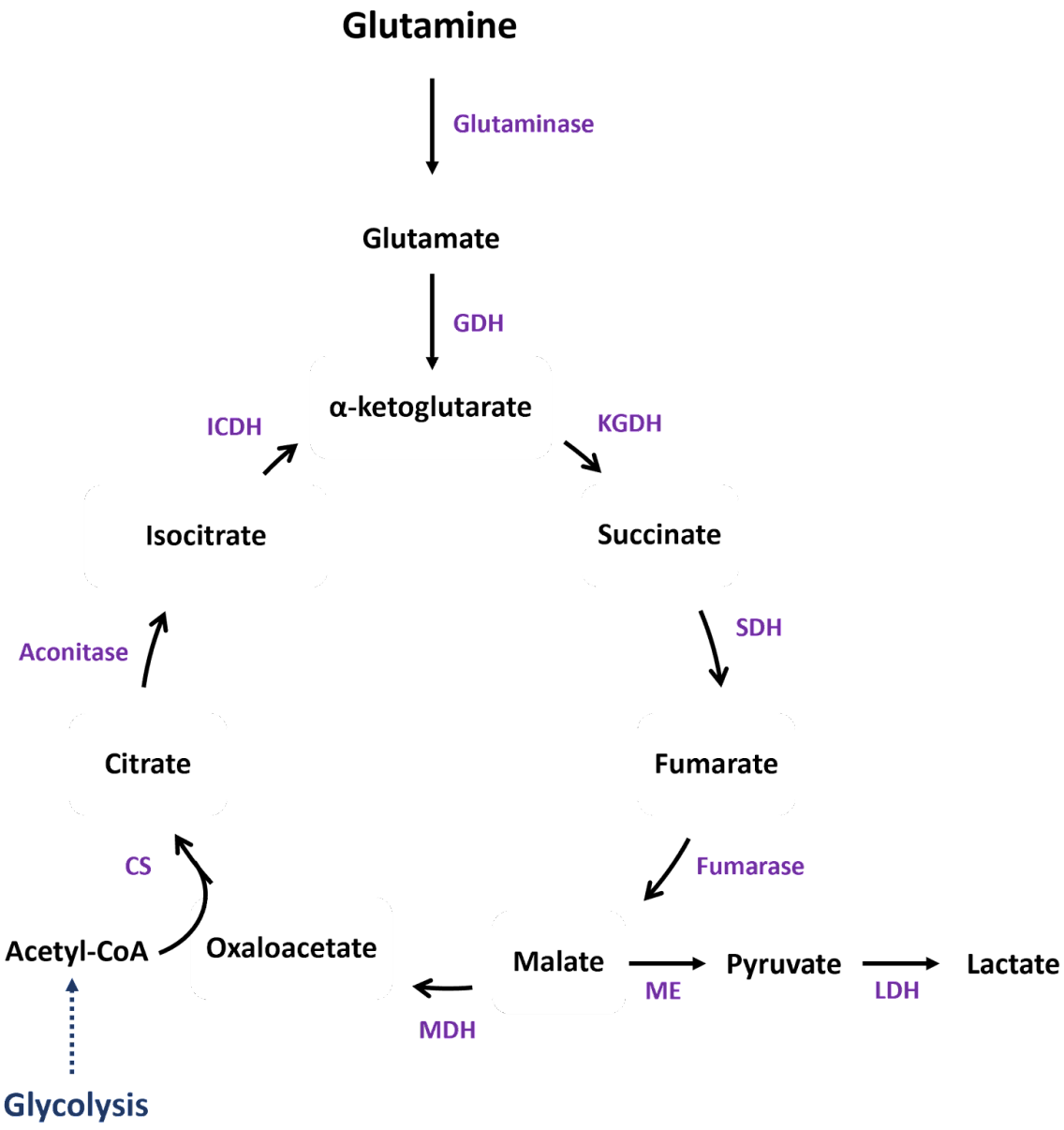

Figure 1.3. Illustration of the TCA cycle pathway. Metabolites are represented in black whereas enzymes involved in the pathway are in purple. Entry point from glutamine is emphasized (top).

1.1.1.3 Oxidative phosphorylation

Oxidative phosphorylation is the last step of cellular respiration. It also proceeds within the mitochondria in higher organisms. In this process, the NADH and $FADH_2$ that are present in the cell and produced from other biochemical pathways are converted into ATP via a series of redox reactions with the aid on membranous enzymes known as the electron transport chain. The electron transport chain is made of five protein complexes, known as Complex I to V that catalyze the different steps in which NADH and $FADH_2$ are converted into energy (Figure 1.4).

The first step of oxidative phosphorylation is the donation of electrons from NADH of $FADH_2$ to complex I, also knows and NADH dehydrogenase. The electrons are transferred through the complex via a series of Fe-S clusters and are then reduce ubiquinone. This is linked to 4 protons (H^+) being shuttled from the cell matrix to the intercellular space.

Complex II, or succinate dehydrogenase, catalyzes the oxidation of succinate to fumarate. Complex II is covalently bound with FAD which is used as a cofactor in the reaction. The electrons generated from this reaction also reduce ubiquinone. This enzyme participates in both the electron transport chain and the TCA cycle. Upon production, the fumarate produced can proceed through the TCA cycle. Complex III, also known as coenzyme Q : cytochrome c oxidoreductase, is the third protein complex of the electron transport chain. It catalyzes the reduction of cytochrome c, a process linked to the oxidation of coenzyme Q. Two electrons and donated to cytochrome c by coenzyme Q, this is paired with 4 protons being pumped into the intermembrane space.

Complex IV, or cytochrome c oxidase, is the next enzyme complex in the electron transport chain. It oxidizes cytochrome c by receiving electrons from it. After four electrons are donated by cytochrome c to Complex IV, they are transferred to two molecules of oxygen and four protons. Two molecules of water are produced from the action of Complex. This mechanism is linked to four protons translocated across the cell membrane. Complex V is the ATP synthase. When protons are translocated in the intermembrane space by Complex I-IV, the proton gradient creates an electrochemical potential. ATP is produced from ADP and Pi with two protons being

pumped back into the cell matrix. Overall, the yield of ATP from a single molecule of NADH is about 2.5 ATP, due to the ATP synthase not being 100% efficient.

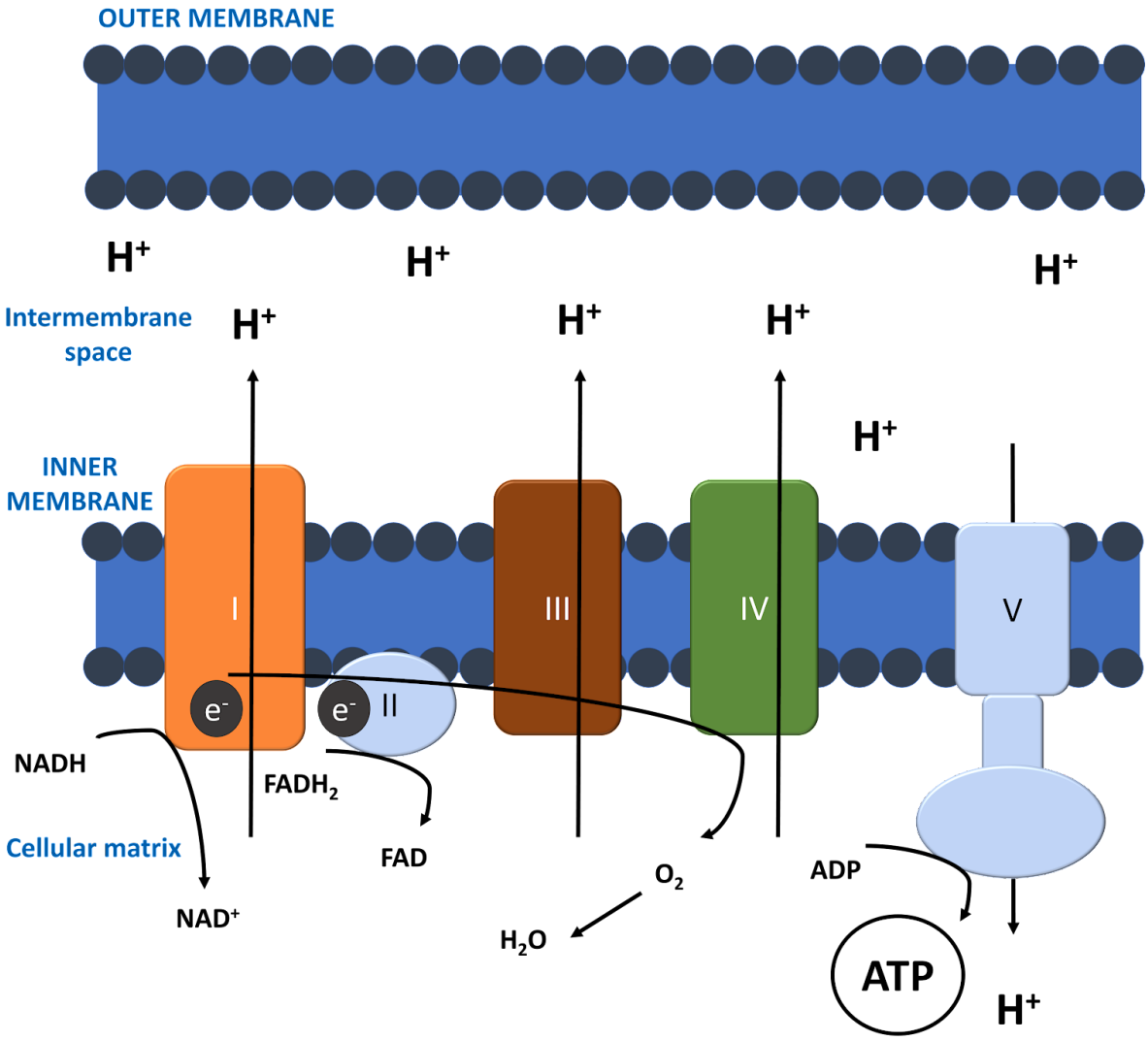

Figure 1.4. Schematic representation of the oxidative phosphorylation. The electron transport chain is made of five protein complexes, known as Complex I to V that catalyze the different steps in which NADH and $FADH_2$ are converted into ATP. Electrons donated by NADH and $FADH_2$ are coupled with protons being pumped into the intermembrane space. This creates a proton gradient. Electrochemical potential allows complex V to make at by shuttling protons back into the cellular matrix. (Adapted from (5))

1.1.2 Antioxidative response

As highlighted above, the TCA cycle is a significant generator NADH molecules. NADH is an oxidative molecule and high production of those will certainly contribute to raising the oxidative burden of the cell. The transmission of electrons from NADH via the electron transport chain to O_2 is associated with occasional electron leakage, which participates in production of ROS. These highly reactive entities consist of peroxide, superoxide and hydroxyl radicals. When oxidative stress is too high, it can lead to DNA damage, lipid peroxidation (6), carbonylation of proteins, as well as oxidation of amino-acids and carbohydrates (7). Considering this, it is of primordial importance for organisms to have mechanisms in order to combat oxidative stress with good efficiency.

The general mechanisms involve enzymes that are able to convert ROS into less toxic components for the cell. For example, superoxides can be converted into hydrogen peroxide (H_2O_2) by superoxide dismutase (SOD). The enzyme catalase (CAT) is responsible for transforming H_2O_2 into innocuous water and oxygen, thus eliminating the threat of those ROS. Glutathione peroxidase can convert H_2O_2 into water as well. It requires glutathione in reduced form. A molecule of NADPH is used as a cofactor to convert the oxidized from of glutathione into its reduced form. Glutathione is one of the main antioxidants found in living cells (5,8). It is a tripeptide of glutamate, cysteine and glycine. It is synthesized by the cell in consecutive reactions involving glutamate-cysteine ligase and glutathione synthetase. The enzyme glutamate-cysteine ligase converts glutamate and cysteine into the dipeptide γ-glutamylcysteine, whereas glutathione synthetase is involved in the addition of a glycine residue as the C-terminal end of γ-glutamylcysteine, forming glutathione (9). The enzymes SOD, CAT and glutathione peroxidase work in tandem to detoxify ROS in living cells (Figure 1.5).

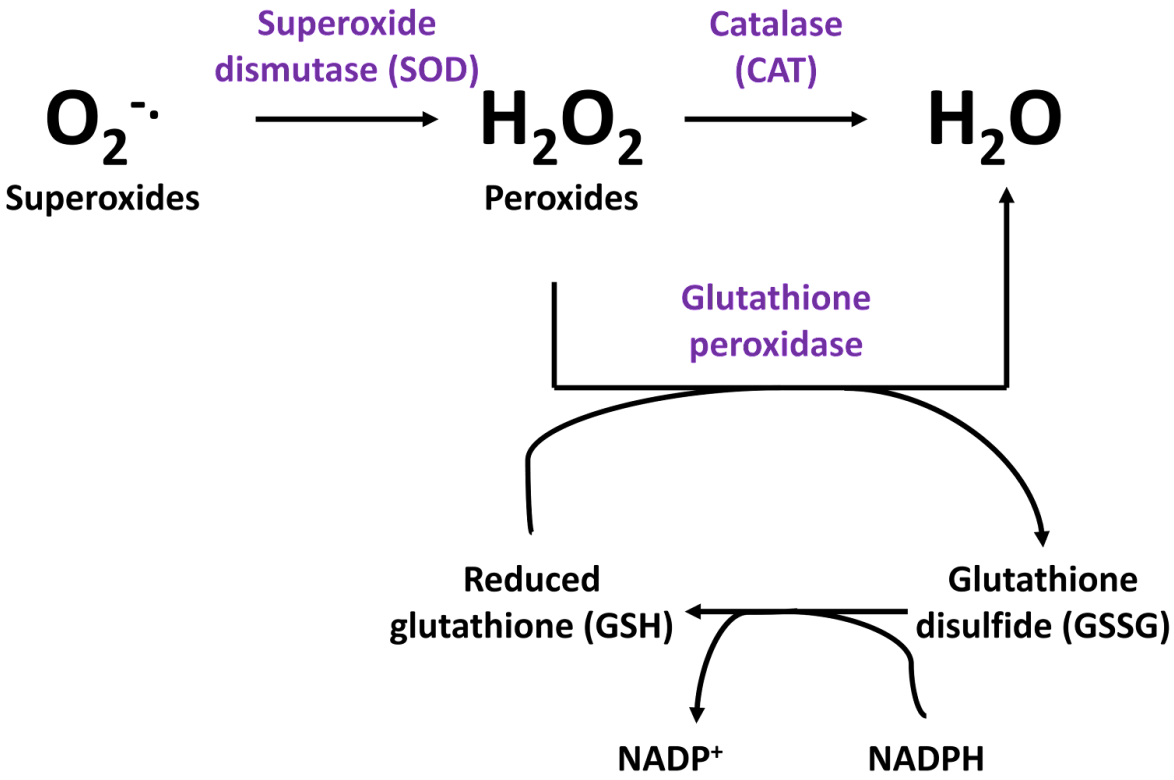

Figure 1.5. Enzymatic systems to detoxify ROS. Superoxides are converted into peroxides by superoxide dismutase (SOD). Peroxides and converted into water by catalase (CAT) and glutathione peroxidase. Reduced form of glutathione is required to detoxify peroxides with this enzyme. A molecule of NADPH is used to reduces glutathione from its disulfide form to its reduces form. (Adapted from (5))

The glutathione system helps immensely in reducing the amount of ROS in the cell, but it does not tackle the problem of ROS production in certain conditions. When the organism is under too much oxidative stress, additional actions must be taken by the cell to avoid cellular death. A major strategy used by microorganisms to shut down production of ROS themselves is modulation the TCA cycle pathway. Metabolism is very flexible. It is a misconception that the TCA cycle is a rigid circular pathway. It is very dynamic and can be adapted under stress conditions. Modulating the TCA cycle as a mean to combat oxidative stress can be done to achieve three goals: 1) producing ketoacids that can act as ROS scavenging molecules, 2)

increasing NADPH production while lowering NADH synthesis and 3) producing ATP without relying on oxidative phosphorylation.

Producing ketoacids can be a good oxidative defense mechanism. They can react with ROS and form the corresponding carboxylic acid as well as a molecule of water and CO_2. The TCA cycle intermediate KG is the ketoacid most often linked to antioxidative activity due to its central position in the energy metabolism. It can be obtained from amino acid metabolism as well as from carbohydrates and even lipid metabolism. Other ketoacids involved in similar processes include glyoxylate, pyruvate and oxaloacetate (10,11). These metabolites can neutralize ROS with the generation of oxalate, acetate, and malonate as by-products. KG is a core intermediate of the TCA cycle that can be regulated by the upregulation of ICDH and the downregulation of KGDH (12). Controlling those enzymes is a way to increase the pool of KG in the cell, which can be utilized to prevent lipid peroxidation (13) and help to prevent oxidative stress (14,15). This modification of the TCA cycle has been shown to help bacterial systems cope with oxidative tension (16,17).

The interplay between NADH/NADPH ratio is crucial to fight off oxidative stress. NADPH is required to obtain reduced glutathione, which is in turn necessary for glutathione peroxidase assisted detoxification of ROS. The TCA cycle being a malleable pathway in which a lot of enzymes are reversible, controlling the amount of NADPH produced can be regulated by modifying the TCA cycle while the cell is in an oxidative environment. Under oxidative stress, it has been shown that enzymes like KGDH and NAD^+-dependent ICDH, that lead to accumulation of NADH, can be shut down. The enzymes producing NADPH like malic enzyme and $NADP^+$-dependant ICDH are upregulated to stimulate NADPH production. This has been demonstrated in microbial systems in different conditions that lead to oxidative stress (15,17-19)

The TCA cycle can also serve as a robust ATP producing machinery even without relying on oxidative phosphorylation. This is done by substrate level phosphorylation (SLP). The process of SLP is defined as the synthesis of high-energy molecule responsible for the conversion of ADP into ATP via the transfer of a phosphate group. The ATP yield from this sort of reaction is not as high as with oxidative phosphorylation, but it has the added value of not contributing to ROS production as much and therefore is a fairly common strategy to produce energy in cases of

oxidative stress. The enzyme succinyl-CoA synthetase is an enzyme that has been shown to participate in SLP under oxidative stress (17). This enzyme can produce ATP from succinyl-CoA, ADP, and phosphate (Pi). Succinate and CoA and byproducts of this reaction. Depending on the nutrients available, thioesters such as oxalyl-CoA can participate in replenishing the pool of succinyl-CoA by reacting with succinate, a process catalyzed by the enzyme oxalyl-CoA: succinate transferase (16,17). In the case of nitrosative stress, the enzyme citrate lyase can be used to convert citrate into oxaloacetate and acetate independently of the presence of ATP. Oxaloacetate can then be converted into PEP by phosphoenolpyruvate carboxylase (PEPC) and in pyruvate and ATP via pyruvate phosphate dikinase (PPDK) (20). Examples of SLP reactions are found in figure 1.6.

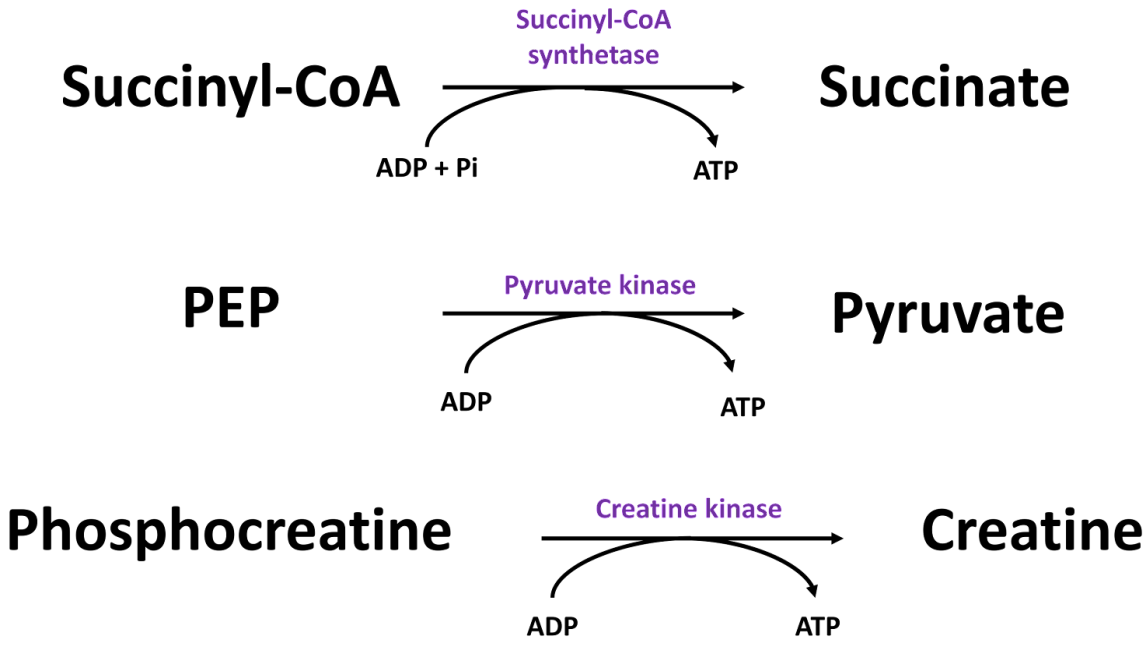

Figure 1.6. Common example of substrate level phosphorylation reaction. Succinyl-CoA synthetase can produce ATP and succinate from succinyl-CoA, ADP and Pi. This is an example of a SLP reaction happening in the TCA cycle. The conversion of PEP into pyruvate with the production of ATP is a SLP reaction happening in glycolysis. Creatine kinase catalyzing the reaction of phosphocreatine to creatine and ATP is a SLP reaction that happens in various tissues, but mostly in skeletal muscles.

1.1.3 Amino acid metabolism

Amino acids are small molecules that, as the name implies, contain a carboxylic group and an amino group. Different amino acids are found in living systems, with 20 of them being the building blocks of proteins. Free amino acids in the cell can be metabolized into different intermediated depending on their nature. There are two groups of amino acids: glucogenic amino acids and ketogenic amino acids. Some amino acids can be in both categories.

Glucogenic amino acids can be broken down into glucose via gluconeogenesis and therefore can be used to generated energy when glucose is rare. Generally, glucogenic amino acids can be broken down into intermediates of the TCA cycle. By going through the TCA cycle, those intermediates can be converted into pyruvate, a starting metabolite of gluconeogenesis. Glucogenic amino acids include arginine, glutamate, glutamine, histidine, proline, isoleucine, methionine, threonine, valine, phenylalanine, tyrosine, asparagine, aspartate, alanine, cysteine, glycine, serine, tryptophan (21).

Ketogenic amino acids can be broken down into ketone bodies. Ketogenic amino acids include lysine, leucine, isoleucine, phenylalanine, threonine, tyrosine and tryptophan. Ketogenic amino acids are broken down into acetyl-CoA or acetoacetyl-CoA and undergo ketogenesis to synthetize ketone bodies. Those ketone bodies can be used as energy in situations where glucose is scarce (21). A schematic representation of amino acid metabolism can be found in figure 1.7.

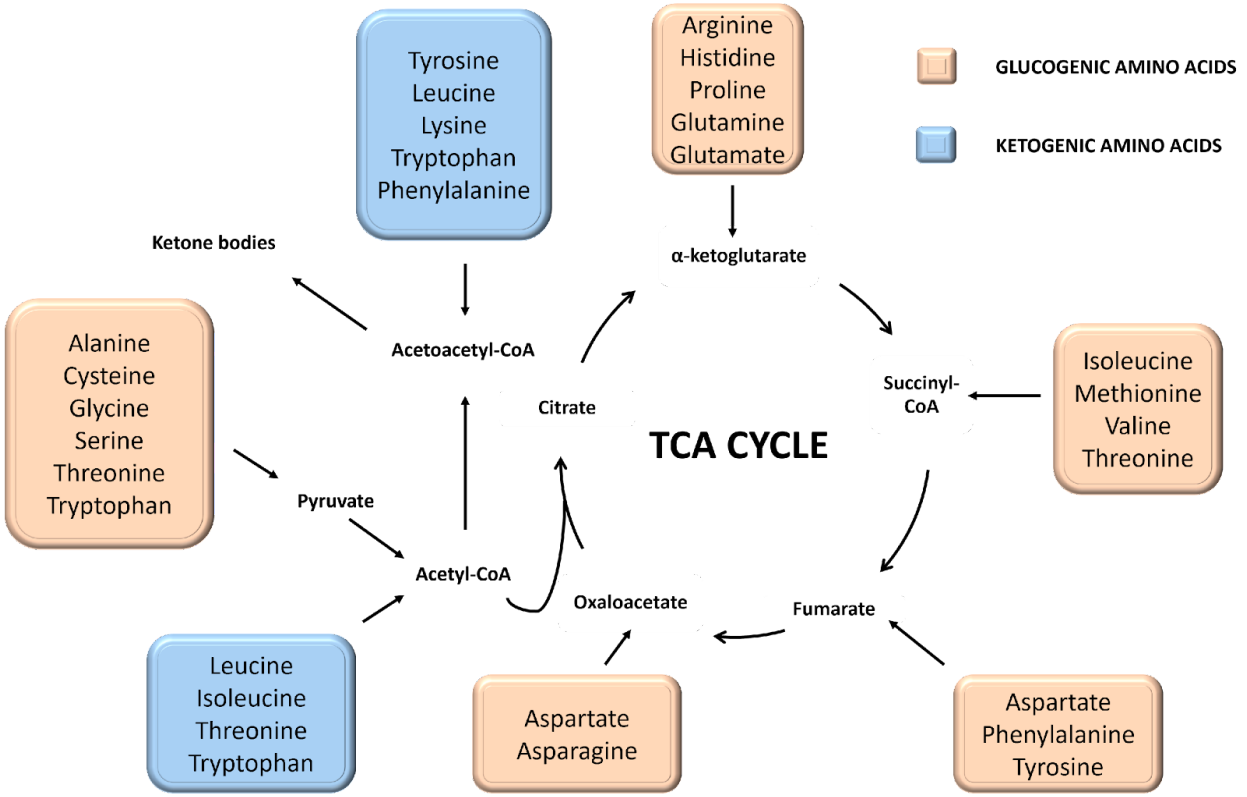

Figure 1.7. Summary of amino acids in the energy metabolism. Glucogenic amino acids are in orange boxes and ketogenic amino acids are in blue boxes. Glucogenic amino acids are converted into pyruvate or intermediates of the TCA cycle. Ketogenic amino acids are converted into acetyl-CoA or acetoacetyl-CoA (22).

1.2 Glutamine

1.2.1 Chemistry of glutamine

Glutamine is an amino acid that, like other amino acids, is an integral part of protein composition. Its chemical structure is very similar to glutamic acid, but the glutamine side chain contains an amide group instead of a carboxylic acid functional group. This amino acid is therefore polar and uncharged. It contains 5 atoms of carbon and two NH_3^+ groups. The molecular weight of glutamine is 146.15 kDa. Its elemental composition is as follows: 41.09% of carbon, 32.84% of oxygen, 19.17% of nitrogen and 6.90% of hydrogen (23).

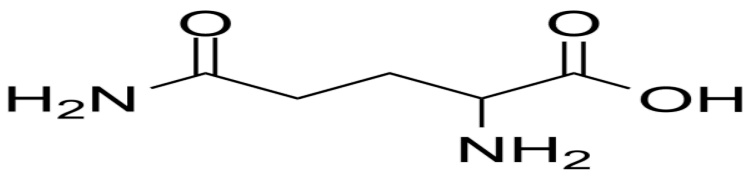

Figure 1.8. Chemical structure of Glutamine

1.2.2 Roles of glutamine

Glutamine is the most abundant free amino acid in human blood (24). This is because it is a very versatile amino acid that contributes to many biological processes. As amino acids are the building blocks of proteins, glutamine is also involved in that, as it accounts for 4.7% to 6% of amino acids incorporated into proteins (24,25), but there are many other functions and benefits of glutamine in every living organism. The metabolism of glutamine can lead to production of nucleotides such as pyrimidines and purines that compose nucleic acids (DNA and RNA). Glutamine can also be the substrate for the production of NADPH, a molecule with antioxidative properties, as well as other antioxidants (26). There are multiple facets of the importance of glutamine in living cells (figure 1.9). This section highlights the role of glutamine as a source of energy, its role in maintain oxidative balance, its function as a nitrogen transporter and as a signaling molecule in bacteria. Roles of glutamine in higher organisms in regard to the immune system are discussed as well as the metabolism importance of glutamine in cancer cells.

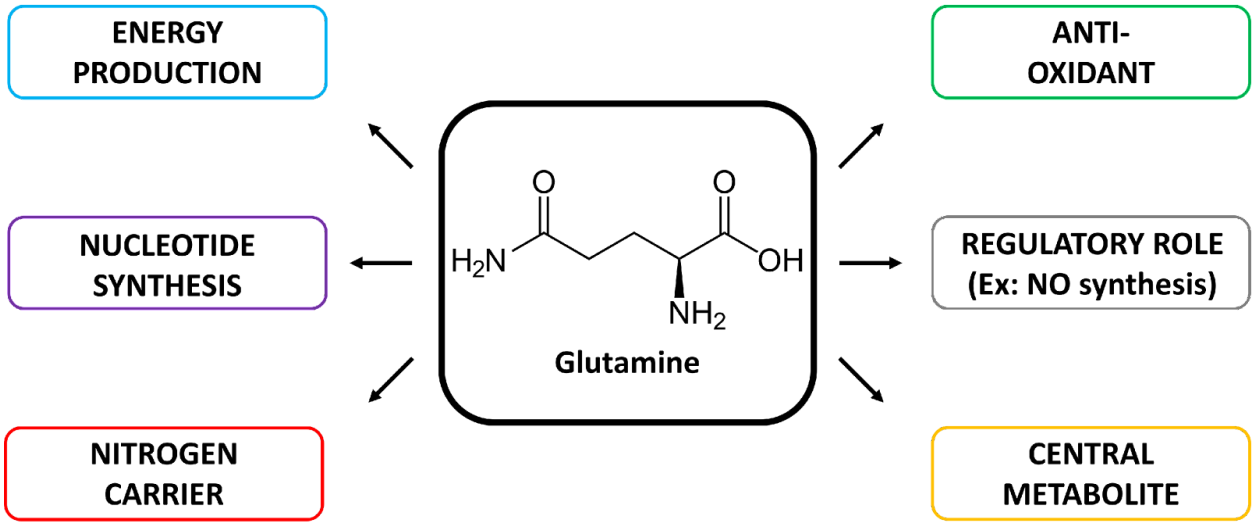

Figure 1.9. Biological functions of glutamine. Roles of glutamine in living cells include energy production, antioxidative defense, nucleotide synthesis, nitrogen transport, regulatory functions and a central metabolite for multiple reaction.

1.2.2.1 Glutamine as a source of energy

Glutamine can be a substrate for energy production. Its central position in the metabolic machinery makes it a very versatile nutrient. In microbial systems, glutamine can be rapidly converted to glutamate by glutaminase or glutamine synthetase. The enzyme glutamine synthetase, which was shown to be activated under oxidative stress in *P. fluorescens* (15) generated a molecule of ATP from glutamine, making glutamine a direct source of energy for the cell. The glutamate produced from this reaction can be converted to KG by glutamate dehydrogenase (GDH) and enter the TCA cycle. The action of GDH leads to the release of ammonia (NH_3) and the production of NADH and NADPH, as this enzyme has a NAD^+ dependent for and a $NADP^+$ utilizing form (27). The NADH produced from GDH and from KG going through the TCA cycle can be processed by the electron transport chain and generate ATP. Therefore, the ability of glutamine to feed the TCA cycle while also producing ATP from GS and NADH from GDH make it an efficient energy source for the cell.

1.2.2.2 Role of glutamine in redox balance

Glutamine is a key regulator of the redox state of living cells. Its implication is reducing oxidative stress is two-fold. First of all, glutamate is required for the biosynthesis of glutathione, one the main components used to combat oxidative pressure in living cells (28). Glutamine is a precursor of glutamate, therefore can lead to glutathione biosynthesis. Glutamine is also a precursor to KG, which has antioxidative properties as well (12). It can modulate the activity of enzymes involved in ROS defense such as SOD, CAT and glutathione peroxidase (13,29). This leads to a decrease in lipid peroxidation, a process during which free radicals can be accumulated in the cell. In bacterial systems, it has been shown that KG can detoxify H_2O_2, superoxides and other ROS when the bacteria is subjected to oxidative stress (14,15,30). This mechanism is essentially a decarboxylation reaction involving the ketone group of KG in which succinate is produced at a by-product (29). The accumulation of KG has been linked to protection against hydrogen peroxide in bacteria (30), insects (31), birds (32) as well as mammalian cells (33).

1.2.2.3 Glutamine as a nitrogen carrier and donor

Glutamine's chemical structure containing two amino groups make it a good nitrogen carrier. Nitrogen donation is very important for many anabolic processes. For example, glutamine acts as a nitrogen donor in the synthesis of purines and pyrimidines, which as part of nucleic acids' structure (34). Glutamine can also act as a nitrogen donor for transamidation reactions (35). In higher organisms, glutamine transport is tightly regulated as its role as nitrogen carrier is central to many biological processes, notable in skeletal muscles where, in humans, 80% of the glutamine in the body is found (36). Glutamine intake is stimulated by hormones such as insulin and insulin-like growth factors (23). The molecules of glutamine are transported inside the cell by an active transport system utilizing sodium ion dependent channels. Transporting a molecule of glutamine inside the cell requires one molecule of ATP.

1.2.2.4 Glutamine and glutamate metabolism in stress response

Glutamine breakdown can go into various directions if the cell is challenged by a stress. In fact, the glutamate produced from glutamine metabolism can be converted into γ-aminobutyric acid (GABA) by glutamate decarboxylase, which can then be converted into succinate by GABA transaminase (GABAt) and succinate semialdehyde dehydrogenase (SSADH). This process is

known as the GABA shunt. This pathway has significant implications in the central nervous system as glutamate is the principal excitatory neurotransmitter whereas GABA is the main inhibitory neurotransmitter (37). The interplay between glutamate and GABA is crucial in regulating many brain functions. In plants, the GABA shunt plays a role in the resistance to numerous abiotic stresses such as temperature changes, lack of oxygen and salinity challenges (38). In microorganisms, the GABA shunt has been linked to bacterial resistance to acidic conditions (39). In fungi, this pathway has been shown to be implicated in oxidative stress resistance (40). The role of the GABA shunt in bacteria is still not fully understood to this day.

1.2.2.5 Glutamine's role in the immune system

Glutamine is also a core metabolite for the immune system. Back in the 70s, evidence already suggested that lack of glutamine led to immunosuppression (41,42) suggesting that it plays an important role for immunity. In immune cells, glutamine can be broken down into glutamate, aspartate and alanine. This process is called glutaminolysis and is important for immune cells (23). Furthermore, the ability of glutamine to participate in the synthesis of pyrimidines and purines required for nucleic acids is also primordial for immune cells. Glutamine also regulates gene expression in immune cells, as the expression of some key genes requires the presence of glutamine. Glutamine has been shown to inhibit the NF-KB (nuclear factor kappa-light-chain-enhancer of activated B cells), STAT (signal transducer and activator of transcription family) and AP-1 (Activator Protein 1) signalling networks as well as activating the HSF1 (Heat Shock Factor 1) and PPAR-γ (peroxisome proliferator activated receptor gamma) pathways. The biological effect of this is reduced inflammation, therefore glutamine in considered an anti-inflammatory molecule.

1.2.2.6 Glutamine's role in cancer cells

Mutations in genes involved in the TCA cycle have been linked to different types of cancer. Notably, mutations in succinate dehydrogenase (Complex II of the electron transport chain), as well as fumarase and isocitrate dehydrogenase have been shown to lead to defects in the TCA cycle in various human cancers (43,44). Since the TCA cycle is impaired and since glucose in cancer cells is oxidized to lactate (a process known as the Warburg effect), cancer cells become reliant on metabolites like glutamine to feed the TCA cycle. Its straightforward path to KG

makes it an ideal fuel for the TCA cycle in such a condition. This phenomenon is often known as ‘glutamine addiction’. In cancer cells, lipid biosynthesis is required, so cancer cells need a pathway to acetyl-CoA, a major precursor of lipids. Recent research has shown than in cancers where the electron transport chain or the TCA cycle were deficient, glutamine is utilized as a nutrient to generate KG and enter the TCA cycle where it produces citrate. Acetyl-CoA is then produced from citrate via the enzyme citrate lyase (45). Citrate lyase has been shown to be upregulated in many different cancers (46). Isocitrate dehydrogenase mutation can affect KG metabolism. Mutations in this enzyme lead to the loss of the ability of the cell to produce KG from isocitrate. Instead, the enzyme gains the ability to catalyze the production of D-2-hydroxyglutarate from KG (47). D-2-hydroxyglutarate is an oncometabolite that prevents cell differentiation (48). The cell becomes very reliant on glutamine in order to generate KG. Finally, glutamine is a precursor of glutathione. Since ROS are present within tumours (49), glutathione synthesis is important in cancer cells. In fact, inhibition of glutamine metabolism in cancer cells leads to accumulation of ROS, thus leading to tumour suppression (50).

1.3 Abiotic stress

Abiotic stress is defined as the effect of non biological factors into living systems. Those factors can include large temperature changes, heavy winds, drought and floods. The effect of insects, fungi or other microorganisms on other living organisms is a biotic stress. The impact of abiotic stress on plants is an ongoing challenge that these organisms have to deal with. This issue can affect food production and agriculture yields. Salt stress in plants is a very common abiotic stress. Too much salt in the soil can inhibit the plant’s health and growth (51). It can limit water uptake by the plant and impact photosynthesis (52). Drought and floods can also obviously impact plants negatively. In animals, temperature change is the most significant abiotic stress. Some examples of abiotic stress are shown in figure 1.10.

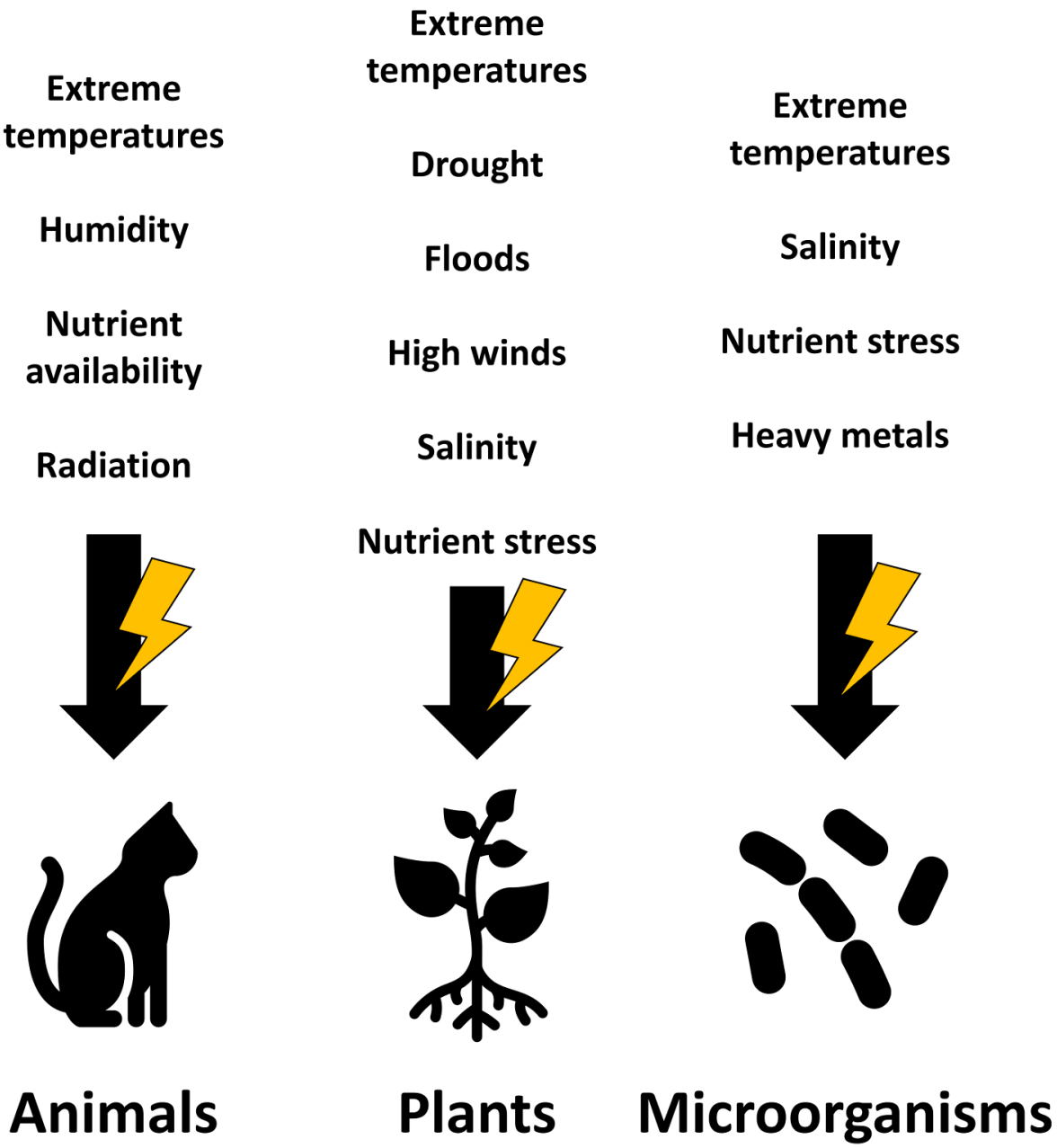

Figure 1.10. Common examples of abiotic stress in animals, plants and microorganisms.

1.4 Sulfur

1.4.1 Roles of sulfur

Sulfur is an essential element for life. It is one of the five macro-elements that are part of biological molecules, along with carbon, oxygen, phosphorus and hydrogen. It is the fifth most abundant element on Earth. In living cells, sulfur is found in proteins, amino acids, vitamins, carbohydrates, and lipids. The amino acids cysteine and methionine contain sulfur and they are part of numerous proteins. Glutathione, discussed above, is also an important molecule that contains sulfur as it is a core player in oxidative stress response. The vitamins biotin and thiamine contain sulfur. Iron-Sulfur clusters (Fe-S clusters) are very important structures of iron and sulfides that are required for the enzymatic function of many enzymes. Proteins that require Fe-S clusters to function are called Iron-Sulfur proteins. Fe-S clusters are crucial for the energy metabolism. The electron transport chain complexes involved in oxidative phosphorylation Complex I, Complex II and Complex III contain a Fe-S cluster (53-56). In the TCA cycle, the enzymes aconitase and fumarase are known to have a Fe-S cluster as well (57-58). Conditions in which Fe-S cluster biosynthesis and assembly is impaired can impact the ability of the cell to make energy. This is not the only biological process in which Fe-S clusters are important. In fact, Fe-S clusters have been shown to be involved in gene expression control, amino acid metabolism, purine synthesis, nitrogen fixation, RNA modifications as well as DNA replication and repair (59-63).

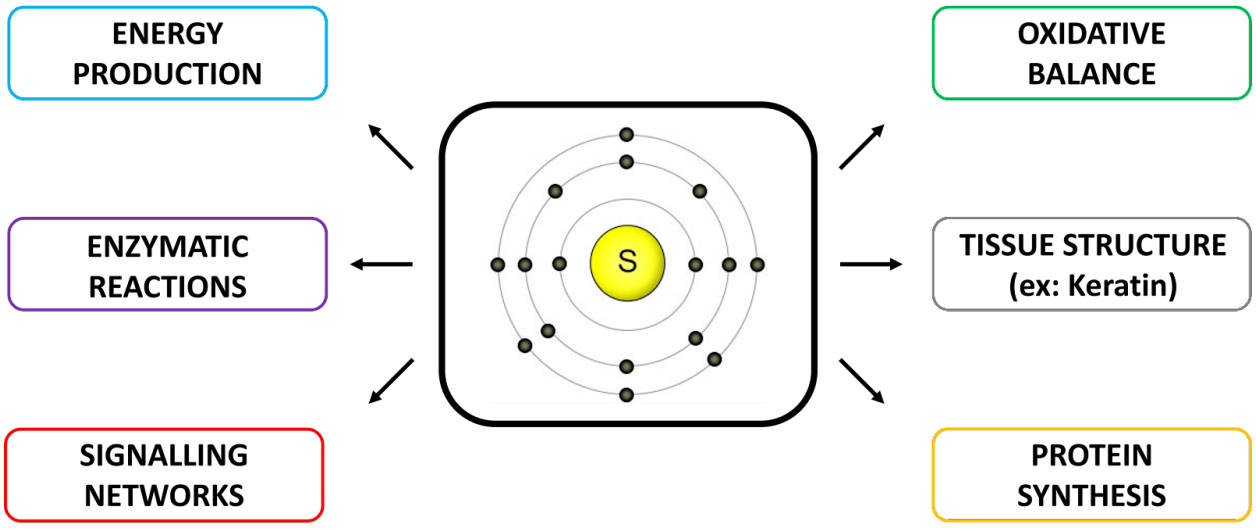

Figure 1.11 Biological functions of sulfur. Sulfur plays a role in energy production, oxidative balance, enzymatic reaction, forming tissue structure, modulating signalling networks as well as protein synthesis.

1.4.2 Sulfur transport

Sulfur is transported into cells by two main transport systems. The first one is ATP-binding cassette type transporter (ABC-type or SulP) and the second one is the major facilitator family-type transport system (SulT) (64). ABC-type transporters can carry molecules across the cell membrane coupled with the hydrolysis of ATP. Thus, this process requires energy. The SulT transport system utilizes electrochemical gradients as the driving force to transport substrates across the cell membrane.

1.4.3 Chemistry of sulfur

Sulfur can be found in different oxidation states in the environment and in living cells. The most oxidized form of sulfur is sulfates (SO_4^{2-}) in which the sulfur has an oxidation state of +6. Sulfides (SO_3^-) have an oxidation state of +4. In chemical compounds like sulfur dichloride (SCl_2), sulfur has an oxidation state of +2. Sulfides like hydrogen sulfide (H_2S) have an oxidation state of -2 and constitute the most reduces form of sulfur found in nature. Elemental sulfur can also be found in nature as well. Bacteria that can oxidize and reduce sulfur are common. In the dissimilatory sulfate reduction pathway, sulfates can be reduced to hydrogen sulfide with the aid of enzymes such as sulfate adenylyltransferase that converts sulfates to adenosine 5'-phosphosulfate (APS), adenylyl-sulfate reductase that reduce APS to sulfites and the membrane complex DsrMKJOP (protein complex made of disulfide reductase subunits M, K, J, O, and P) that catalyze the formation of sulfides. Oxidation of sulfur by microbes can happen through two distinct pathways: the Sox pathway (65), a pathway aided by thiosulfate-oxidizing multi-enzyme (TOMES) complex, and the sulfide:quinone oxidoreductase pathway, that involves formation of intermediates such as sulfites and APS (66).

1.4.4 Sulfur starvation

Sulfur is not always abundant in the environment and the effects of sulfur starvation can be multiple. For example, in yeast, it has been demonstrated that sulfur starvation led to various

effects such as sporulation, cell cycle defects, autophagy and inhibition of protein translation (67). In plants, sulfur starvation leads to lower height of the plant as well as less chlorosis of the leaves (68). In response to sulfur starvation, plants root growth is stimulated (69). Genetically, the expression of genes involved in sulfur assimilation and transport are also upregulated under sulfur starvation (70). In bacteria, it was identified that a significant amount of proteins present under sulfur starvation in microbial systems contained a lower amount cysteine and methionine residues (71, 72). Bacterial cells subjected to sulfur starvation also have a lesser amount of intracellular thiols (73). The ABC family transporters are upregulated during sulfur deficiency (64). Oxidative stress is also observed in microorganisms under condition where sulfur is scarce (74). Despite this knowledge, the molecular mechanisms underlying the response to sulfur starvation are not fully understood.

1.5 Phosphate

1.5.1 Roles of phosphate

Phosphorus is the 15th element of the periodic table. It is highly reactive, therefore it is not found in elemental form naturally in the environment unlike sulfur. In biological systems as well as in the biosphere, phosphorus is found in the form of phosphates. Phosphate (Pi) is essential for life. Nucleic acids (DNA, RNA) contain phosphate groups. Other complex molecules that contain phosphate include phospholipids, part of the cell membrane, and proteins, that can be phosphorylated on certain residues. Roles of phosphorus are summarized in figure 1.12. In humans, phosphate deficiency has been linked to proximal myopathy, dysfunctions in hemoglogin’s interaction with oxygen, dysfunction in the nervous system (apathy, weakness and tremors) (75).

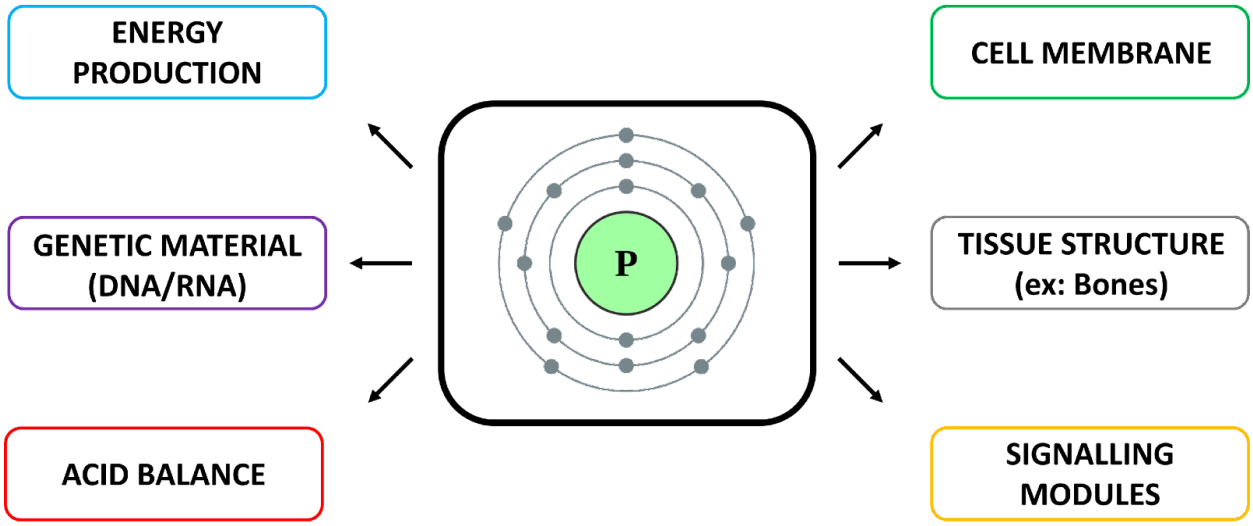

Figure 1.12. Biological roles of phosphorus. Functions of phosphorus in living cells include energy production, building the cell membrane, building the genetic material (DNA/RNA), tissue structure, maintaining acid balance (pH) and regulating signalling networks.

Protein phosphorylation is a crucial biochemical process involving phosphate. Proteins can be phosphorylated on key residues in order to accomplish different functions. Proteins can be phosphorylated to change protein-protein interactions in the cell (76), to regulate signaling networks, to trigger protein degradation (77), to regulate enzyme activity and more. This induces a conformational change in the protein due to the negative charge present on the phosphate group. Protein kinases catalyze the addition of phosphate groups unto proteins.

1.5.2 Phosphate in the environment

Phosphate in the environment is in relatively low concentrations. In ocean water, the concentrations of phosphate can go as low as in the nanomolar range (78). In conditions where the soil is too alkaline or under heavy metal pollution, phosphate levels go down significantly (79), making it hard for vegetation to thrive. Many organisms have developed ways to deal with a lack of phosphate, notably the expression of phosphate starvation-inducible genes, or psi genes. These genes encode for proteins involved in phosphate sensing, metabolism, transport and uptake (80). The Pho regulon is the main regulator of phosphate starvation (81). In cases where phosphate is not readily available, expression of phosphatases is stimulated in an effort to free up some phosphate groups from polyphosphate reserves for usage where it would be more essential.

Other macromolecules can be affected. For example, phospholipids can have their phosphate cleaved and are replaced by an amino group in the cell membrane. However, metabolic mechanisms underlying the response to phosphate starvation are not fully understood and could provide good knowledge for the industry and society, especially in microorganisms. There is growing need for efficient biofertilizers in order to help regreening efforts around the world. A lot of fertilizers contain phosphates as it helps plant growth. However, using bacteria as biofertilizers would provide a very green and cheap alternative.

1.6 *Pseudomonas fluorescens*

The microbe *Pseudomonas fluorescens* is a gram-negative rod-shaped bacterium. It is commonly found in soil and sea water. It was first characterized in agricultural soils (82). Some *P. fluorescens* strains can grow on plant leaves and contribute positively to plant growth and health (83). *P. fluorescens* is a good model organism to study metabolism. Although its optimal temperature of growth is 25°C, it can survive in a wide range of temperature as well as pH and salinity, which is very practical for research purposes. Additionally, it has a good variety of industrial applications as well. *P. fluorescens* can be used as a bioreactor to generate antibiotics as well as other compounds. Wood pulp is a key material in the paper production industry. *P. fluorescens* is used to aid in the pulping process (84). A significant number of bioremediation technologies use *P. fluorescens*. It has been shown to be able to remove ammonia from wastewater (85). It has even been shown to degrade petroleum products (86). Taken together, those characteristics make *P. fluorescens* a prime candidate as a model organism for biochemical research (2-4,14,15).

2 Objectives of the thesis

The general objective of the thesis is to characterize glutamine utilization under stress conditions and the metabolic response to sulfur starvation and phosphate starvation in a model microbial system. The nutrient-versatile microbe *Pseudomonas fluorescens* is an excellent organism to decipher metabolic reprogramming triggered by nutrient stress. Sulfur is a key element in physiology. It is incorporated in many biological molecules that directly contribute to the energy metabolism such as iron-sulfur clusters. It is also essential for cell signaling as well as maintaining oxidative balance. Phosphate groups, similarly, are integral part of many macromolecules, such as lipids and proteins, and ATP, the main molecule utilized as energy in living cells. Considering the importance of those micronutrients, the working hypothesis for this study is that the metabolic pathways happening in *P. fluorescens* undergoing sulfur starvation and phosphate starvation will be altered in order to avoid ROS accumulation and in order to produce energy without depending on the TCA Cycle and oxidative phosphorylation pathways.

In order to test this hypothesis, *P. fluorescens* will be cultured in defined mineral media using glutamine as the only source of carbon and nitrogen. Cells will be grown in a control media as well as a 'low sulfur' media that doesn't contain any added sulfur or a 'low phosphate' media that contain ~2,600 times less phosphate than the control media. The cultures will be grown until stationary phase and spun down using various centrifugation steps. Metabolite profiles of control and stressed cells can be assessed by using a C-18 reverse phase high performance liquid chromatography approach (HPLC) using this metabolite profile, some candidate enzymes that can be upregulated or downregulated can be identified. The activity of enzymes can be determined using blue native polyacrylamide gel electrophoresis (BN-PAGE) coupled with the formazan precipitate method. With this kind of strategy, the data obtained will permit to put the pieces of the puzzle together to map metabolic pathways utilized in response to abiotic stress (Figure 2.1). The stress response to sulfur starvation will be investigated from two facets: NADPH homeostasis and ROS scavenging. The response to phosphate starvation will be aimed at understanding energy production under a lack of phosphate. In all those conditions, a map of metabolic pathways that are favored is presented.

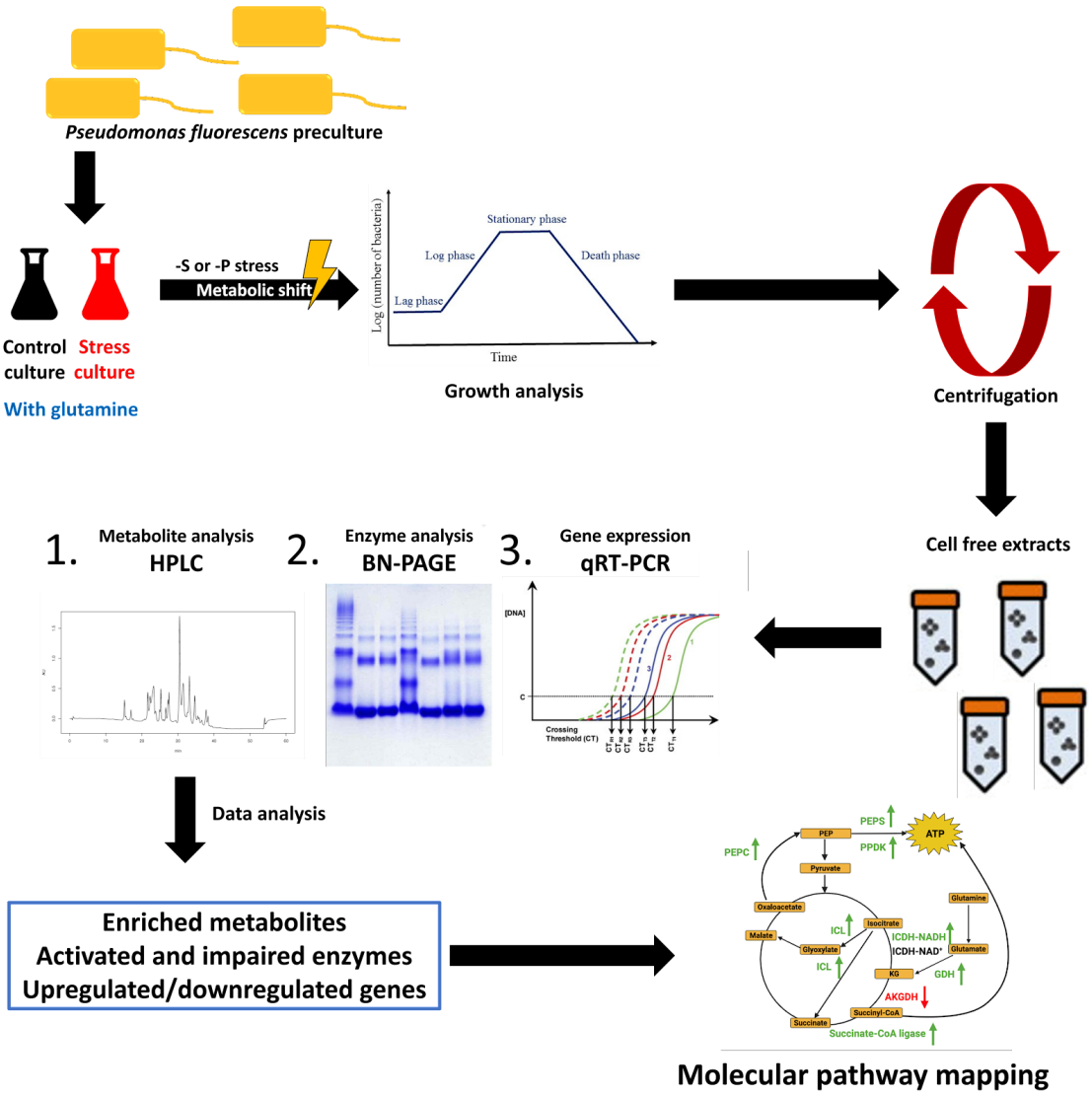

Figure 2.1. Schematic representation of the bacteria culturing methods and experimental tools utilized in this project. Bacteria will be grown in a control medium and a stress medium until stationary phase or late logarithmic phase. Bacteria will be subjected to abiotic stress, that will trigger a metabolic shift in the bacteria. They will then undergo centrifugation steps in order to pellet the bacteria cells. Cells are sonicated and fractionated by centrifugation. This gives the cell free extracts that are utilized for downstream experiments (HPLC, BNPAGE, etc.). The data obtained will allow for analysis of enriched metabolites, activated and impaired enzymes as well as upregulated and downregulated genes. Taken together, mapping metabolic networks favored under those stress conditions is possible.

3 The metabolic network to maintain NADPH homeostasis in *P. fluorescens* subjected to sulfur starvation

Metabolic networks are very fluid. The pathways used by living cells can be adapted to respond to certain stimuli or stress. This chapter covers the metabolic response of *P. fluorescens* to sulfur starvation in order to maintain NADPH homeostasis. With sulfur's vital role in maintaining oxidative balance in the cell, it is expected that lack of sulfur will lead to an oxidative environment that the microbe will have to deal with. NADH and NADPH balancing is key for combatting oxidative environments, as they are respectively oxidant and antioxidant. This chapter demonstrates that sulfur starvation does indeed induce oxidative stress and will highlight the different mechanisms engineered by *P. fluorescens* to maintain a high amount of NADPH (antioxidant) and a low amount of NADH (oxidant). This aspect is a key factor of stress response to a lack a sulfur since NADPH is used in the glutathione system.

The key finding of this study suggest that enzymes that use NAD^+ as a cofactor and lead to the production of NADH are shut down to avoid NADH accumulation. Additionally, enzymes that produce NADPH such as malic enzyme and the cytoplasmic ICDH are more active, which provide the cell with sufficient NADPH. However, this mechanism comes at the cost of having a big pool of NAD^+ in the cell. This is fixed by the enzyme NAD Kinase (NADK) which converts NAD^+ to $NADP^+$ at the cost of a molecule of ATP.

The work presented in this chapter establishes the basis of microbial systems' stress response to a low sulfur environment. This chapter has been published. It is based on the following research article:

Legendre, F., Tharmalingam, S., Bley, A.M., MacLean, A., Appanna, V.D., 2020. Metabolic adaptation and NADPH homeostasis evoked by a sulfur-deficient environment in Pseudomonas fluorescens. Antonie Van Leeuwenhoek 113, 605–616. https://doi.org/10.1007/s10482-019-01372-7

Metabolic adaptation and NADPH homeostasis evoked by a sulfur-deficient environment in *Pseudomonas fluorescens*

Félix Legendre, Sujeenthar Tharmalingam, Anondo Michel Bley, Alex MacLean and Vasu D. Appanna*

Department of Chemistry and Biochemistry,

Laurentian University

Sudbury, ON P3E 2C6

Canada

*Corresponding author

Email: vappanna@laurentian.ca

Phone: 705-675-1151 ext: 2112

Abstract

Sulfur is essential for all living organisms due to its ability to mediate a variety of enzymatic reactions, signalling networks, and redox processes. The interplay between sulfhydryl group (SH) and disulfide bond (S–S) is central to the maintenance of intracellular oxidative balance. Although most aerobic organisms succumb to sulfur starvation, the nutritionally versatile soil microbe *Pseudomonas fluorescens* elaborates an intricate metabolic reprogramming in order to adapt to this challenge. When cultured in a sulfur-deficient medium with glutamine as the sole carbon and nitrogen source, the microbe reconfigures its metabolism aimed at the enhanced synthesis of NADPH, an antioxidant and the limited production of NADH, a pro-oxidant. While oxidative phosphorylation (OXPHOS) and tricarboxylic acid (TCA) cycle, metabolic modules known to generate reactive oxygen species are impeded, the activities NADPH-producing enzymes such as malic enzyme, and glutamate dehydrogenase (GDH) $NADP^+$-dependent are increased. The α-ketoglutarate (KG) generated from glutamine rapidly enters the TCA cycle via α-ketoglutarate dehydrogenase (KGDH), an enzyme that was prominent in the control cultures.

In the S-deficient media, the severely impeded KGDH coupled with the increased activity of the reversible isocitrate dehydrogenase (ICDH) that fixes KG into isocitrate in the presence of NADH and HCO_3^- ensures a constant supply of this critical tricarboxylic acid. The up-regulation of ICDH-$NADP^+$ dependent in the soluble fraction of the cells obtained from the S-deficient media results in enhanced NADPH synthesis, a reaction aided by the concomitant increase in NAD kinase activity. The latter converts NAD^+ into NADP in the presence of ATP. Taken together, the data point to a metabolic network involving isocitrate, KG, and ICDH that converts NADH into NADPH in *P. fluorescens* subjected to a S-deprived environment.

Key words: Sulfur stress, NADH, NADPH, isocitrate dehydrogenase, α-ketoglutarate, NAD kinase, glutamine.

INTRODUCTION

Sulfur (S) is an essential nutrient in all living organisms as it is involved in a variety of vital biological functions (Ulrich and Jakob 2019; Rouault 2019). For instance, oxidative phosphorylation (OXPHOS), a process central in ATP synthesis during aerobic respiration cannot operate in absence of S. This moiety is a component of most of the enzymes participating in the electron transport chain (ETC). Here, the Fe–S clusters mediate the transfer of electrons (e^-) located within the reducing factors (NADH and $FADH_2$) to O_2 (3,14,33,87). The tricarboxylic acid (TCA) cycle that supplies the reducing factors for OXPHOS is ineffective if enzymes like aconitase, fumarase and α-ketoglutarate dehydrogenase (KGDH) are devoid of their S-containing reactive constituent. The latter contains lipoic acid, a moiety that requires S while the former two enzymes are dependent on Fe–S clusters (88-90) The synthesis of amino acids such as cysteine and methionine necessitates the participation of S. Cysteine is also pivotal in maintaining the proper redox potential in a cell due to its involvement in the biosynthesis of glutathione, a key antioxidant. The homeostasis of the oxidized and reduced forms of this tripeptide is known to orchestrate the fine-reducing balance all cellular systems need in order to survive in an aerobic environment (91).

Numerous redox sensing networks that living systems rely on to gauge intracellular oxygen tension are dependent on cysteine and Fe–S containing biomolecules. Upon oxidation of the sulfhydryl (SH) group into disulfide S–S and other oxidized S moieties, proteins are able to relay

this information into actionable physiological responses (92). For instance, the transcription factor SOXR upon reacting with superoxide ($O\cdot^{-2}$) is activated following the modification of SH in a cysteine residue (93). This conformational change enables this protein to interact with the promoter region in the genetic machinery responsible for triggering a set of proteins involved in the detoxification of reactive oxygen species (ROS), thus diminishing oxidative tension. As part of our investigation to decipher the metabolic networks aimed at the survival of living organisms subjected to abiotic stress (11,33,94), we have examined how the soil microbe *Pseudomonas fluorescens* adapts in an environment deficient in S. The microorganism was grown in a mineral medium with no added S in the presence of glutamine as the source of carbon and nitrogen.

Here we report that the oxidative stress evoked by S stress compels *P. fluorescens* to reprogram its metabolic pathways in order to limit the production of the pro-oxidant NADH and enhance the synthesis of NADPH, an antioxidant. The modulation of isocitrate dehydrogenase (ICDH-$NADP^+$ and NAD^+ dependent) coupled with the concomitant activation of NAD-kinase (NADK) is central in combatting the oxidative stress induced by S deficiency as it essentially results in the conversion of NADH into NADPH. This strategy also promotes a sharp decline in the TCA cycle and oxidative phosphorylation, two metabolic processes known for their ROS-generating attributes.

MATERIAL AND METHODS

Bacterial cultures and biomass measurement

Pseudomonas fluorescens was obtained from the American Type Culture Collection (ATCC 13525). It was grown in a defined mineral medium with glutamine (19 mM) as the sole source of carbon and nitrogen. The salt and trace metals were added as described in (Anderson et al. 1992; Aldarini et al. 2017). The control medium contained 0.8 mM of $MgSO_4$ while the stress medium had no added sulfate. Instead $MgCl_2$ (0.8 mM) was utilized. Media were dispensed in 200 mL aliquots in 500 mL Erlenmeyer flasks and autoclaved for 20 min at 121 °C. The cultures were inoculated with 1 mL of *P. fluorescens* preculture as previously described (95) and grown on a Gyrotory® Water Bath Shaker Model G76 (New Brunswick Scientific) at ambient temperature. To measure cellular biomass, 10 mL of microbial culture was spun down at 12,000 × g for

20 min. The pellet was resuspended in 1 mL 0.5 M NaOH. Biomass was determined by measuring the amount of soluble proteins with a Bradford assay (96).

Cell fractionation and metabolic profiling

Bacteria cultures were spun down at 12,000 × g for 20 min. The pellets were washed with ~ 100 mL of 0.85% m/v NaCl and the samples were centrifuged again. Following suspension of the cellular pellet in 1 mL of Cell Storage Buffer (CSB) (50 mM Tris–HCl, 1 mM phenylmethylsulfonyl fluoride, 1 mM dithiothreitol, pH 7.6), the bacteria was broken down with ultrasonic waves using an ultrasonic processor (Johns Scientific). Resuspended cells were sonicated for 15 s, five times, with a three minutes interval between each sonication in an ice-bath. Centrifugation at 110,000 × g for 3 h at 4 °C resulted in a soluble fraction (supernatant) and a membrane fraction (pellet). The membrane fraction was resuspended in 1 mL of CSB. The cell free extracts were stored at 4 °C for a maximum of 7 days and were used for analytical studies including High Performance Liquid Chromatography (HPLC) analysis, Blue Native Polyacrylamide Gel Electrophoresis (BN-PAGE) and enzymatic assays.

HPLC analysis was performed on a Waters 2695 Separation Module HPLC system with a Synergi 4 μm Hydro-RP 80A column (Phenomenex) with dimensions of 250 × 4.6 mm at a flow rate of 0.2 mL/min. A Waters 2478 Dual λ absorbance detector, set at wavelengths of 210 nm to identify organic acids and 254 nm to monitor nucleotides. The mobile phase consisted of 5% v/v acetonitrile, 20 mM KH_2PO_4 diluted in Milli-Q water, pH 2.9 at room temperature. The mobile phase was vacuum filtered using a Stericup® Vacuum Driven Disposable Filtration System. The funnel used for the filtration had a 0.22 μm Millipore Express® PLUS Membrane filter. To monitor the metabolites and appropriate standards, samples were prepared and run in the HPLC as previously described (17). Metabolite amounts were determined from the area under the curve of the corresponding peaks using the Empower software (Waters Corporation).

Blue native polyacrylamide gel electrophoresis (BN-PAGE) and enzyme activity

The activity of enzymes of the TCA cycle as well as enzymes involved in NADH/NADPH production was probed by BN-PAGE. In order to obtain optimal protein separation, gels containing a 4–16% linear gradient of polyacrylamide were cast with the MiniProteanTM2 gel

system (Bio-Rad Laboratories) with 1.0 mm spacers. The final concentration of the protein samples prepared was 4 mg/L. For membrane proteins, a concentration of 1% (m/V) of η-dodecyl β-D-maltoside was added in order to solubilize the proteins. A mass of 60 µg of proteins was loaded into each well and the proteins were migrated under native conditions (50 mm ϵ-aminocaproic acid, 15 mM Bis–Tris, pH 7.0 at 4 °C). The electrophoresis was carried out at 75 V and 15 mA with blue cathode buffer (50 mM Tricine, 15 mM Bis–Tris, 0.02% (m/v) Coomassie G-250, pH 7.0 at 4 °C) until the migration front reached the resolving gel, then the voltage and current were changed to 150 V and 25 mA respectively. When the migration was halfway through the gel, the blue cathode buffer was swapped for a colourless cathode buffer (50 mM Tricine, 15 mM Bis–Tris, pH 7.0 at 4 °C) to allow for better visualization.

Detection of enzymatic activity was performed using formazan precipitation. Gels were incubated in a reaction mixture containing substrates and cofactors utilized by the enzyme of interest as well as 0.4 mg/mL or iodonitrotetrazolium (INT) and 0.2 mg/mL of either phenazine methosulfate (PMS) or dichlorophenolindophenol (DCPIP). The reaction buffer contained 25 mM Tris–HCl and 5 mM MgCl2, pH 7.4 at room temperature. To prevent complete utilization of substrates in the experiments with membrane preparations, KCN (5 mM) was included (97). Complex I activity was tested on the membrane fraction using 0.5 mM NADH, 0.4 mg/mL INT while Complex IV activity was visualized with 5 mg/mL diaminobenzidine, 13.3 mM of sucrose and 10 mg/mL of cytochrome C. Malic enzyme (ME) and malate dehydrogenase (MDH) were probed using 5 mM malate, 0.5 mM $NADP^+$, 0.2 mg/mL PMS and 0.4 mg/mL INT in the soluble and membrane fractions respectively. Fumarase activity was identified in the membrane fraction using 5 mM fumarate, 0.5 mM NAD^+, 1 unit of malate dehydrogenase, 0.2 mg/mL PMS and 0.4 mg/mL INT. Isocitrate dehydrogenase (ICDH) NAD^+ dependant was assessed in the membrane fraction while ICDH-$NADP^+$ dependant was monitored in the soluble fraction using 5 mM isocitrate, 0.5 mM of $NADP^+$, 0.2 mg/mL PMS and 0.4 mg/mL INT respectively. The reverse ICDH was assessed in the membrane fraction with 5 mM α-ketoglutarate, 5 mM sodium bicarbonate, 0.5 mM of NADH, 0.2 mg/mL DCPIP and 0.4 mg/mL INT while in the soluble faction the reverse ICDH was probed with NADPH (0.5 mM) as the co-factor. Glutamate dehydrogenase was probed as described in (15). To further confirm the nature of the enzymes, the activity bands were excised and incubated in the reaction buffer with the appropriate

substrates. This reaction mixture was then analysed by HPLC for the formation of the products and the utilization of the substrates (11,20,98,99)

Enzyme activity analysis by spectrophotometry

Spectrophotometric analysis was used to quantify the activity of some selected enzymes by monitoring the presence or absence of NADH/NADPH at 340 nm. For enzymes of interest, 200 µg of protein was added to 2 mM of substrate and 0.5 mM of NAD^+/$NADP^+$ or NADH/NADPH based on the enzyme in a volume of 1000 µL of the Reaction Buffer (25 mM Tris–HCl and 5 mM $MgCl_2$ in water, pH 7.4 at ambient temperature). Proteins were added last and the spectrophotometer was blanked before adding the proteins. After the addition of proteins, the mixture was allowed to react and the change in absorbance was recorded after 60 s to measure the reaction rate. For KGDH, 2 mM of α-ketoglutarate and 0.5 mM of NAD was used. For ICDH-NAD^+, 2 mM of isocitrate and 0.5 mM of NAD^+ were used. For GDH-NAD^+, 2 mM of glutamate was used with 0.5 mM of NAD^+. For Reverse-ICDH-NADH, 2 mM of α-ketoglutarate, 2 mM of sodium bicarbonate and 0.5 mM of NADH was used.

Superoxide dismutase and catalase assays

The activity of catalase (CAT) was determined with the aid of the reagent p-anisidine, and the absorbance at 458 nm was monitored. 200 µg of protein equivalent from control or sulfur deprived proteins were incubated with 15 mM hydrogen peroxide (H_2O_2). 10 mM p-anisidine was added immediately in a final volume of 1.0 mL and the absorbance was measured after 60 min. Blanks were prepared similarly lacking the peroxide component. The activity of the control enzyme was normalized to 100% and the activity of the enzyme in the absence of sulfur was quantified as fold change compared to control (100).

The activity of SOD was obtained by using iodonitrotetrazolium violet (INT), with an oxidized absorbance of 485 nm € = 11 mM−1 cm−1 (101). Two hundred micrograms of control or sulfur deprived protein were incubated with 5 mM menadione, 15 µL of INT (4 mg/mL stock) was added for a final volume of 1.0 mL and the absorbance was measured after 60 min. Blanks were prepared similarly lacking the presence of menadione. The activity of the control enzyme was

normalized to 100% and the activity of the enzyme in the absence of sulfur was quantified as fold change compared to control.

Free sulfhydryl measurement

The amount of free sulfhydryl groups in the cell free extracts of control and stressed cells was calculated with the aid of the Ellman's reagent (102). A 100 µg protein equivalent of cell free extract from control cells and cells grown in a media without added sulfur was incubated with 500 µM of 5,5′-dithio-bis-2-nitrobenzoic acid (DTNB) and was incubated for 30 min at room temperature. All dilutions were done using an aqueous buffer containing 0.4 M Tris–HCl and 0.1 M EDTA. Free sulfhydryl concentration was monitored by measuring the absorbance at 420 nm after the incubation period. A standard curve using reduced glutathione concentration ranging from 0.1 to 1.0 mM was made to calculate the concentration of free sulfhydryl groups in solution. The data is represented as relative concentration, with the control being assigned a value of 1.

ICDH-NADP and NAD kinase activity analysis by HPLC

The activity of ICDH-NADP and NADK was monitored by HPLC. For ICDH-$NADP^+$, 200 µg of protein was added to 2 mM isocitrate and 0.5 mM of NAD^+. For NADK, 200 µg of protein was added to 2 mM ATP and 0.5 mM of NAD^+. The reactions were completed to a final volume of 1000 µL with Reaction Buffer (25 mM Tris–HCl and 5 mM $MgCl_2$ in water, pH 7.4 at ambient temperature) in an Eppendorf 1.5 mL microtube. The mixture was reacted for 30 min., then heat inactivated by boiling the samples in a water bath for 10 min. A volume of 100 µL was added to 900 µL of HPLC-grade water in a 2.0 mL scintillation vial and 10 uL was injected unto a Synergi 4 µm Hydro-RP 80A column (Phenomenex) with dimensions of 250 × 4.6 mm at a flow rate of 0.7 mL/min. A Waters 2478 Dual λ absorbance detector, set at wavelengths of 210 nm to identify the amount of α-ketoglutarate produced from ICDH and 254 nm to identify the amount of NADP produced by NADK, was utilized. The mobile phase consisted of a filtered 20 mM KH_2PO_4 solution diluted in Milli-Q water, pH 2.9 at room temperature similarly to what was used for metabolic profiling. $NADP^+$ and α-ketoglutarate standards were run in parallel to identify their retention time in the column.

RNA extraction and cDNA synthesis

Total RNA was extracted using the nucleic acid extraction kit from Qiagen (Cat #80234) according to manufacturer's instructions. Purified RNA with 260/280 absorbance (ND-1000 spectrophotometer) ratios below 1.8 were excluded from analysis. Contaminating genomic DNA was removed from the purified RNA samples using the DNAse kit (Sigma) according to manufacturer's instructions. The DNAse treated RNA samples were reverse transcribed using random primers (Sigma), oligo dT (VWR), and M-MLV reverse transcriptase (Promega) according to manufacturer's instructions to obtain complementary DNA (cDNA).

Real time quantitative polymerase chain reaction (RT-qPCR)

RT-qPCR reactions were performed using QuantStudio5 (ThermoFisher) to obtain threshold cycle (Ct) values. Each reaction was performed in 15 µL volumes containing 1 × POWERUP SYBR Master Mix (ThermoFisher), 600 nM forward/reverse primers and 10 ng cDNA. The cycling conditions were as follows: (a) 60 °C for 2 min, (b) 95 °C for 2 min, (c) 95 °C for 10 s (cDNA denaturation), (d) 56 °C for 10 s (primer annealing), (e) 72 °C for 20 s (template extension), (f) plate read and data collection, and (g) steps c to f repeated for 40 cycles. DNA melt curve analysis was performed at the end of each qPCR run to confirm specificity.

Forward and reverse primer pair sequences for genes of interest were designed using Primer-BLAST (NCBI). The complete list of primer sequences can be found in Table 3.1. All primer pairs were subjected to stringent validation tests as demonstrated previously (2). All samples were normalized to two independent control housekeeping genes (16S rRNA and cpn60). The relative mRNA transcript level of each gene was reported according to the ΔΔCT method as mRNA fold increase (2,103).

Table 3.1. RT-qPCR primer sequences. Accession numbers for genes of interest were identified from NCBI database for *Pseudomonas fluorescens* Pf0-1 (NC_007492.2) or *Pseudomonas fluorescens* strain ATCC 13525 (AY123661.1 and AF094725.1). Forward and reverse primer sequences were designed using Primer-BLAST.

Gene Name	Genome ID [Gene Location]	Sequence (5'→3')		PCR Product Size (bp)	Annealing Temp. (^{0}C)
ICDH NADP	NC_007492.2 [4060263 - 4061519]	Forward Primer:	GAATTTCATCCATGGGCCGC	79	56
		Reverse Primer:	CTTCAAGGACTGGGGCTACG		
ICDH Kinase	NC_007492.2 [1590514 - 1592235]	Forward Primer:	AACATCTTTCCCGGCGACAT	109	56
		Reverse Primer:	GGAAGTTGGCTTCGGTGAGA		
16S rRNA	NR_114476.1	Forward Primer:	TGGGAGGAAGGGCATTAACC	111	56
		Reverse Primer:	TTAACGCTTGCACCCTCTGT		
Cpn60	AY123661.1	Forward Primer:	AAAAACCTGTCCAAGCCATGC	81	56
		Reverse Primer:	GATGGAGCTGTCGGAGTTGG		

Statistical Analysis

Statistical analysis was performed using Student's t test. All experiments were executed in duplicate with at least three biological replicates.

RESULTS AND DISCUSSION

Pseudomonas fluorescens multiplied in a mineral medium without added S. Glutamine, the sole of carbon and nitrogen was consumed more rapidly in the control cultures compared to those deficient in S. At stationary phase of growth, the biomass was relatively higher in the control cultures (Figure 3.1a). The soluble cell-free extracts (CFE) obtained at stationary phase of growth revealed a disparate profile of nicotinamide adenosine nucleotides. The cells grown in the S-deficient medium was characterized with a higher amount of NADPH and lower concentration of NADH compared to the cultures with added S (Figure 3.1b). As lack of S is known to trigger oxidative stress, enzymes involved in the detoxification of ROS were monitored. Superoxide dismutase (SOD), an enzyme that nullifies $O_2\cdot^-$ and catalase, an enzyme that neutralizes H_2O_2 were monitored. An increase in activity of SOD was observed in the cultures deficient in S (Figure 3.1c). Free sulfhydryl measurements were performed in order to assess the effect of S

starvation in SH groups availability. The cell free extracts from cells grown in a media without added sulfur did show free sulfhydryl, but in a lesser amount than the cells grown in control media (Figure 3.1c). The presence of S in the other mineral salts utilized may account for this observation. Regardless, its diminished level is known to pose an oxidative challenge (74). Since oxidative tension was higher in the stressed cultures, its impact on select enzymes in the TCA cycle and electron transport chain (ETC) was assessed. The activities of such enzymes as ICDH-NAD$^+$, fumarase and Complex I, were significantly down-regulated in cells harvested from the media with no added S while there did not appear to be a significant change in the activity of MDH (Figure 3.1d).

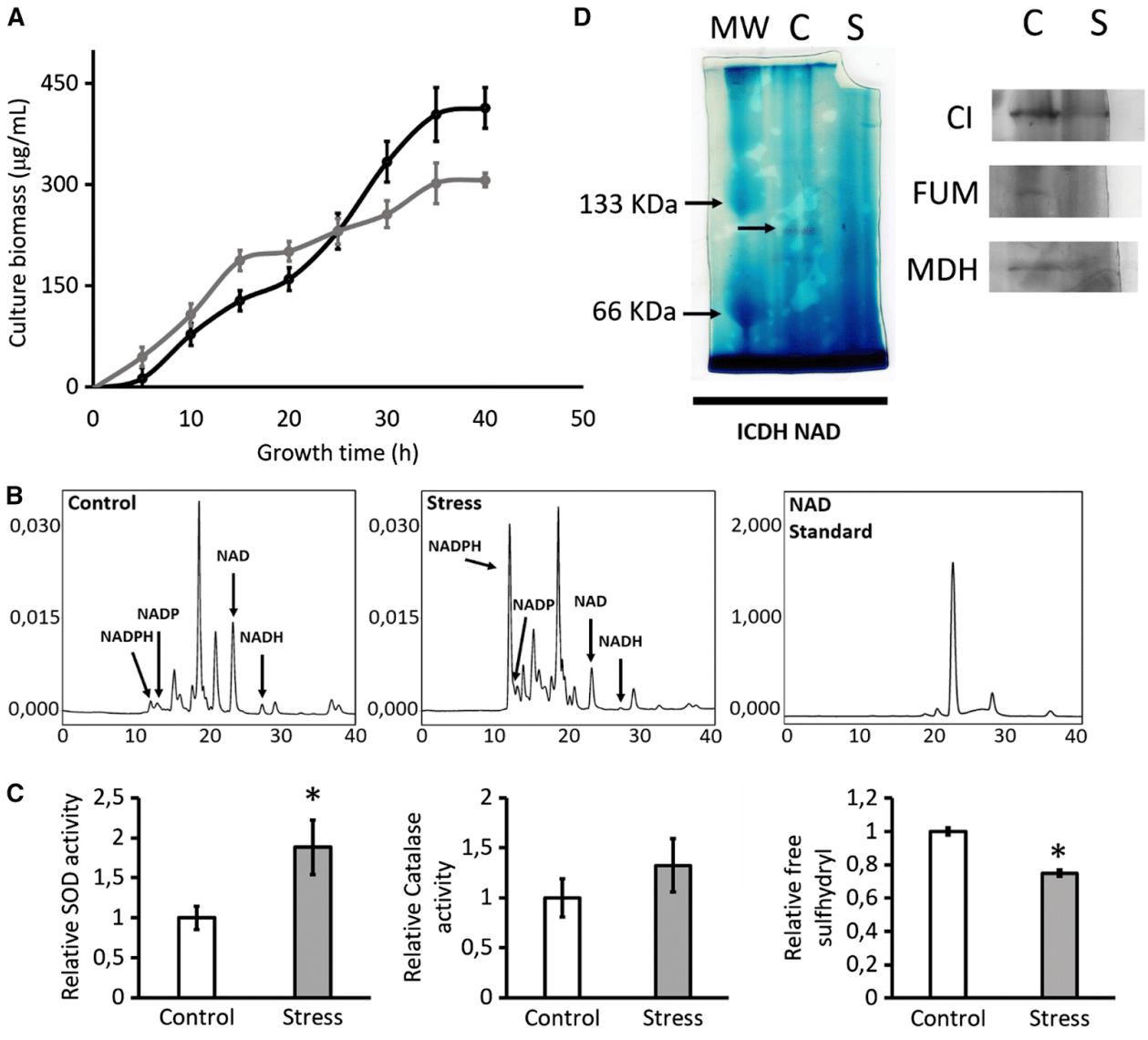

Figure 3.1. Sulfur starvation induces oxidative stress in *P. fluorescens*. A. Growth curve of *P. fluorescens* cultures in glutamine media with (black) and without no added S (grey). B. Nicotinamide nucleotide profiles in *P. fluorescens* obtained from control (left) and S-deficient cultures (middle) at stationary growth phase. NAD^+ standard (right) is shown as an example. C. SOD (left panel) and Catalase (middle panel) activity assay and free sulfhydryl measurement (right). Catalase activity was monitored at 485 nm after 60 min. Superoxide dismutase activity was monitored at 458 nm after 60 min. Activity is presented as fold change relative activity, where the control activity was assigned a value of 1. Free sulfhydryl was quantified at 420 nm after 30 min. D. Activity analysis of ICDH-NAD^+ (full gel), Complex I (CI), Fumarase (FUM) and malate dehydrogenase (MDH) by Blue Native polyacrylamide gel electrophoresis (C = control, S = stress, MW = molecular mass markers). Results are shown as mean ± standard deviation. Results are representative of three independent experiments. Statistical significance was determined at $p < 0.05$ (*) using student's t test

As there was a marked shift in oxidative metabolism in the S-deficient cultures, it became important to examine the fate of nicotinamide adenosine dinucleotides in these conditions as there was a significant difference in the amounts of these moieties in stressed cells compared to the controls (Figure 3.1a). These observations prompted the investigation of enzymes involved in the synthesis of NADH and NADPH. We have previously reported that under oxidative stress induced by H_2O_2, *P.fluorescens* generates glutamate from glutamine in an energy efficient manner (15). Glutamate can subsequently be metabolized to KG, a reaction mediated by GDH-NAD/NADP dependent. The activity of GDH-NAD^+ dependent was more pronounced in the control cells than in the stressed cells. On the other hand, the activity of GDH-NADP dependent was elevated in the stressed cells compared to the control (Figure 3.2A). The KG formed can either follow the reductive or oxidative TCA cycle. The enzyme KGDH, a pivotal participant in the formation of NADH was virtually absent in the S-deficient cultures. No discernible activity band was observed even after 4h of incubation. On the other hand, malic enzyme (ME) known to decarboxylate malate with the concomitant formation of NADPH was elevated in the stressed with a lack of S (Figure 3.2B). The reductive TCA cycle propelled by the enzyme ICDH was markedly elevated in the stressed cultures. This reaction converts KG into isocitrate in the presence of HCO_3^- and NADH/NADPH. NADH was a preferred co-factor for the

enzyme located in the membrane component of the stressed cells. The reductive decarboxylation mediated by ICDH that results in the formation of KG, NADH and CO_2 was more pronounced in control cells. Hence, it became quite evident that the membrane fractions isolated from cells grown in the S-deficient cultures possessed isocitrate-producing enzyme that consumed NADH more rapidly than their control counterparts. The NADH-generating attribute of these fractions was more elevated in the controls. However, in the soluble CFE where the enzyme of the ICDH-NADP is located, the activity was sharply increased in the stressed cells (Figure 2C). The activity was evident even when the co-factor ($NADP^+$) was decreased 10-fold in the reaction mixture (data not shown). The reaction of the excised activity band was readily followed by HPLC where the utilization of isocitrate and the formation of KG were recorded (Figure 3.2D). Hence, the dearth of S has compelled *P.fluorescens* to produce more NADPH and limit the synthesis of NADH.

These findings were further confirmed by the ability of the soluble CFE from the stressed cells to readily generate KG upon incubation with isocitrate and $NADP^+$. It was numerous fold higher compared to the controls as evidenced by the production of KG. This trend to reconfigure the metabolic pathways dedicated to NADPH formation coupled to a decrease in the production of NADH was further tested by examining malic enzyme (ME), an enzyme that liberates NADPH following the decarboxylation of malate and α-ketoglutarate dehydrogenase (KGDH) , an enzyme that generates NADH via the decarboxylation of KG. While the later was decreased, a marked increase was observed with the former (Figure 3.2D) When the soluble CFE from the stressed cultures was incubated with NAD^+ and ATP, $NADP^+$ with the concomitant formation of ADP was readily obtained' thus revealing the presence of enhanced NAD kinase (NADK). This reaction was sharply reduced in the controls (Figure 3.2E). These BN-PAGE studies were further confirmed by the spectrophotometric analyses of these enzymes. While KGDH was barely evident in the stressed cells, the reversible ICDH-NADH was 10-fold higher (Table 1). The drastic down-regulation of KGDH has also been observed in the enhanced production of KG in *P. fluorescens* cultured in a glycerol in the presence of manganese (2,99). RT-qPCR analyses pointed to a significant increase in the mRNA transcripts of ICDH-$NADP^+$ and ICDH kinase, two enzymes that are known to contribute to NADPH synthesis (Figure 3.3).

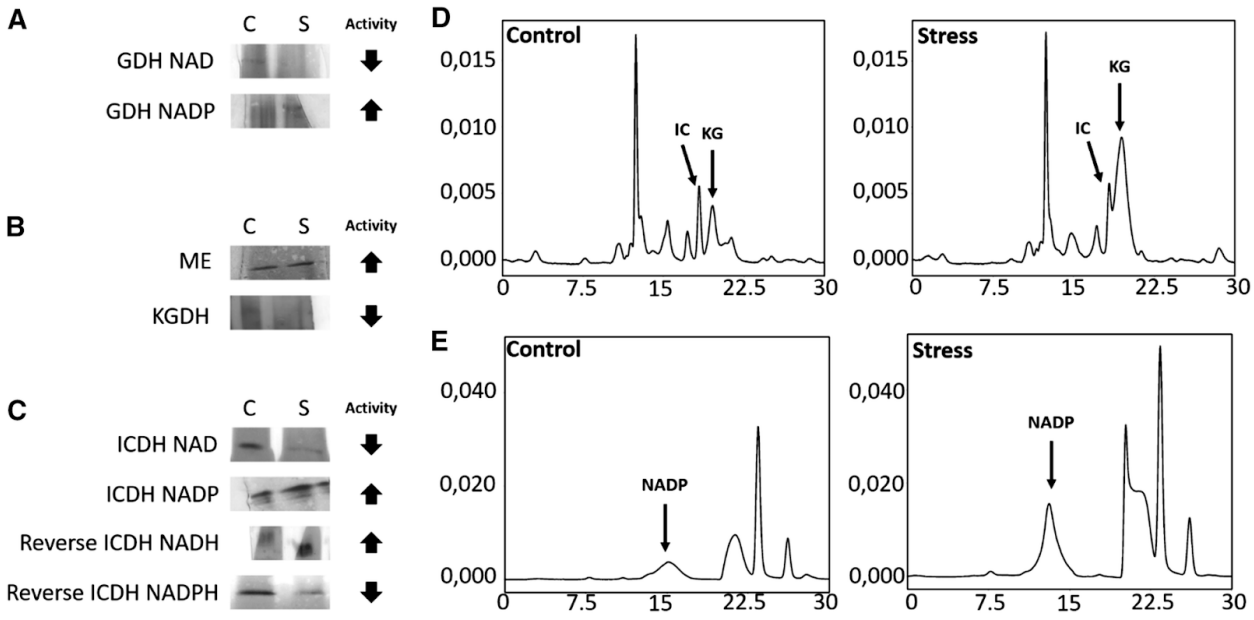

Figure 3.2. NADH and NADPH homeostasis in control and stressed cultures. A. BN-PAGE activity analysis of GDH NAD^+/$NADP^+$ dependent. **B**. Activity analysis of ME and αKGDH. **C**. BN-PAGE Activity analysis of ICDH-NAD^+/$NADP^+$ dependent. C = control cell free extract, S = cell-free extract from sulfur starved culture. **D**. HPLC analysis of ICDH-$NADP^+$ dependent activity. 200 µg of protein was incubated with 2 mM isocitrate and 0.2 mM of $NADP^+$ and incubated for 1h. Samples were analyzed by a C-18 reverse-phase HPLC column at a flow rate of 0.2 mL/min and monitored at 210 nm. The production KG and consumption of isocitrate were followed. **E**. NADK activity analysis by HPLC. 200 µg of protein was incubated with 2 mM ATP and 2 mM NAD^+ and incubated for 1 hr. Samples were then ran unto a C-18 reverse phase HPLC column and detected using a UV lamp set at 254 nm. $NADP^+$ formation was monitored via the characteristic $NADP^+$ peak (showed by arrow) at 12 minutes. NADK activity is increased under sulfur starvation.

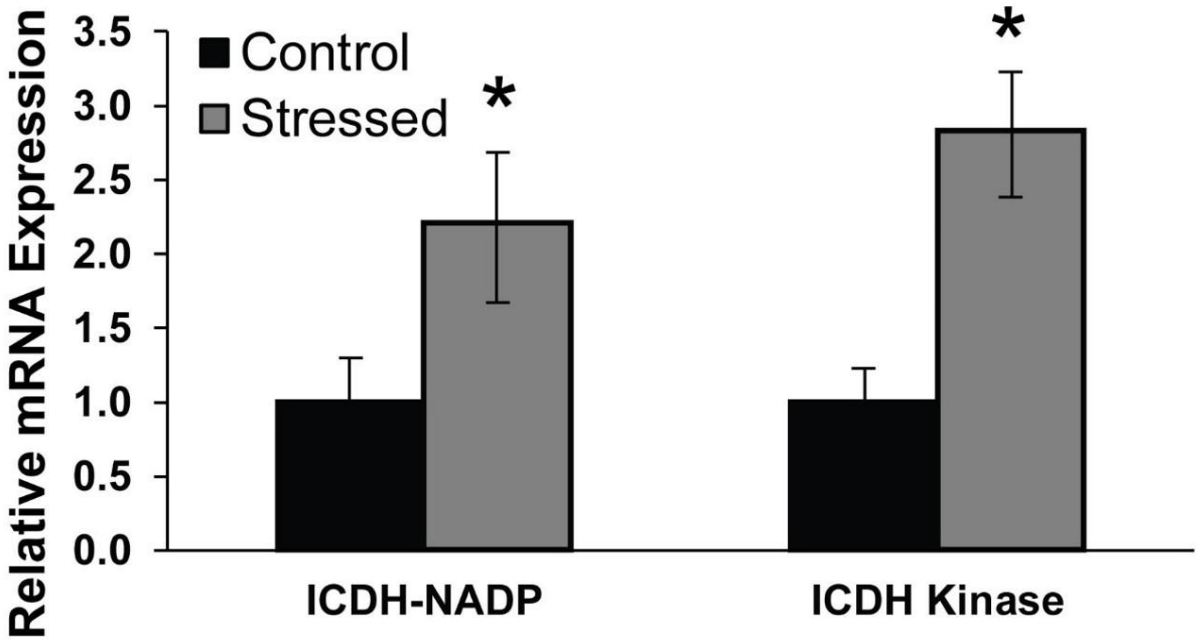

Figure 3.3. mRNA expression analysis of metabolic enzymes in stressed and control cultures by RT-qPCR analysis. mRNA transcripts of isocitrate dehydrogenase $NADP^+$ dependent (ICDH-$NADP^+$) and isocitrate dehydrogenase kinase (ICDH Kinase) were determined relative to 16S rRNA and chaperonin 60 reference genes. Stress cultures demonstrated approximately 2.5 and 3.0 fold increased expression of ICDH-$NADP^+$ and ICDH kinase respectively. Results are representative of 3 independent experiments. Statistical significance was determined at $p < 0.05$ (*) using student's t-test.

The aforementioned data demonstrate the ability of *P.fluorescens* to reconfigure its metabolism in order to fend the oxidative stress triggered by a S-deficient environment. Sulfur that helps maintain a reductive milieu is essential for the survival of all aerobic organisms. In this instance, the microbe opts for a metabolism geared towards the reduction in the production of the pro-oxidant NADH and an increase in the synthesis of the NADPH, an anti-oxidant. The increased in activities of the enzymes, catalase and SOD in the S-deficient culture pinpoint to an oxidative stress encountered by the microorganism when subjected to this challenge (33,104). To quell this situation, *P.fluorescens* impedes the TCA cycle and O.P., two metabolic networks known to be the major generator of ROS. Furthermore, the consumption of NADH is enhanced by the ability of the reductive TCA cycle to consume NADH through its interaction with KG and

HCO_3^-. This not only decreases the intracellular levels of NADH but also enables the ICDH localized in the soluble CFE to generate NADPH with the subsequent formation of KG. The latter can then again fuel the fixation of NADH and the production of isocitrate, a moiety whose decarboxylation is coupled to the synthesis of NADPH by the ICDH residing in the soluble CFE. This metabolic cycle indeed provides an effective route to convert NADH into NADPH by activating enzymes located in different cellular fractions and in this instance fending off an oxidative assault induced by a dearth of S. A metabolic network involving malate, oxaloacetate and pyruvate and the enzymes malate dehydrogenase, malic enzyme and pyruvate carboxylase has been shown to convert NADH into NADPH (98,105,106).

This fine-balancing act in modulating the homeostasis of NADH and NADPH is further aided by NADK, an enzyme that police the availability of NAD^+ and $NADP^+$ in the cells. An up-regulation of the activity of the enzyme will tilt the balance towards $NADP^+$ while a reduction in activity will favour the synthesis of NAD^+. Such an adjustment of the $NAD^+/NADP^+$ ratio will have major implication of the downstream enzymes that require these cofactors for their activities. The lack of NAD^+ is known to arrest the TCA cycle, a metabolic module that incorporates numerous enzymes dependent of this nicotinamide moiety. Hence, in this instance where the aim is to limit ROS production due to a scarcity of S, the enhanced activity of NADK restricts the availability of NAD^+ and subsequently turns the TCA cycle and O.P., two metabolic machines known to release ROS either by design or accidentally. The S-deficient microbe has to impede this if it is to survive this toxic situation. The enhanced formation of $NADP^+$ will undoubtedly promote enzymes committed to the synthesis of NADPH, a well-known biological anti-oxidant. Indeed, an augmentation in activities of numerous NADPH–generating enzymes were observed in this study.

In conclusion, this report illustrates the plasticity of cellular metabolism and how it can be moulded to enable the adaptation of living organisms confronted by nutritional challenges. The dearth of S that precipitates an oxidative stress is averted by a metabolic reconfiguration mediated by ICDH, an enzyme that can modulate the two effectors of oxidative tension NADH and NADPH. This cyclic metabolic module converts NADH into NADPH with the aid of the substrates isocitrate and KG. The cross-talk involving NADK helps support this system by modulating the concentration of $NADP^+$ and NAD^+. NADK resembles a molecular key that turns

on and off the activity of NAD^+ and $NADP^+$ dependent. Hence, the metabolic adaptation orchestrated by molecular partners ICDH, ICDH, NAD^+, $NADP^+$, isocitrate and KG helps provide an effective stratagem to counter the S-triggered oxidative stress (Figure 3.4).

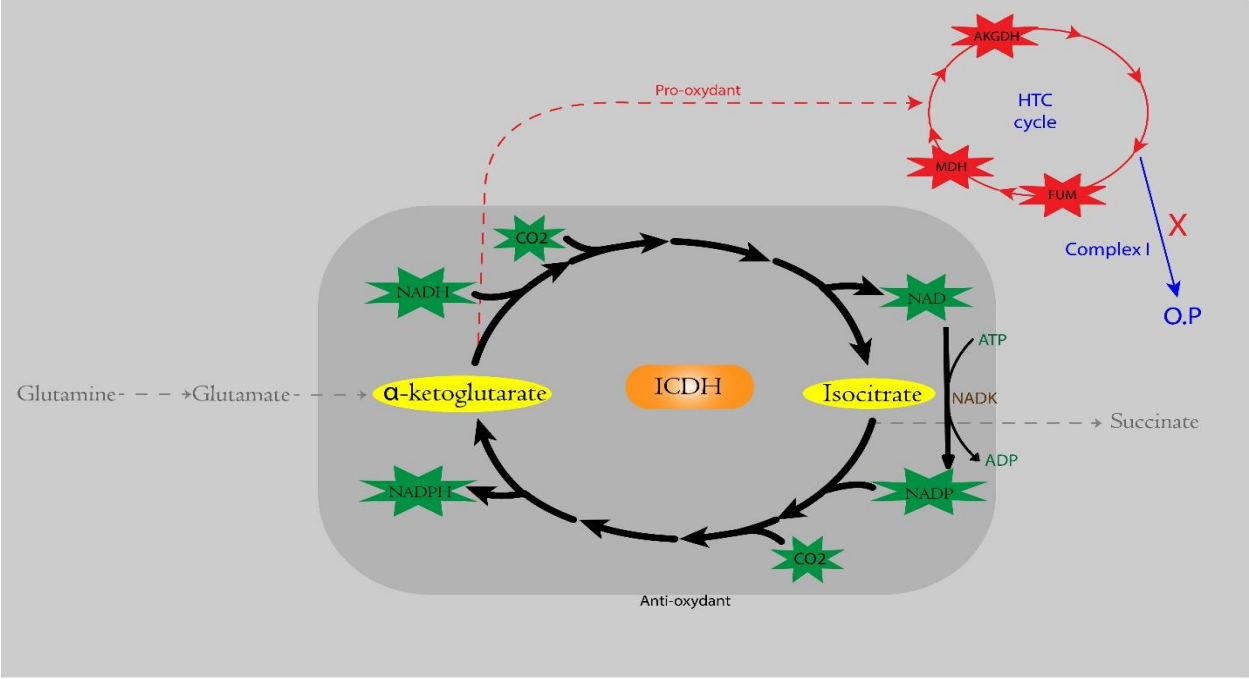

Figure 5 : Schematic representation of NADPH homeostasis in a sulfur deficient

Figure 3.4. Schematic representation of NADPH homeostasis in a sulfur-deficient environment. As Glutamine is the sole source of carbon and nitrogen, it is converted into KG through Glutamine Synthase and Glutamate dehydrogenase (GDH). $NADP^+$-dependent GDH is upregulated, whereas NAD^+-dependent GDH is impaired to avoid the production of NADH, a pro-oxidant molecule. KG is converted into isocitrate using Isocitrate dehydrogenase (ICDH). $NADP^+$-dependent GDH is upregulated, whereas NAD^+-dependent GDH is inactivated. ROS generating metabolic modules such as the TCA cycle and Oxidative Phosphorylation are shut down in this system. This allows the accumulation of the antioxidant molecule NADPH. NAD^+ is utilized by NAD Kinase NADK in order to maintain a high pool of $NADP^+$ in the cell.

4 The metabolic network aimed at production of α-ketoglutarate, an antioxidant, under sulfur starvation

The response to ROS stress involves more than just managing NADH and NADPH homeostasis in the cell. With glutamine as the only source of carbon and nitrogen in the system, it provides a straightforward way to produce KG, a molecule with powerful antioxidant properties, as it is a direct product of glutamate dehydrogenase. KG can detoxify ROS, which leads to the production of succinate as a byproduct. However, KG has a very central position in the metabolic tree and it is needed for more than just detoxify ROS.

This chapter highlights the metabolic pathways that is utilized in *P. fluorescens* in order to respond to ROS accumulation that is aimed towards production of KG from succinate. The data suggest a mechanism where the succinate that is accumulated in the cell following ROS detoxification is transformed into succinate semialdehyde by succinate semialdehyde dehydrogenase (SSADH). This succinate semialdehyde can then be converted back into KG via the enzyme α-ketoglutarate decarboxylase (KGDC). This process is aided by enzymes that produce succinate, such as isocitrate lyase (ICL) and fumarate reductase (FRD). In parallel, the enzymes GABA transaminase (GABAt) and glutamate decarboxylase work together to produce additional succinate semialdehyde.

This mechanism is a novel pathway in which KG is regenerated at low cost for the cell, as the succinate produced at the end of the ROS detoxification reaction can be cycled back into KG. The results of this chapter have been published in the journal Antioxidants.

A metabolic network mediating the cycling of succinate, a product of ROS detoxification into α-ketoglutarate, an antioxidant

Félix Legendre, Alex Maclean, Sujeenthar Tharmalingam and Vasu D. Appanna*

Department of Chemistry and Biochemistry

Laurentian University

Sudbury, Ontario

Canada

P3E 2C6

* Corresponding Author

ABSTRACT

Sulfur is an essential element for life. However, the soil microbe *Pseudomonas (P.) fluorescens* can survive in a low sulfur environment. When cultured in a sulfur-deficient medium, the bacterium reprograms its metabolic pathways to produce α-ketoglutarate (KG) and regenerate this keto-acid from succinate, a by-product of ROS detoxification. Succinate semialdehyde dehydrogenase (SSADH) and KG decarboxylase (KGDC) work in partnership to synthesize KG. This process is further aided by the increased activity of the enzymes glutamate decarboxylase (GDC) and γ-amino-butyrate transaminase (GABAT). The pool of succinate semialdehyde (SSA) generated is further channeled towards the formation of the antioxidant. Spectrophotometric analyses, HPLC experiments and electrophoretic studies with intact cells and cell-free extracts (CFE) pointed to the metabolites (succinate, SSA, GABA) and enzymes (SSADH, GDC, KGDC) contributing to this KG-forming metabolic machinery. Real-time polymerase chain reaction (RT-qPCR) revealed significant increase in transcripts of such enzymes as SSADH, GDC and KGDC. The findings of this study highlight a novel pathway involving keto-acids in ROS scavenging. The cycling of succinate into KG provides an efficient means of combatting an

oxidative environment. Considering the central role of KG in biological processes, this metabolic network may be operative in other living systems.

Keywords: sulfur stress; oxidative stress; KG; succinate recycling; metabolic network; glutamate decarboxylase

INTRODUCTION

Sulfur is an essential element for life. It is present in macromolecules and plays a key role in redox processes, in large part due to sulfhydryl groups of proteins. In fact, the interplay between sulfhydryl groups (-SH) and disulfide bonds (S-S) is at the center of the oxidative state of living organisms from bacteria to humans (107-109). Free sulfhydryl moieties are required for the proper functioning of numerous enzymes (87). Sulfur also participates in the synthesis of Fe-S clusters, which are essential for the activity of enzymes involved in energy metabolism, including the TCA cycle and oxidative phosphorylation. For instance, aconitase, fumarase, and electron transport chain enzymes contain Fe-S (33,110,111). Abnormal biosynthesis and maintenance of these clusters lead to the accumulation of free cytosolic iron and the creation of free radicals through the Fenton reaction (112,113). As a result, sulfur starvation contributes to a highly oxidative environment where the TCA cycle and oxidative phosphorylation are severely impeded (114).

The metabolite α-ketoglutarate (KG) is an intermediate of the TCA cycle. Its central position in energy metabolism makes it a pivotal regulatory component in different biological processes, ranging from amino acid homeostasis to genetic modifications as well as cell signaling (20, 109,115). The metabolite KG has been recognized for its ability to combat oxidative stress generated by reactive oxygen species (ROS) (16,29,30,115). It can readily neutralize ROS with the concomitant formation of succinate, carbon dioxide and water. This attribute makes KG an important protective asset against cellular oxidative stress arising from exposure to hydrogen peroxide to metal stress, metabolic dysfunctions, and a range of other challenges (17,30). In fact, high concentrations of metals like iron and gallium have been shown to exert toxic effects on biological systems in a manner that perturb Fe-S cluster biosynthesis (18,112). An increase in NADPH, superoxide dismutase, catalase and glutathione peroxidase coupled with the enhanced

synthesis of keto-acids like KG are associated with the core anti-oxidative defense strategies in numerous organisms (17,18,116).

The soil microbe *Pseudomonas (P.) fluorescens* is a nutrient-versatile bacterium found in diverse environments including soil and water bodies. It can orchestrate tightly regulated metabolic adaptations to grow and thrive under different abiotic challenges such as oxidative, metal and nutrient stress (3,4,17,117). When grown in a glutamine mineral medium without added sulfur, *P. fluorescens* switches its metabolism towards NADPH production and NADH utilization to better survive in the oxidative environment triggered by sulfur starvation, a stress responsible for the superoxide and H_2O_2 (15,114). This pathway involves using the NAD^+ pool in the cell to produce $NADP^+$ through NAD^+ kinase. $NADP^+$-dependent glutamate dehydrogenase and isocitrate dehydrogenase are upregulated to produce the antioxidant NADPH. In this study, the ability of the organism to reprogram its metabolic networks aimed at the production of the antioxidant KG was investigated. Here, we report that oxidative stress evoked by sulfur starvation triggered a metabolic reconfiguration aimed at enhanced synthesis and regeneration of KG. A novel pathway, reliant on the enzymes succinate semialdehyde dehydrogenase (SSADH) and alpha-ketoglutarate decarboxylase (KGDC), orchestrates the cycling of succinate, a by-product of ROS neutralization into KG, the antioxidant. Glutamate decarboxylase (GDC), fumarate reductase (FRD) and isocitrate lyase (ICL) participate in increased formation of KG. The efficacy of this metabolic adaptation involving the enzymes of the glyoxylate cycle, GABA shunt and the TCA directed towards intracellular oxidative environment provoked by sulfur stress is also discussed. These findings further highlight the significance of metabolism and keto-acids in modulating ROS.

MATERIAL AND METHODS

Bacterial Cultures and Biomass Measurement

Pseudomonas fluorescens 13525 was obtained from the American Type Culture Collection. It was cultured in a defined mineral medium with glutamine (19 mM) as the only source of carbon. The control medium contained 42 mM Na_2HPO_4, 22 mM KH_2PO_4 and 0.8 mM of $MgSO_4 \cdot 7H_2O$. In the stressed medium $MgSO_4 \cdot 7H_2O$, was substituted by $MgCl_2$ (0.8 mM). Trace metals were added to the culture as previously described in (95). Media was autoclaved for 20 min at 121 °C.

The cultures had a volume of 200 mL and were inoculated with 1 mL of *P. fluorescens* preculture as previously described in (95) and grown on a Gyrotory® Water Bath Shaker Model G76 (New Brunswick Scientific, Midland, ON, Canada) at ambient temperature. Biomass measurements were taken using the Bradford assay (96) to quantify the amount of soluble protein as the indicator of cellular biomass. Ten milliliters (mL) of microbial culture were spun down at 12,000× g for 20 min. The pellet containing the bacterial cells was resuspended in 1 mL of 0.5M NaOH and soluble proteins were assayed in triplicate.

Cell Fractionation and Metabolic Profiling

The pellets harvested after centrifugation were washed with approximately 100 mL of 0.85% m/v sodium chloride and the samples were centrifuged at 12,000 × g for 20 min. The pellet containing whole cells was resuspended in 1 mL of Cell Storage Buffer (CSB) (50 mM Tris-HCl, 1 mM phenylmethylsulfonyl fluoride, 1 mM dithiothreitol, pH 7.6) and disrupted using an ultrasonic processor (Johns Scientific, Toronto, ON, Canada). Cellular membrane fraction (mCFE, outer and inner membrane) and soluble fraction (sCFE) were obtained by centrifugation at 110,000 × g for 3 h at 4°C. The mCFE was resuspended in 1 mL of CSB and sCFE were stored at 4 °C for a maximum of 7 days and were used for follow-up experimentation.

The HPLC analysis was performed on a Waters 2695 Separation Module HPLC system with a Synergi 4 μm Hydro-RP 80A column (250 × 4.6 mm, San Francisco, CA, USA). The flow rate utilized was 0.2 mL/min. The mobile phase consisted of 5% (v/v) acetonitrile, 20 mM KH_2PO_4 diluted in Milli-Q water at a pH 2.9 at ambient temperature. Detection of metabolites was done using a Waters 2478 Dual λ absorbance detector, set at a wavelength of 210 nm to detect organic acids. Samples were prepared and run in the HPLC as described previously (17). Metabolite amounts were determined from the area under the curve of the corresponding peaks using the Empower software (Milford, MA, USA) and identified by comparing their elution time to known standard solutions. The peaks were confirmed by spiking the samples with the appropriate standards and keto-acids were further confirmed by the 2,4-dihydrophenylhydrazine (DNPH) assay (11,117,118). All enzymatic assays with the intact cells, and cell-free extracts were performed with cells obtained at a similar growth phase (late logarithmic phase) in control and sulfur-deficient media.

Blue Native Polyacrylamide Gel Electrophoresis (BN-PAGE) and Enzyme Activity

Activity of specific enzymes was detected by Blue Native Polyacrylamide Gel Electrophoresis (BN-PAGE). A 4–16% acrylamide linear gradient native gel was prepared (50 mM ϵ-aminocaproic acid, 15 mM Bis–Tris, pH 7.0, 4 °C). The gel was cast using the MiniProteanTM2 gel system (Bio-Rad Laboratories, Mississauga, ON, Canada). A spacer of 1.0 mm was used to prepare the gel. A quantity of 60 μg of proteins was loaded into gel wells. The gel chamber was filled with anode buffer (50 mM Bis–Tris, pH 7.0, 4 °C), whereas the space between gels was filled with blue cathode buffer (50 mM Tricine, 15 mM Bis–Tris, 0.2 g/L Coomassie Blue G250, pH 7.0, 4 °C. Membrane protein samples contained 1% (m/V) η-dodecyl β-D-maltoside to help proteins solubilize. Electrophoresis was carried out at a voltage of 75 V and a current of 15 mA until the proteins entered the resolving gel as described in (97,119,120). Enzymatic activity was detected using the formazan precipitation method, where the gel slices are incubated in a reaction buffer (25 mM Tris-HCl, 5 mM MgCl2, pH 7.4) with appropriate substrates and redox markers. The compounds iodonitrotetrazolium (INT) in reduced form produces the formazan precipitate. Phenazine methosulfate (PMS) and dichlorophenolindophenol (DCPIP) are used as electron transfer intermediates to allow the reduction of INT. The concentration of INT and DCPIP/PMS was 0.4 mg/mL for all reactions.

The activity of fumarase (FUM) was probed using a mixture of 5 mM fumarate, 0.5 mM nicotinamide adenine dinucleotide (NAD^+) and 2 units of malate dehydrogenase (MDH) per lane. Fumarate reductase (FRD) activity was monitored in the membrane fraction using 5 mM fumarate and 0.5 mM nicotinamide adenine dinucleotide reduced form (NADH). Complex I activity was assessed on the membrane fraction using 0.5 mM NADH, without PMS, while Complex IV activity was visualized with 5 mg/mL diaminobenzidine, 13.3 mM of sucrose and 10 mg/mL of cytochrome C. α-ketoglutarate dehydrogenase (KGDH) was tested by using 5 mM α-ketoglutarate, 0.5 mM NAD^+ and 1 mM CoA. α-ketoglutarate decarboxylase activity was assessed as previously described (2). Enzymatic activity of alanine transaminase was detected by using a mixture of 5 mM alanine, 5 mM α-ketoglutarate, 0.5 mM NAD^+ and 5 units of glutamate dehydrogenase. Enzymatic activity of isocitrate lyase was detected by using 5 mM isocitrate, 0.5 mM NAD^+ and 5 units of lactate dehydrogenase. Succinate semialdehyde enzymatic reaction was observed with 5 mM succinate and 0.5 mM NADH.

Detection of Enzymatic Activity by HPLC and Spectrophotometric Assays

Detection of enzymatic activity was also performed by using HPLC and colorimetric assays. Cell free extract (200 μg) from control and stressed cultures were incubated with substrates of interest and reacted for 30–120 min. Following inactivation of the reactions by heat, the products/reactants were monitored. The activity of glutamate decarboxylase (GDC) was determined by monitoring GABA with glutamate as the substrate. The activity of GABA transaminase (GABAT) was detected by incubating 200 μg protein equivalent of cell free extract with 5 mM of GABA and 5 mM of pyruvate. In this instance, alanine and succinate semialdehyde (SSA) were monitored. The activity of fumarate reductase was tested by incubating 200 μg of protein from the cell free extracts of control and stressed cultures with 2 mM fumarate and 0.2 mM of NADH. The activity of succinate semialdehyde dehydrogenase was assessed using 2 mM succinate and 0.2 mM NAD^+ whereas the activity of α-ketoglutarate dehydrogenase (KGDH) was assessed by using 2 mM KG and 0.2 mM NAD^+. The absorbance of NADH at 340 nm was monitored by UV-Vis spectrophotometer for 60 s. Relative activity was calculated by dividing the rate of NADH consumption or production of the stressed cell free extract reaction by the rate of the control. The control activity was arbitrarily set to 1. To further confirm the nature of the enzymes, activity bands were excised and incubated in appropriate substrates. Product peaks were monitored by HPLC and by the DNPH assay. Intact (whole) cells were utilized to evaluate the metabolic networks enabling *P. fluorescens* to adapt to sulfur starvation. Four milligrams of these cells isolated from control and stressed cultures were incubated with 10 mM glutamate and the conversion of glutamate to GABA was monitored by incubation of the intact cells with the aid of HPLC. Four milligrams of these cells isolated from control and stressed cultures were incubated with 10 mM succinate and 10 mM sodium bicarbonate resulting in the formation of KG and SSA.

Gene Expression Profiling Using Quantitative Real Time Polymerase Chain Reaction (qRT-PCR)

Total RNA from control and stressed cells was extracted using TRIzol Reagent following the provider's instructions. Samples were treated with DNAse I to avoid genomic DNA contamination. The reverse transcription reaction as well as qRT-PCR reaction were carried out as previously described (2,114). Primer sequences were designed using Primer-BLAST and

NCBI genome databases. Forward/reverse primer pairs for selected genes were subjected to a validation test by plotting Ct values against cDNA serial dilution concentrations. To be considered acceptable for qRT-PCR experiments, primer pairs had to show a R^2 value > 0.99 and an efficiency between 90% and 110%. The efficiency was calculated using the formula: efficiency = 10(−1/slope) -1. The housekeeping genes used to normalize the samples were rpoA and cpn60. The relative mRNA transcript level of each gene was shown as fold change using the ΔΔCT method described in (103) as mRNA fold change where the low sulfur mRNA level is compared to the control mRNA level. The list of primers used can be found in Table 4.1. Accession numbers were obtained from the NCBI database for *Pseudomonas fluorescens* Pf0-(NC_007492.2) or *Pseudomonas fluorescens* strain ATCC 13525 (NZ_LT907842.1).

Table 4.1. List of primers used for the qRT-PCR analysis.

Gene Name	**Enzyme Symbol**	**Genome ID (Gene Location)**	**Forward Primer [5′ to 3′]**	**Reverse Primer [5′ to 3′]**
Succinate dehydrogenase (sdhB)	**SDH**	NZ_LT907842.1 (4306753–4307457)	CTCGACGGTCTGTACG AGTG	CTGGACCCAGGAACT TGTCC
Fumarate reductase (sdhA)	**FRD**	NZ_LT907842.1 (2366315–2368087)	GATCGCGACGACGAA AACTG	GGAACTGTCTTCGGCG AGAA
Glutamate Decarboxylase (Gldc)	**GDC**	NZ_LT907842.1 (5096095 5096823)	TTTCGACCTGCCGGAA ATGA	TTCACCTCATGGGCCT GTTC
Alpha-ketoglutarate decarboxylase (alkB)	**KGDC**	NZ_LT907842.1 (3673836–3674501)	CCCCAGAAGATCGCCT TGTT	TCGGCATCACCCCATG AAAA
Isocitrate dehydrogenase (NAD^+) (AceK)	**ICDH (NAD^+)**	NZ_LT907842.1 (4980207–4981922)	CCCGAGGATGAGATG GCTTC	AAGGCGGGAATTCTTC AGGG
Succinate semialdehyde	**SSADH**	NC_007492.2 (225316–226758)	GTCGTCAGCTGATGTC GGAA	GTCGAACACGATGAAT GGCG

dehydrogenase (SSADH)				
Isocitrate lyase (AceA)	**ICL**	NZ_LT907842.1 (6193725–6195050)	CCCACGGGTCTTCTTT CAGG	ACAAAGTCGGCTACTG GTCG
Housekeeping Gene: Chaperonin 60 (cpn60)	**N/A**	NZ_LT907842.1 (5505175–5506821)	GCGACATGATCGAAAT GGGC	GCCAGTCGAGCCTTCT TTCT
Housekeeping Gene: DNA-directed RNA polymerase subunit alpha (rpoA)	**N/A**	NZ_LT907842.1 (6028685–6029686)	TCCTGTTGTCCTCAAT GCCC	TGCAGCTTGATAGCCA GACC

RESULTS

Oxidative environment evoked by lack of sulfur leads to succinate accumulation in *P. fluorescens*

Although there was no significant change in the growth profile of the microbe grown in control and sulfur-deficient media, a marked difference was observed in the metabolic processes occurring under these conditions. The spent fluid obtained from the sulfur deficient cultures revealed prominent peaks attributable to succinate, pyruvate, isocitrate and KG by HPLC analyses. These peaks were barely discernable in the control cultures (Figure 4.1A,B). This elevated amount of the dicarboxylic acid, a known product of ROS neutralization characteristic of KG, prompted the evaluation of select enzymes responsible for the TCA cycle and oxidative phosphorylation that are known to be perturbed by oxidative stress in this instance triggered by sulfur starvation. The BN-PAGE analysis of enzymatic activity revealed that fumarase (FUM), KGDH, and complexes I and IV, all sulfur dependent proteins, had decreased activity (Figure 4.1C*). Inversely, fumarate reductase (FRD), that converts fumarate to succinate, and isocitrate lyase (ICL) that mediates the transformation of isocitrate to succinate and glyoxylate were upregulated in the stressed cultures. The excised band responsible of FRD activity readily generated succinate upon incubation with fumarate and NADH (Figure 4.1D). Spectrometric

studies of select enzymes further confirmed the increased activity of FRD and diminished activity of KGDH in the stressed cells (Figure 4.1E).

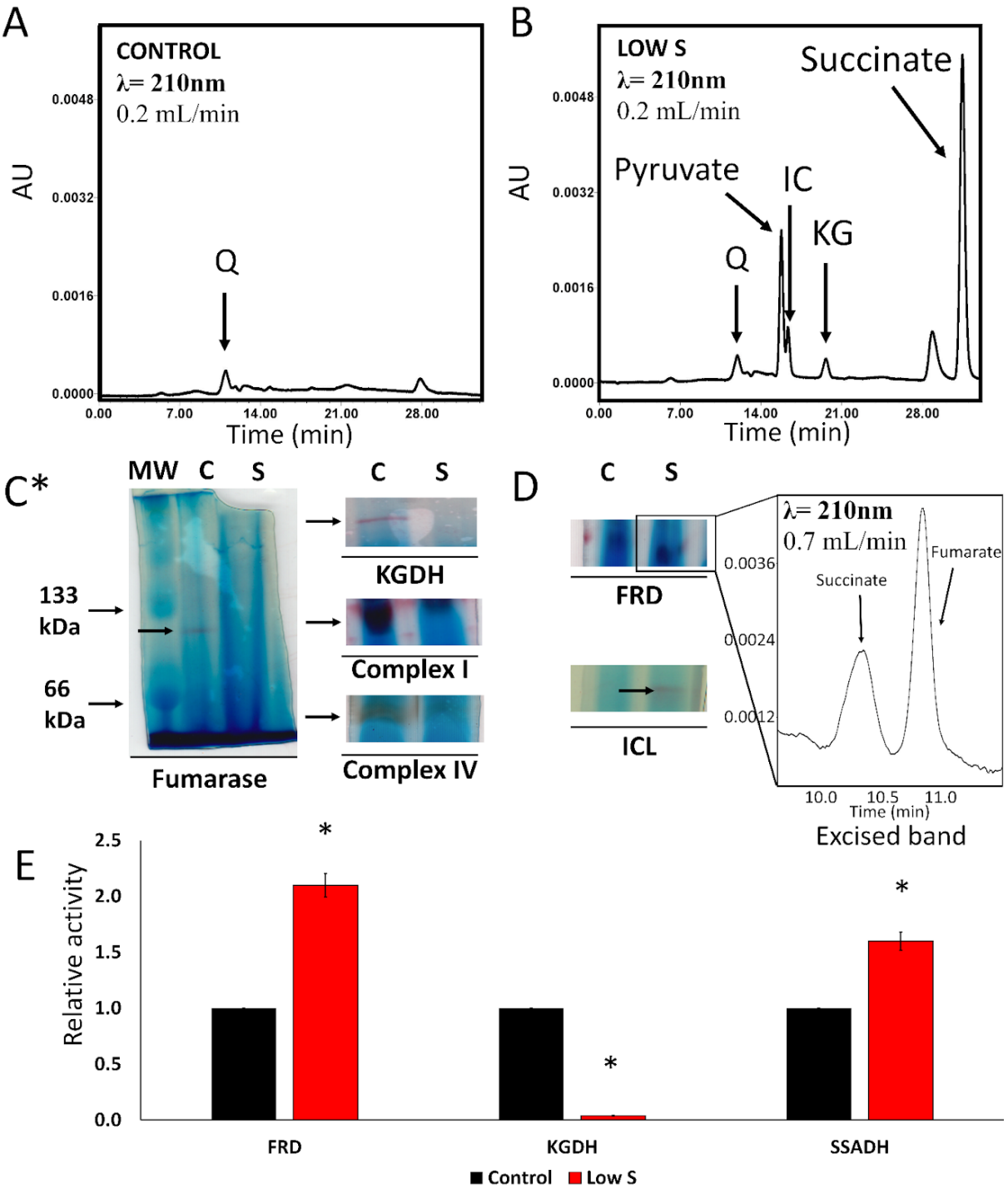

Figure 4.1. Oxidative stressed provoked by sulfur starvation leads to succinate accumulation in *P. fluorescens*. (A). HPLC chromatogram of a spent fluid sample from *P. fluorescens* grown in control conditions. (B). HPLC chromatogram of a spent fluid sample from *P. fluorescens* grown in media with no added sulfur. The X axis shows retention time in minutes and the y axis shows absorbance at 210 nm in arbitrary units (AU). (C*). Enzymatic activity analysis of TCA cycle and oxidative phosphorylation enzymes by Blue Native polyacrylamide gel electrophoresis (BN-PAGE). Fumarase, α-ketoglutarate dehydrogenase (KGDH) and (Complex I-IV) activities are decreased in the stressed cells. (D). Enzymatic activity analysis of fumarate reductase (FRD) and isocitrate lyase (ICL). FRD and ICL activities are increased under sulfur starvation. The nature of FRD was confirmed by cutting the band and incubating it in reaction buffer with 2 mM fumarate and 0.2 mM NADH. Detection of succinate was done by running the reaction mixture in the HPLC after 24 h. C = Control, S = Low sulfur. (E). Enzymatic assays of select enzymes with appropriate substrates by measuring the absorbance of NADH at 340 nm. The rate of reaction was calculated using the slope of absorbance change per minute. The control sample was normalized to 1 and the stressed rate was compared to it, data is shown as relative activity. (Q = glutamine, IC = isocitrate, KG = α -ketoglutarate) Data are represented as means ± standard deviation and is representative of three (3) distinct experiments. n = 3, * = $p < 0.05$.

Metabolite and Enzyme profiles in cell-free extracts (CFEs) from control and S-deficient cultures

To further assess the nature of the metabolic shift resulting in the elevated presence of succinate in the spent fluid and probe the diminished activity of enzymes involved in aerobic energy formation, the metabolite and the enzymatic profiles of the CFEs were examined. The HPLC chromatogram of soluble CFEs of *P. fluorescens* cells grown under a lack of S consistently showed higher amounts of KG, γ-aminobutyric acid (GABA) and succinate semialdehyde (SSA) (Figure 4.2A–C). Additionally, peaks attributable to moieties like isocitrate that were evident in the stressed cells were barely discernable in the controls (Figure 4.2C). The prominence of GABA in the soluble CFE led us to investigate the ability of the intact cells to consume glutamate and generate GABA. The HPLC analysis showed that *P. fluorescens* harvested from the sulfur-limited culture produced more GABA than the controls when incubated in the presence of glutamate (Figure 4.2D–F). As succinate was a prominent metabolite in the spent

fluid, it was important to decipher if the intact cells were capable of producing KG upon incubation with this dicarboxylic acid and HCO_3^-. Indeed, SSA and KG were detected. The former was readily carboxylated to KG. These peaks were not evident in the control cells (Figure 4.2G).

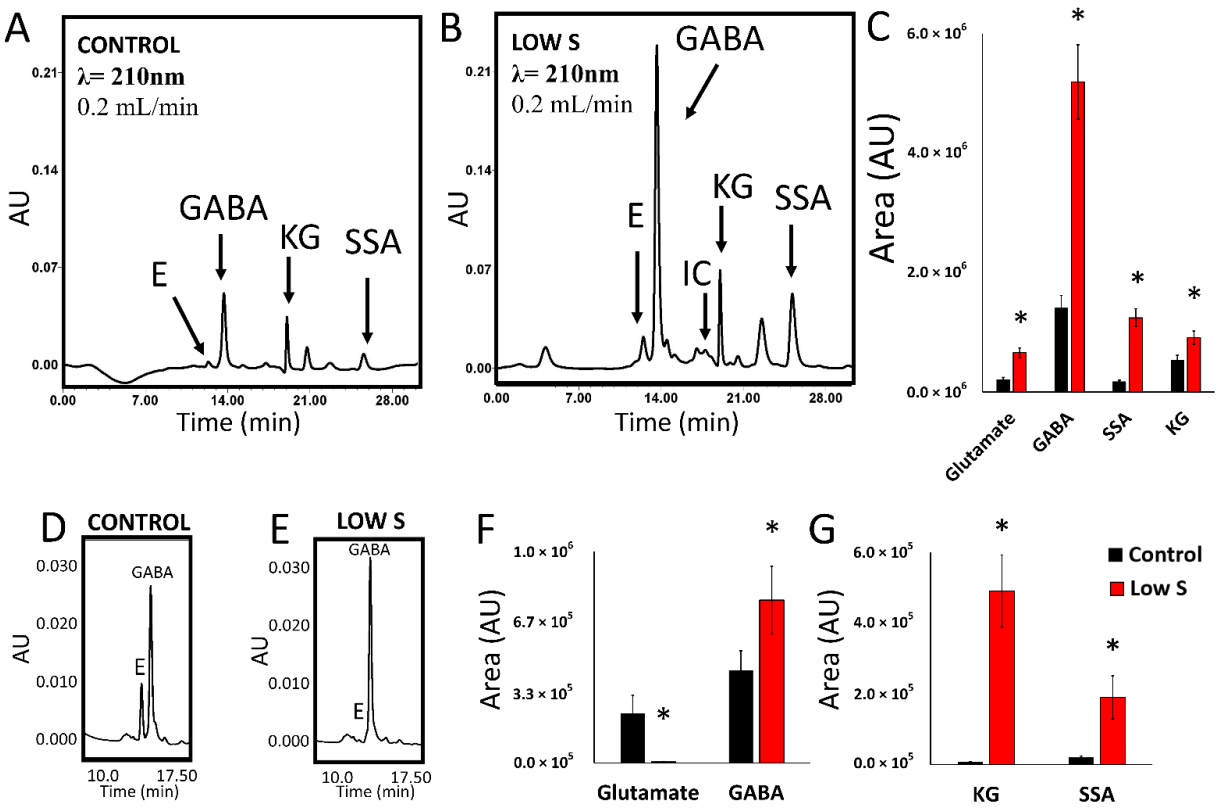

Figure 4.2. Metabolite profiling in *P. fluorescens* cell free extract and intact cells in control and sulfur-deficient conditions. (A). HPLC chromatogram of a cell free extract from *P. fluorescens* grown in control conditions. (B). HPLC chromatogram of a cell free extract sample from *P. fluorescens* grown in a media with no added sulfur. Peaks corresponding to glutamate (E), isocitrate (IC), γ-aminobutyric acid (GABA), α-ketoglutarate (KG) and succinate semialdehyde (SSA) are shown. (C). Quantification of select metabolites in cell free extract samples of *P. fluorescens* grown in control and sulfur-deficient (Low S) conditions. Enrichment in GABA, SSA and KG is seen in sample from sulfur-deficient grown cells. (D,E). HPLC chromatogram of whole cells *P. fluorescens* control (D) and low sulfur (E) cells incubated with 10 mM glutamate for two hours. (F). Quantification of metabolites in whole *P. fluorescens* cells

grown in control and sulfur-deficient (Low S) conditions fed with 5 mM glutamate and incubated for two hours. (G). Quantification of metabolites in whole *P. fluorescens* cells grown in control and sulfur-limited (Low S) conditions fed with 10 mM succinate, 10 mM HCO_3^- and incubated for two hours. Succinate metabolism leads to enrichment in KG. Data are represented as means ± standard deviation. n = 3, * = $p < 0.05$.

Experiments were performed with cell-free extracts in the presence of glutamine, isocitrate and succinate to further assess the nature of the metabolic network resulting in the cycling of succinate into KG. The metabolism of glutamine in the soluble CFE yielded increased amounts of succinate, SSA, KG and isocitrate in the stressed cells. Incubation in the presence of isocitrate gave peaks reflective of pyruvate, KG and succinate. In the presence of succinate and HCO_3^-, the sCFE extracts generated KG and isocitrate (Figure 4.3A–C). Membrane mCFE isolated from the stressed cells readily produced alanine and SSA in higher amounts compared to the control mCFE when incubated with GABA and pyruvate. This pointed to an increased activity of GABA transaminase (GABAT) in the cell free extracts from the culture grown without added sulfur (Figure 4.3D). To further understand the biochemical networks resulting in the elevated amounts of KG, pyruvate and SSA in the stressed cells, select enzymatic activities were assessed by BN-PAGE. In the stressed cells, KGDC, an enzyme involved in the carboxylation of SSA to KG, was increased concomitant with the augmentation of SSADH activity, an enzyme modulating the synthesis of SSA. As alanine transaminase (ALA-T) can be a source of elevated pyruvate, a precursor to KG, this enzyme was also analyzed by BN-PAGE. A noticeable increase was observed in the stressed cells (Figure 4.3E). Addition of stressed cells into a control medium readily reversed this biochemical trend (personal observation).

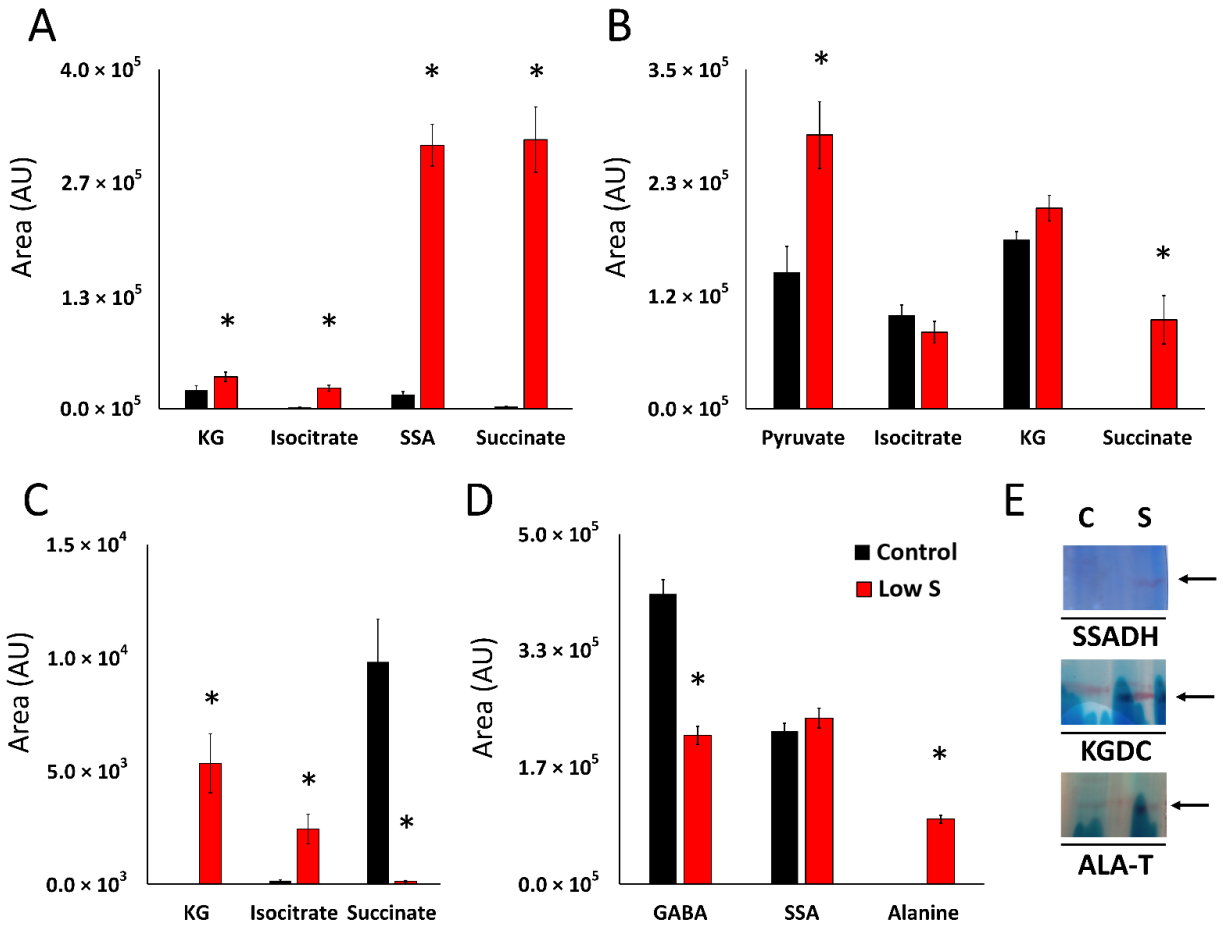

Figure 4.3. Multiple routes to α-ketoglutarate in *P. fluorescens* subject to sulfur starvation. (A). Quantification of metabolites in membrane cell free extracts of *P. fluorescens* grown in control and limited-sulfur (Low S) conditions incubated with 5 mM glutamine for 60 min. Glutamine utilization leads to enrichment of KG, Isocitrate, SSA and succinate. (B). Quantification of metabolites in cell free extracts of *P. fluorescens* grown in control (black) and sulfur-limited (red) conditions incubated with 5 mM isocitrate for 60 min. Isocitrate metabolism leads to enrichment of KG, succinate and pyruvate. (C). Quantification of metabolites in cell free extracts of *P. fluorescens* grown in control and sulfur-limited (Low S) conditions incubated with 5 mM succinate, 10 mM HCO_3^- for 60 min. Succinate metabolism results in the production of isocitrate and KG. (D). Quantification of metabolites in membrane cell free extracts of *P. fluorescens* grown in control and sulfur-deficient (Low S) conditions incubated with 5 mM GABA, 5 mM pyruvate for 60 min. Production of alanine, a by-product of GABAT is identified.

(E). Activity analysis by BN-PAGE of succinate semialdehyde dehydrogenase (SSADH), α-ketoglutarate decarboxylase (KGDC) and alanine transaminase (ALA-T). SSADH, KGDC and ALA-T. c = control, s = low sulfur. Data are represented as means ± standard deviation. n = 3, * = $p < 0.05$.

Gene expression profiling in *P. fluorescens* under sulfur starvation

Gene expression profiling studies were performed to evaluate if the enzymes in the cycling of succinate to KG observed under sulfur starvation were upregulated during transcription. Quantitative real time polymerase chain reaction (qRT-PCR) experiments revealed that genes responsible for glutamate decarboxylase (GDC), isocitrate lyase (ICL), α-ketoglutarate decarboxylase (KGDC), succinate semialdehyde dehydrogenase (SSADH) and fumarate reductase (FRD) were indeed upregulated significantly in cells from cultures grown in sulfur-deficient media, whereas diminished expression of genes resulting in the enzymes isocitrate dehydrogenase (ICDH-NAD^+) and succinate dehydrogenase (SDH) were observed. A 15-fold increase KGDC transcript was observed while mRNA responsible for SDH was decreased 2-fold (Figure 4.4).

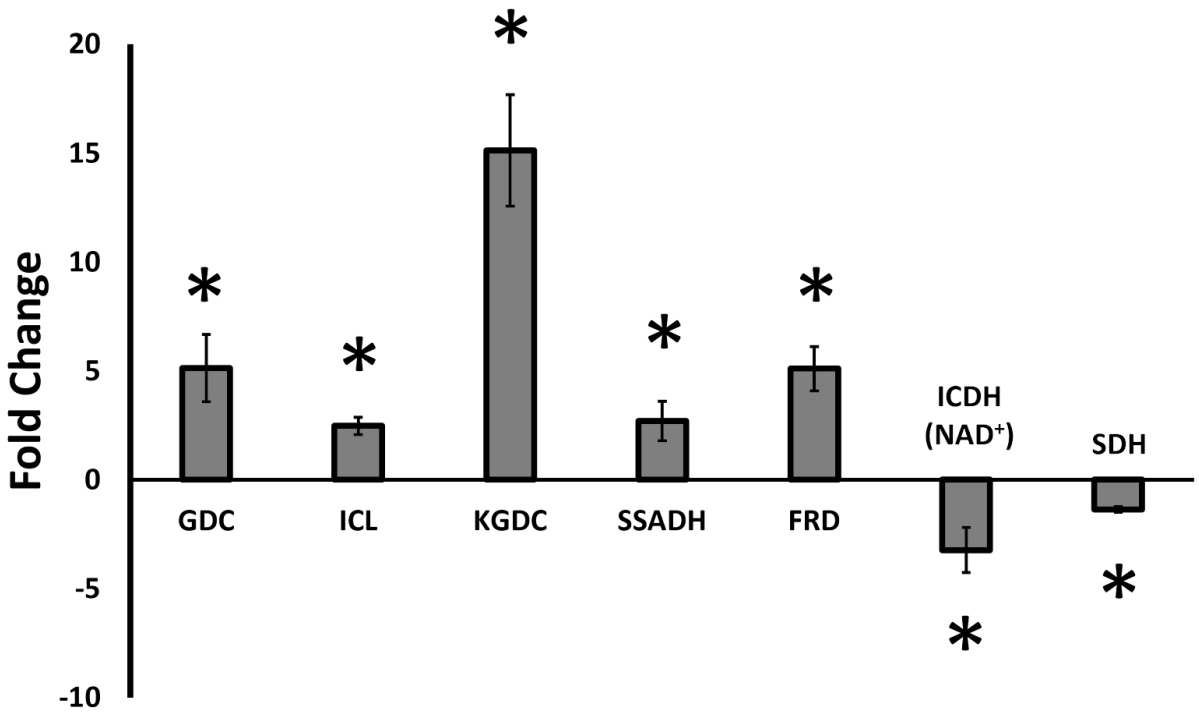

Figure 4.4. Gene expression profiling of genes involved in KG regeneration under sulfur starvation in *Pseudomonas fluorescens*. qRT-PCR experiments were performed using primer pairs from Table 4.1. Relative expression of mRNA transcripts in comparison to control conditions in cells at the late exponential phase was determined using the ΔΔCt method. GDC = glutamate decarboxylase, ICL = isocitrate lyase, KGDC = α-ketoglutarate decarboxylase, SSADH = succinate semialdehyde dehydrogenase, FRD = fumarate reductase = ICDH (NAD^+) = NAD^+-dependent isocitrate dehydrogenase, SDH = succinate dehydrogenase. N = 4, *= $p<0.05$.

DISCUSSION

The data in this report demonstrate the ability of *P. fluorescens* to survive a sulfur deficient medium by reprogramming its metabolism aimed at the cycling of succinate to KG, an antioxidant. Succinate generated because of ROS detoxification by KG is converted into SSA and subsequently into KG. This provides an elegant cycle to scavenge ROS without an onerous burden on the organism. Sulfur deprivation is known to impose oxidative stress in all organisms, as sulfur is an important component of the redox potential living systems must maintain to live in

an aerobic environment. We have recently shown that in a medium with glutamine as the sole carbon source, this microbe elaborates a metabolic network to produce enhanced NADPH and consumption of NADH (19,114). In this instance, the oxidation carboxylation of KG by ICDH leads to the synthesis of isocitrate and the utilization of NADH. The tricarboxylic acid subsequently supplies NADPH, a process mediated by the enzyme ICDH-$NADP^+$ dependent. This strategy of antioxidative defense is complemented with the increased production of KG, an antioxidant. Keto-acids are excellent neutralizers of reactive oxygen and nitrogen species (RONS) (12,30). While KG produces succinate upon detoxification of RONS, pyruvate is decomposed to acetate following decarboxylation triggered by oxidative stress. Glyoxylate decomposes RONS to release formate (14,122). These keto-acids are widely utilized as antioxidants in vivo and in vitro in medications and nutrient supplements (122-124).

The TCA cycle intermediate KG is a molecule with known antioxidative properties that have been studied from bacteria to humans (2,30,107-109, 125). However, the metabolic routes to KG in an environment where sulfur is limiting has not been well-characterized. The involvement of KG in mitigating the oxidative stress evoked by sulfur starvation is apparent from the fact that a significant amount of succinate is found in the spent media of the cultures grown in the absence of added sulfur (Figure 4.1B). The metabolite KG can readily detoxify ROS with the generation of succinate, a moiety that is also known to act as a signaling metabolite (126). In fact, aluminum toxicity resulting from the disruption of Fe-S cluster triggers modulation of the TCA cycle and enhanced synthesis of KG and succinate, an observation that has also been reported during oxidative stress and sulfur starvation (12,17,127-129). Not only key enzymes of the TCA cycle are affected but the electron transport chain is also severely perturbed as revealed by the marked inhibition of complexes I and IV (Figure 4.1). This metabolic shift promotes the utilization of KG in ROS detoxification and reduction in ROS formation because of diminished oxidative phosphorylation. Thus, sulfur starvation, metal toxicity and elevated amounts of H_2O_2, all known to increase oxidative tension elicit the reconfiguration of cellular metabolism (14,114,117,129). The utilization of glutamine, as the only source of carbon and nitrogen in the present study, permits the further exploration of the homeostasis of the antioxidant KG, as this amino acid has to transit via the keto-acid to be further processed in any organism (12,14).

Metabolite profiling of *P. fluorescens* under sulfur-limited conditions showed a higher amount of GABA, SSA and KG compared to the controls (Figure 4.2). This metabolite fingerprint points to a prominent role of GABA shunt in the sulfur-deficient cells. This metabolic network is known to be responsible for various brain functions in higher organisms while in prokaryotes it acts a compatible solute and helps regulates pH (15,130,131). The enzymes GABA transaminase (GABAT) and glutamate decarboxylase (GDC) are key contributors to this metabolic module and showed increased activity in sulfur-stressed cells (Figure 4.3C–F). Although this pathway does not directly result in KG production, it generates SSA, a moiety that can be converted to KG with the assistance of KGDC. The activity and expression of this enzyme was markedly elevated. In fact, a 15-fold increase in the transcript was observed (Figures 4.3G and 4.4). The increased activity and expression of isocitrate lyase (ICL) and fumarate reductase (FRD) may help supplement the pool of succinate, a metabolite that reacts with NADH to generate SSA with the aid of SSADH, an enzyme that was upregulated more than 2-fold. The significance of the enzyme in the enhanced production of KG in glycerol medium supplemented by micromolar amounts of manganese (Mn) was recently demonstrated (2). In the present study where sulfur starvation resulting in oxidative stress compels the microbe to augment its KG production. The latter is then utilized in the elimination of ROS leading to the formation of succinate. Succinate is then channeled towards KG synthesis, a process further promoted by the downregulation of SDH, an enzyme reliant on sulfur and the electron transport chain. Increased production of KG orchestrated by glutamate dehydrogenase and ICDH-$NADP^+$ has also been shown in *P. fluorescens* in a glutamine culture exposed to H_2O_2 (15). Succinate generated by ICL, FRD and following the ROS-mediated decomposition of KG is routed by SSADH to SSA. The latter is further supplemented by the transamination of GABA and is subsequently transformed into the antioxidant KG. This metabolic reprogramming provides an elegant and potent antioxidative strategy to quell the oxidative environment triggered by sulfur starvation in *P. fluorescens*. The pool of succinate is replenished by isocitrate lyase and fumarate reductase that are known to participate in disparate stress responses in numerous microbial systems (87,126). The scheme shown in Figure 4.5 illustrates the metabolic reprogramming occurring in *P. fluorescens* to transform succinate into KG, an antioxidant aimed at the oxidative tension evoked by sulfur starvation.

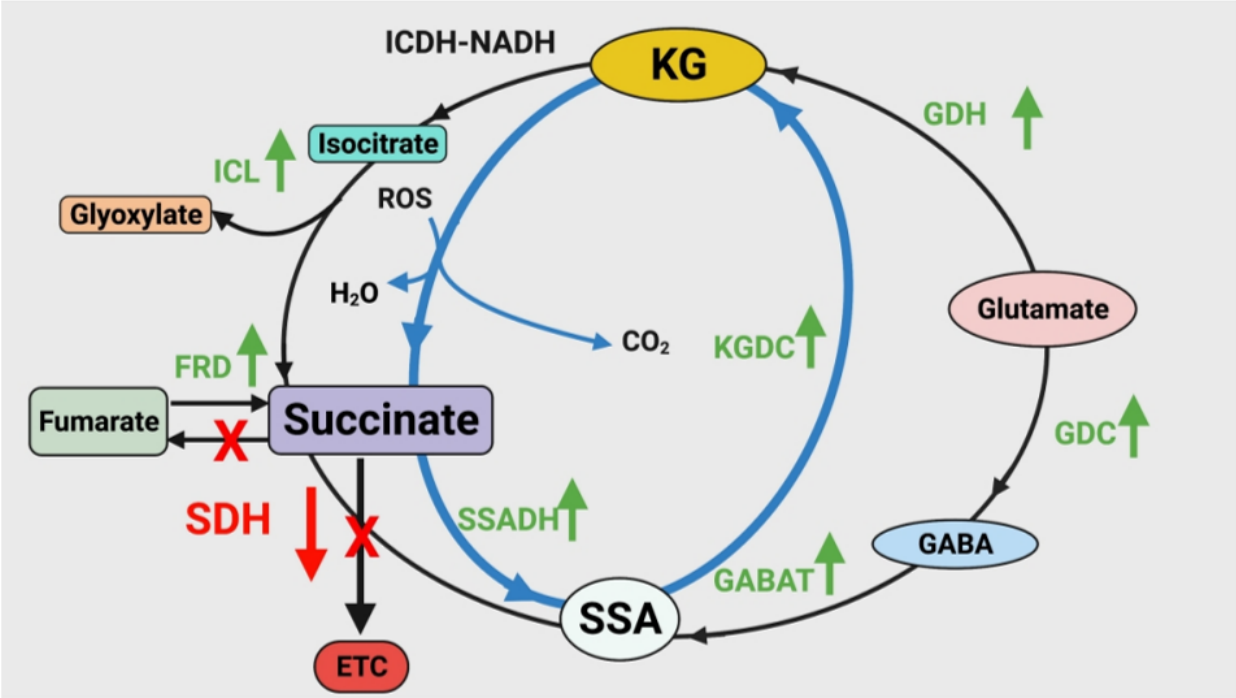

Figure 4.5. Schematic representation of the metabolic pathway used by *P. fluorescens* to combat sulfur starvation. KG, resulting of glutamine metabolism, acts as an ROS scavenging molecule and detoxifies ROS, leading to succinate production with CO_2 and H_2O as by-products. Succinate is not used in the electron transport chain (ETC). Succinate is regenerated into KG by SSADH and KGDC, creating an efficient mechanism for KG enrichment. The enzymes ICL and FRD contribute to increasing the pool of succinate available, whereas SDH is shut down. Degradation of glutamate into GABA is also a way to produce SSA via GABAT. ICL = isocitrate lyase, FRD = fumarate reductase, SSADH = succinate semialdehyde dehydrogenase, SDH = succinate dehydrogenase, KGDC = α-ketoglutarate decarboxylase, GABAT = GABA transaminase, GDC = glutamate decarboxylase, GDH = glutamate dehydrogenase.

CONCLUSION

In conclusion, *P. fluorescens* invokes a major metabolic reprogramming to combat the sulfur starvation-induced oxidative stress. KG is the potent antioxidant utilized to detoxify ROS in a medium where glutamine is the sole source of carbon and nitrogen. The pooling and channelling of succinate to SSA provides an efficient route to KG that can be regenerated. The malleability of metabolic pathways and ability of organisms to utilize different enzymatic systems usually

dedicated to diverse physiological functions represent a unique strategy to fend off abiotic insults. In this instance, the glyoxylate and GABA shunts coupled with components of the TCA cycle enable *P. fluorescens* to neutralize the toxicity associated with a sulfur-limited environment. The fluxes in the concentrations isocitrate, succinate, GABA, succinate semialdehyde and fumarate are the main effectors fuelling the formation of KG, a metabolite in high demand under sulfur starvation. This further confirms phenotypic changes mediated by metabolites are central to physiological adaptation most organisms have to resort.

Acknowledgements

This research project has been supported and funded by the Northern Ontario Heritage Fund. Félix Legendre is supported by the Queen Elizabeth II Graduate Scholarship in Science and Technology (QEII-GSST), the Ontario Graduate Scholarship program (OGS) and is a recipient of an Alexander Graham-Bell Canada Graduate Scholarship — Doctoral (CGS D) from the Natural Sciences and Engineering Research Council of Canada (NSERC). Dr. Sujeenthar Tharmalingam is supported by research funds from Bruce Power and the Northern Ontario School of Medicine.

Conflict of interest statement

No conflicts of interest declared by authors.

5 The metabolic network aimed at energy production in *P. fluorescens* subjected to phosphate starvation

In chapter 3 and 4, metabolic pathways describing the stress response to a low sulfur environment using glutamine as the only source of carbon were characterized. The current chapter focuses on stress response to phosphate starvation. Phosphate groups are integral parts of many molecules such as ATP, the main energy fuel used by all living organisms, and macromolecules such as proteins and lipids. Since phosphate is one of the building blocks for ATP and that many microbial systems that colonize the environment can grow using low amounts of phosphate, studying the metabolic mechanism used by microbes to produce energy in those conditions is of great interest.

This chapter presents a mechanism aimed at energy production in which the KG produced from glutamine metabolism will be converted into isocitrate by ICL, and will undergo the glyoxylate shunt, producing glyoxylate and succinate as products. Glyoxylate can then be converted to malate by malate synthase (MS) and progress towards oxaloacetate, whereas succinate seems to be shuttled towards succinate semialdehyde in a mechanism very familiar to the previous chapter. Both those branches of the metabolism can lead to ATP generation by substrate level phosphorylation. Oxaloacetate can be transformed into PEP by phosphoenolpyruvate carboxylase (PEPC), and into pyruvate and ATP by phosphoenolpyruvate synthase (PEPS) and pyruvate phosphate dikinase (PPDK). Succinate can be transformed into KG by SSADH and KGDH, and then made into succinyl-CoA. Using succinate-CoA ligase, ATP can be generated.

The manuscript covering this study is currently under review for publication.

Phosphate starvation triggers an ATP producing-metabolic network mediated by the reprogramming of the glycolytic and tricarboxylic acid cycles in *Pseudomonas fluorescens*

Félix Legendre, Alex MacLean, Sujeenthar Tharmalingam and Vasu D. Appanna*

Department of Chemistry and Biochemistry

Laurentian University

Sudbury, Ontario

Canada

P3E 2C6

* Corresponding Author

ABSTRACT

Phosphate (Pi) is essential for life as it is an integral part of the universal chemical energy adenosine triphosphate (ATP), and macromolecules such as, DNA, RNA proteins and lipids. Pi is often a limiting nutrient for bacterial and plant growth in natural environments. Despite the core roles of this nutrient in living cells, some bacteria can grow in environments that are poor in Pi. The metabolic mechanisms that enable bacteria to proliferate in a low phosphate ecosystem are not fully understood. In this study, the soil microbe *Pseudomonas (P.) fluorescens* was cultured in a control and a low Pi (stress) medium with glutamine as the only source of carbon and nitrogen in order to delineate how energy homeostasis is maintained. Although there was no significant variation in biomass yield in these cultures, metabolites like isocitrate, oxaloacetate, pyruvate and phosphoenolpyruvate (PEP) were markedly increased in phosphate-starved condition. Components of the glycolytic and tricarboxylic acid cycles operated in tandem to generate ATP by substrate level phosphorylation (SLP). The α-ketoglutarate (KG) produced glutamine was transformed into phosphoenol pyruvate (PEP) and succinyl CoA (SC), two high energy moieties. The metabolic reprogramming orchestrated by isocitrate lyase (ICL),

phosphoenolpyruvate carboxylase (PEPC), phosphoenolpyruvate synthase (PEPS), pyruvate phosphate dikinase (PPDK), α-ketoglutarate dehydrogenase (KGDH) and succinyl CoA synthetase resulted in ATP synthesis. Cell free extract experiments confirmed ATP synthesis in the presence of PEP, oxaloacetate and isocitrate. Gene expression profiling revealed high transcript levels associated with enzymes like ICL, PEPS, pyruvate carboxylase (PC), malate synthase (MS), pyruvate kinase (PK), and succinyl CoA synthetase (SCS). The latter two enzymes are known to generate ATP directly from PEP and SC respectively. This metabolic adaptation enables *P. fluorescens* survive Pi stress, a characteristic that may contribute to biological activity in phosphate-deficient ecosystems.

INTRODUCTION

Metabolism is the foundation of life and Pi is central to metabolic activity as it participates in a wide range of biological processes. A major part of metabolism results in energy production. The main source of energy in living cells is ATP, a moiety liberated from the breakdown of nutrients and contains three phosphoryl groups. The phosphoanhydride bonds are very energy rich and possess a free energy (ΔG) of about -30.5 KJ/mol (132). Thus, phosphate groups play a central role in storing and transporting energy in living organisms and they are also constituents in nucleotides that form (DNA, RNA) and in numerous other macromolecules, such as phospholipids that are an integral part of the cell membrane in all organisms (133). Additionally, Pi is required for a wide variety of metabolic and cell regulation actions such as amino acid metabolism, carbohydrate metabolism and post-translational modifications of proteins by phosphorylation (135). Hence, it is not surprising that most organisms succumb in a phosphate deficient ecosystem, conditions prevalent in alkaline and metal-polluted environments (79,135). The Pi is not readily bioavailable due to its insolubility, a situation detrimental to the survival of bacteria and plants. However, some microorganisms are able to grow and thrive under very limited concentrations of Pi (136-139).

Bacteria have developed disparate strategies to cope with a dearth of Pi including the expression of phosphate starvation-inducible genes, often referred as psi genes. These genes encode for proteins involved in Pi sensing, metabolism, transport and uptake (80). The Pho regulon is the main regulatory machinery used by microbes to counter Pi limitations (81). For instance, the

expression of phosphatases is increased in order to cleave phosphate groups from polyphosphate reserves of the cell and sometimes from macromolecules such as phospholipids (140,141). In fact, phospholipids are replaced by aminolipids as the major constituent of cell membrane in Pi-deprived conditions. Nearly 10% of the genes devoted to respond to phosphate starvation in Escherichia coli has been reported (142). Although the importance of the Pho regulon in response to Pi starvation has been studied extensively, the metabolic adaptations that lead to ATP production in microorganisms able to survive in an environment that lack Pi are not fully understood. The plasticity of metabolic processes renders them malleable and susceptible to manipulation under stress conditions.

P. fluorescens is a gram-negative rod-shaped bacterium that is found abundantly in soil and sea water. In oceanic environments, the concentrations of Pi can sometimes be in the nanomolar range (78). *P. fluorescens* is a very nutrient versatile microbe and has been a successful model to study metal stress, such as zinc, aluminum and gallium toxicity (17,18,117). The mechanisms by which these contaminants are countered involved production of metabolites to immobilize the metal toxicants and the maintenance of ATP homeostasis. Zinc can react with free sulfhydryl groups of proteins, which are essential for enzymatic function and maintaining oxidative balance, thus creating an oxidative environment that the cell has to deal with (144). Aluminum can substitute for iron in biochemical processes, which leads to disruption of Fe-S clusters that are required for enzymatic activity mediating energy metabolism (17,127,128). Oxalate production leads to aluminum sequestration in *P. fluorescens* (17). Gallium is also an iron mimetic, its toxicity is countered by aspartate production (18,144).

In this study, *P. fluorescens* is subjected to a Pi-limited environment in order to elucidate the metabolic networks responsible to maintain ATP homeostasis. The metabolite profile, enzymatic activity and gene expression were monitored in in a mineral medium with glutamine as the sole source of carbon. Here, we report involvement of a metabolic adaptation orchestrated by SLP responsible for ATP homeostasis. Modified glycolytic and TCA cycles channel the high-energy metabolites PEP and succinyl COA into the production of ATP. The participation of phosphoenol pyruvate carboxylase (PEPC), phosphoenol pyruvate synthase (PEPS), pyruvate phosphate dikinase (PPDK), pyruvate kinase (PK) and succinylCoA synthetase in this process is elaborated and the pivotal role metabolism plays in countering Pi-stress is discussed The

significance of these findings in mitigating the impact of Pi-deficiency in metal-polluted and alkaline ecosystems is commented on.

MATERIAL AND METHODS

Culture media and bacterial culture growth

Pseudomonas fluorescens (strain 13525) was obtained from the American Type Culture Collection (ATCC). It was grown in a defined mineral medium that had glutamine at a concentration on 19 mM, as the only source of carbon and nitrogen. The control medium contained 42 mM Na_2HPO_4 as well as 22 mM KH_2PO_4 as phosphate sources and 0.8 mM of MgSO4·7H2O. In the low phosphate medium, the components used were the same, except the concentration of Na2HPO4 was 16 μM and the quantity of KH_2PO_4 was 8.5 μM. (total Pi concentration was ~2600 fold less). Trace metals were added as previously described (95). Both culture media were autoclaved for 20 minutes at 121°C. The cultures were grown on a Gyrotory® Water Bath Shaker Model G76 (New Brunswick Scientific) at ambient temperature. The volume of the culture was 200 mL, with 1 mL of preculture utilized, as previously described in (145). The growth curve was determined by measuring the amount of soluble proteins present at different times of growth. The Bradford method was used (96). A volume of 10 mL of culture was centrifuged at 12,000 × g for 20 minutes. The pellet was resuspended in 1 mL of 0.5M NaOH and analysed for proteins in triplicate.

Bacteria sample processing

Once the cultures reached stationary phase, they were harvested and the pellets were washed with approximately 100 mL of 0.85% m/v sodium chloride, after which a second centrifugation using the same settings was done. The pellet (whole cells) was resuspended in 1 mL of Cell Storage Buffer (CSB) (50 mM Tris-HCl, 1mM phenylmethylsulfonyl fluoride, 1mM dithiothreitol at pH 7.6) and broken down using an ultrasonic processor (Johns Scientific). Centrifugation at 110,000 × g for 3 hours at 4°C permitted the separation of the soluble cell free extract (sCFE) and membrane fraction (mCFE). The mCFE was resuspended in 1 mL of CSB. Fractions were stored at 4°C and downstream experiments were performed within a maximum of 7 days.

Metabolite analysis by HPLC

HPLC analysis was performed on a Waters 2695 Separation Module HPLC system with a Synergi 4 μm Hydro-RP 80A column with dimension of 250 × 4.6 mm (Phenomenex). The flow rate utilized was 0.2 mL/min for the metabolic profiling. The mobile phase consisted of 5% acetonitrile, 20 mM KH_2PO_4 diluted in Milli-Q water at a pH 2.9 at ambient temperature. Detection of metabolites was done using a Waters 2478 Dual λ absorbance detector, set at wavelengths of 210nm to identify molecules with carbonyl groups. Metabolite amounts were determined from the area under the curve of the corresponding peaks using the Empower software and identified by matching their elution time to standard solutions. The peaks were confirmed by spiking the samples with the appropriate standards (2).

Detection of enzymatic activity by Blue Native Polyacrylamide Gel Electrophoresis (BN-PAGE)

A 4%-16% acrylamide linear gradient native gel was prepared (50 mM ϵ-aminocaproic acid, 15 mM Bis–Tris at pH 7.0). The gel was cast using the MiniProteanTM2 gel system from Bio-Rad Laboratories and spacers of 1.0 mm. An amount of 60 μg of proteins from either the control or stress sample was loaded into each well. Membrane protein samples were prepared with 1% (m/V) η-dodecyl β-D-maltoside to help proteins solubilize. Gel chamber was filled with anode buffer (50 mM Bis–Tris at pH 7.0), and the space between gels was filled with blue cathode buffer (50 mM Tricine, 15 mM Bis–Tris, 0.2 g/L Coomassie Blue G250 at pH 7.0). Electrophoresis was carried out as described in (97,119,120). Enzymatic activity was detected using the formazan precipitation method, where gel slices are incubated in a reaction buffer containing 25 mM Tris-HCl and 5mM MgCl2 at pH 7.4 with appropriate substrates and colorimetric redox markers. Iodonitrotetrazolium (INT) in reduced form the formazan precipitate and produces a red band on the gel indicative of positive enzymatic activity. Phenazine methosulfate (PMS) and dichlorophenolindophenol (DCPIP) are used as electron transfer intermediates to allow the reduction of INT. The concentration of INT and DCPIP/PMS is 0.4 mg/mL for all reactions.

Isocitrate dehydrogenase was probed using 5 mM isocitrate and 0.5 mM NAD^+ (forward reaction) or 5 mM KG, 5mM HCO_3^- and 0.5mM NADH (reverse reaction). Enzymatic activity of isocitrate lyase was detected by using 5 mM isocitrate, 0.5 mM NAD^+ and 5 units of lactate

dehydrogenase. Complex I activity was assessed on the membrane fraction using 0.5 mM NADH, without PMS. The enzymes PEPS, PPDK and PEPC were detected as previously described (120). ICDH was confirmed by excising the band and incubating it in 2 mM isocitrate and 0.2 mM NAD^+ (forward) or 2 mM KG, 2 mM HCO_3^- and 0.2 mM NADH (reverse) for 24 hours, after which the reaction mixture was subjected to an HPLC run to detect the products. Densitometric readings were performed using ImageJ as previously described (3).

Cell free extract experiments and nucleotide detection

Cell free extract experiments were performed using oxaloacetate and PEP. Approximately 200 µg of protein from the control cell free extract and the cell free extract from the low phosphate cultures was incubated separately with 2mM of PEP or oxaloacetate, as well as 0.2 mM of AMP and 0.2 mM of Na_2HPO_4 (Pi). The reaction was incubated at ambient temperature for 24 hours. The sample were then heat inactivated by boiling for 10 minutes and ran through the HPLC column. For this analysis the flow rate utilized was 0.7 mL/min and the detection was done at both 210 nm to detect metabolites and 254 nm to detect nucleotides such as ATP. Quantification was done using the area under the curve as described above.

Gene expression probing by real time polymerase chain reaction (qRT-PCR)

Total RNA from control and low phosphate stressed cells was extracted using TRIzol Reagent and then purified using the DNAse kit (Millipore Sigma). The RNA samples underwent reverse transcription using random primers (Millipore Sigma), oligo dT (VWR) and M-MLV reverse transcriptase (Promega) to obtain complementary DNA. Real-time quantitative polymerase chain reaction was conducted using the software QuantStudio5. Each reaction was done in 15 µL volumes containing 1 × Perfecta qPCR FastMix from Quanta Biosciences, 600 nM forward/reverse primers, and 10 ng of complementary DNA from the reverse transcription. The cycling conditions utilized were: 1) 95°C for 2 min, 2) cDNA denaturation at95°C for 30 s, 3) primer annealing at 57°C for 30 s, 4) template extension at 72°C for 30 s, 5) plate read and data collection, and 6) steps 2–5 repeated for 40 cycles. To confirm specificity of products obtained, a DNA melt curve analysis was performed at the end of each qPCR experiment. Forward and reverse primer pair sequences for genes of interest were designed using Primer-BLAST, using NCBI gene databases. All primer pairs underwent validation tests by plotting Ct values against

cDNA serial dilutions. Primers with amplification efficiency between 90 and 110% [efficiency = 10(−1/slope) − 1], and R2 value greater than 0.99 were acceptable for further analysis. All samples were normalized to two independent control housekeeping genes (rpoA and cpn60). The relative mRNA transcript level of each gene was reported according to the ΔΔCT method as mRNA fold increase (103). The list of primers used can be found in Table 5.1.

Statistical analysis

All experiments were done in triplicates with three or four biological replicates. Statistical analysis was performed using Student's T Test (paired; two-tail) on Microsoft Excel, from Microsoft Office 365.

RESULTS AND DISCUSSION

Growth and metabolic profiles of *P. fluorescens* in low phosphate conditions

6 When grown using a low phosphate mineral medium with glutamine as the sole source of carbon and nitrogen, a fairly similar growth pattern is observed in the low phosphate cultures (24.5 uM) in comparison to the control condition (64 mM). Both cultures consistently reach the stationary phase of growth after 24 hours of growth with comparable biomass, albeit slightly lower in the Pi-stress medium. The low phosphate cultures had a characteristic green coloration compared a whitish hue in the control (figure 5.1A). This points to the ability of this microbe to produce sufficient energy despite scant Pi in the stressed conditions. In order to further explore this, the metabolite profile of both cultures was obtained using a C-18 reverse-phase HPLC approach, which allows for detection of organic acids. Metabolites of the indicative of glycolytic, TCA and glyoxylate cycles were monitored. The HPLC analysis revealed that *P. fluorescens* cells had an increased amount of pyruvate, isocitrate, phosphoenolpyruvate (PEP) and oxaloacetate in comparison to control cells (figure 5.1B-D). There are not many possibilities in the initial steps of glutamine metabolism. Glutamine is converted

to glutamate and then to KG by glutamate dehydrogenase to enter the energy-generating machinery (114) As glutamine is the only source of carbon, the presence of isocitrate in the cell free extracts of the cells grown in low phosphate indicates that KG is possibly converted into isocitrate. It has been shown that under certain stressed conditions, the isocitrate dehydrogenase enzyme favors the reverse reaction to produce isocitrate from KG, NADH and HCO_3^- (114). This strategy can help the cell to manage its NADH pool, as it is a pro-oxidant molecule. The presence of pyruvate, PEP and oxaloacetate indicates a possible progression the TCA cycle albeit in a modified manner, as those are key metabolites of the energy metabolism. Isocitrate can readily enter the glyoxylate shunt, a situation prevalent under environmental challenge (2,146). Isocitrate can undergo a transformation into glyoxylate and succinate by the enzyme isocitrate lyase. The metabolites may then progress into the TCA cycle to generate oxaloacetate, PEP and pyruvate in order to make energy as the levels of ATP were relatively similar in these conditions.

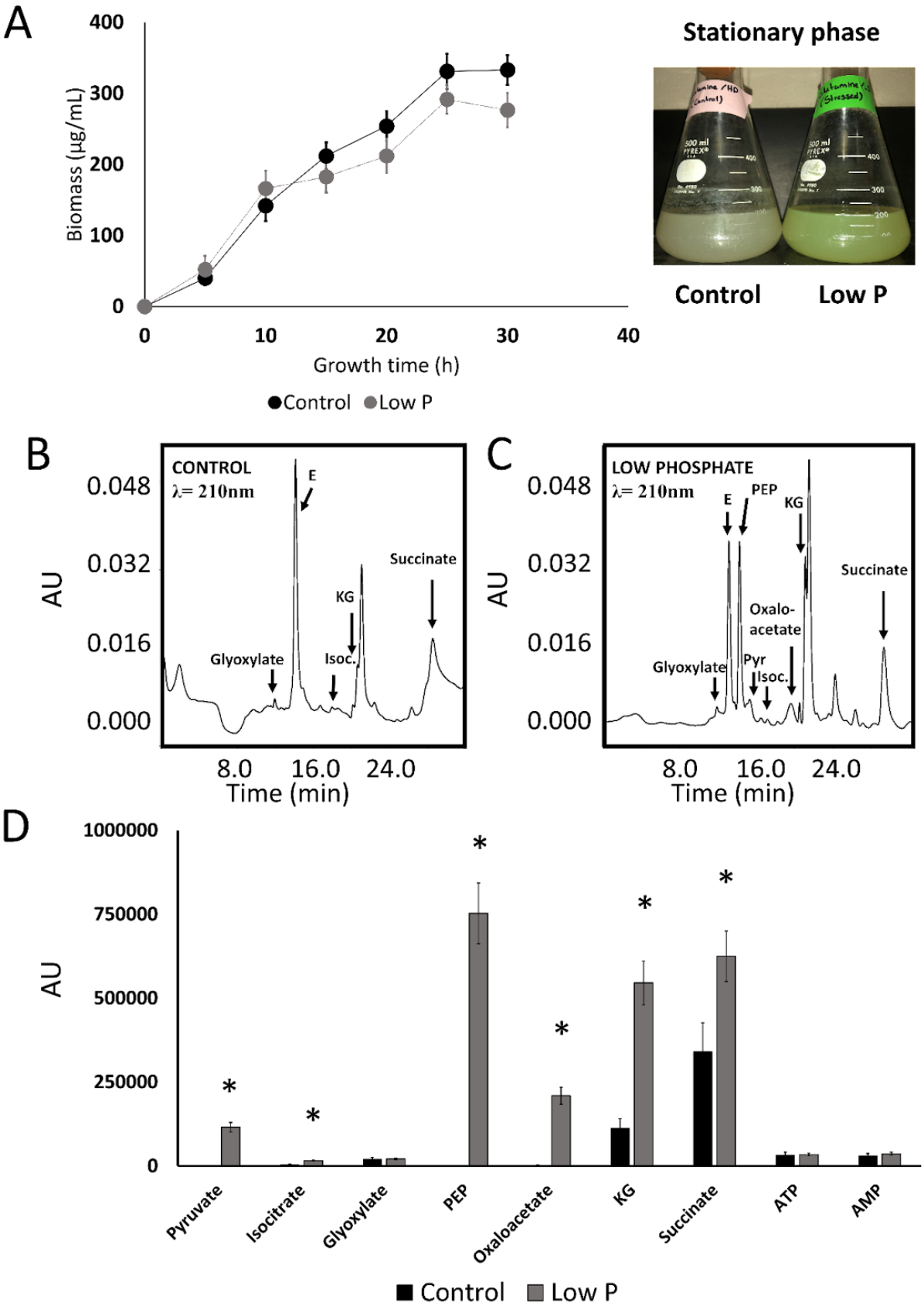
A
Biomass (µg/mL)
400
300
200
100
0
0
10
20
30
40
Growth time (h)
Control
Low P
Stationary phase
Control
Low P
B
CONTROL
λ= 210nm
E
Succinate
KG
Glyoxylate
Isoc.
AU
0.048
0.032
0.016
0.000
8.0
16.0
24.0
Time (min)
C
LOW PHOSPHATE
λ= 210nm
E
PEP
KG
Succinate
Oxalo-
acetate
Glyoxylate
Pyr
Isoc.
AU
0.048
0.032
0.016
0.000
8.0
16.0
24.0
Time (min)
D
AU
1000000
750000
500000
250000
0
Pyruvate
Isocitrate
Glyoxylate
PEP
Oxaloacetate
KG
Succinate
ATP
AMP
Control
Low P

Figure 5.1. Growth and metabolite profiles in *P. fluorescens* subjected to Pi stress. A. Growth profile of *P. fluorescens* cultures. Biomass is determined by measuring the concentration of soluble proteins. At stationary phase, the Pi-starved culture exhibits a green color compared to the control's white color. B-C. HPLC chromatogram of a cell free extract from *P. fluorescens* grown in control (B) and low phosphate (C) conditions. The detection was performed with a UV lamp set at 210 nm. Peaks corresponding glyoxylate, glutamate, pyruvate, PEP, isocitrate, succinate, oxaloacetate and KG are shown. X axis shows retention time in minutes and y axis shows absorbance at 210 nm in arbitrary units (AU). D. Quantifications of HPLC peaks from panels B-C. n = 3, *= $p<0.05$.

Enzymatic activity analysis of *P. fluorescens* cells under phosphate starvation

To map out the metabolic pathways utilized by *P. fluorescens* in an environment with low phosphate, a targeted proteomic approach using blue native polyacrylamide gel electrophoresis strategy was utilized. As the metabolite analysis suggested, the NAD^+ dependent isocitrate dehydrogenase that converts isocitrate into KG was shut down in the low phosphate conditions. The reverse reaction however was increased in the stressed conditions (figure 5.2A). To probe the activity of ICDH, the band obtained by the formazan precipitation method was excised and incubated with the substrates of ICDH forward and reverse and ran through the HPLC column to detect the products of the reaction. The forward reaction produced KG in control cells and the reverse reaction showed isocitrate in the stressed cells, which further confirmed these enzymes (figure 5.2B). Next, enzymes that transform or produce isocitrate, pyruvate, PEP and oxaloacetate were assessed in order to establish if a pathway to ATP independent of oxidative phosphorylation (OXPHOS) may be operative. The enzyme isocitrate lyase is more active under low phosphate conditions, as well as phosphoenolpyruvate carboxylase (PEPC), pyruvate phosphate dikinase (PPDK) and phosphoenolpyruvate synthase (PEPS) (figure 5.2C). Complex I, the first complex of the electron transport chain that takes electrons from NADH as the first step of oxidative phosphorylation, is markedly diminished (figure 5.2C). The gel results were analyzed by densitometric reading, which allows to approximate quantification of enzymatic activity visible in the gels (figure 5.2D). These results suggest that energy is not predominantly generated via oxidative phosphorylation but by an alternative mechanism such as substrate level phosphorylation. Isocitrate generated from KG is channeled towards succinate and glyoxylate

production as shown by the increased ICL activity. This bypasses a part of the TCA cycle. Succinate and glyoxylate can progress towards oxaloacetate, PEP and pyruvate. The enzyme PEPC is the key enzyme to produce phosphoenolpyruvate in this system. Following production of PEP, the enzymes PEPS and PPDK can lead to ATP production by converting PEP to pyruvate. PEPS can concert PEP, AMP and Pi to pyruvate and ATP, whereas PPDK converts PEP, AMP and pyrophosphate into pyruvate, ATP and Pi. This could be a strategy used by *P. fluorescens* under Pi starvation to generate ATP. The perturbation of OXPHOS triggered by a variety of abiotic stresses has been shown to favour the reconfiguration of metabolic networks such the glycolytic and TCA cycles (17,114).

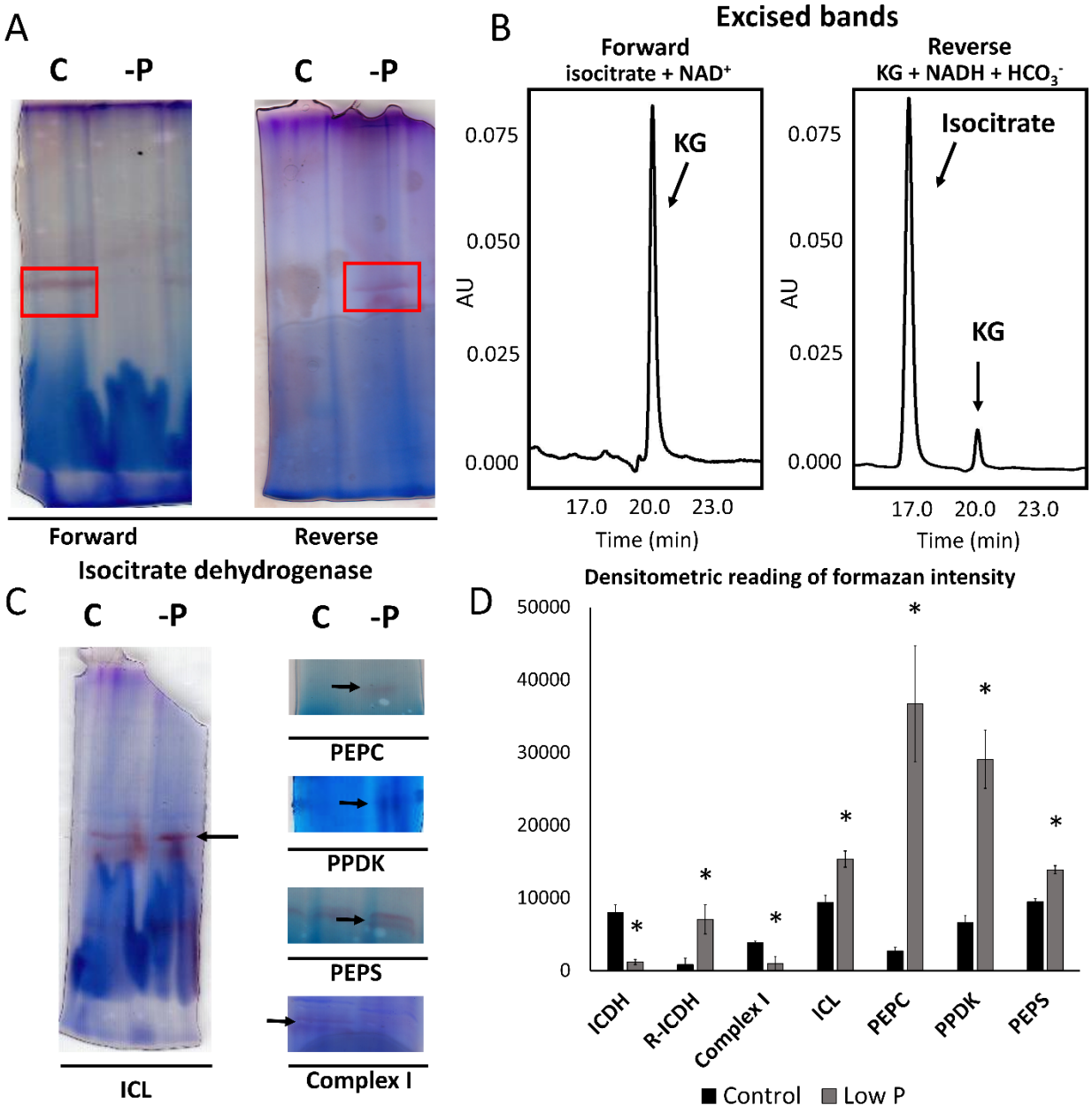

Figure 5.2. Analysis of enzyme activities in control and Pi-stressed *P. fluorescens*. A. Detection of isocitrate dehydrogenase activity by BN-PAGE. The conversion of isocitrate into KG is inhibited under low phosphate conditions (forward reaction), whereas the conversion of KG and HCO_3^- into isocitrate is favored (reverse reaction). B. HPLC chromatograms of reaction mixtures containing the reactants of isocitrate dehydrogenase forward and reverse reactions incubated with the excised band from the BN-PAGE gel. Reactions were allowed to proceed for 24 hours. Peaks corresponding to isocitrate and KG are shown and confirm the nature of the

enzyme detected on the BN-PAGE gel. C. Detection of isocitrate lyase (ICL), PEPC, PPDK, PEPS and Complex I was performed. The enzymes ICL, PEPC, PPDK, PEPS were upregulated under a lack of Pi whereas Complex I was inhibited. D. Densitometric reading of formazan intensity. Results are representative of three distinct experiments. n = 3, *= $p<0.05$. C= Control; -P= Pi stress.

Oxaloacetate, PEP and isocitrate degradation lead to ATP production in *P. fluorescens* under phosphate stress

The metabolic analysis and enzymatic activity analysis suggest a mechanism where glutamine is converted into KG, which is in turn transform into isocitrate by reverse-ICDH. Isocitrate is then cleaved into succinate and glyoxylate by ICL and the metabolites progress through the rest of the TCA cycle until oxaloacetate, which is converted into PEP, which can serve as a substrate for ATP production by PPDK and PEPS in a modified version of the glycolytic cycle. To investigate whether ATP is produced by *P. fluorescens* grown in a low phosphate medium via such a mechanism, cell free extract experiments were performed in order to see if degradation of PEP, and oxaloacetate can lead to ATP production. Cell free extract experiments in which control cells and cells grown in low Pi conditions were incubated with oxaloacetate or PEP, AMP and Pi in a reaction buffer solution were performed and resulting metabolites were detected by HPLC analysis where nucleotides were detected at 254 nm (figure 5.3A-B). In comparison to control conditions, the low Pi cell free extracts fed with oxaloacetate showed an increased production in ATP and ADP (figure 5.3C). Detection of nucleotides at 254nm for the cell free extracts exposed to PEP showed an increase in ATP and AMP (figure 5.3C). Those results are in agreement with the enzymatic analysis that showed PEPS being more active in low Pi conditions and provide an elegant demonstration that ATP is produced from PEP degradation. Isocitrate a metabolite that is distant precursor of PEP was also incubated with AMP and Pi. The HPLC analysis performed at 254 nm (figure 5.3E-F) showed increased production of ATP in the stressed cell-free extracts (figure 5.3G). Analysis of metabolites resulting from isocitrate breakdown resulted in the enrichment of oxaloacetate and glyoxylate (figure 5.3H). Hence, the evidence points to SLP as an important contributor to ATP homeostasis under Pi starvation.

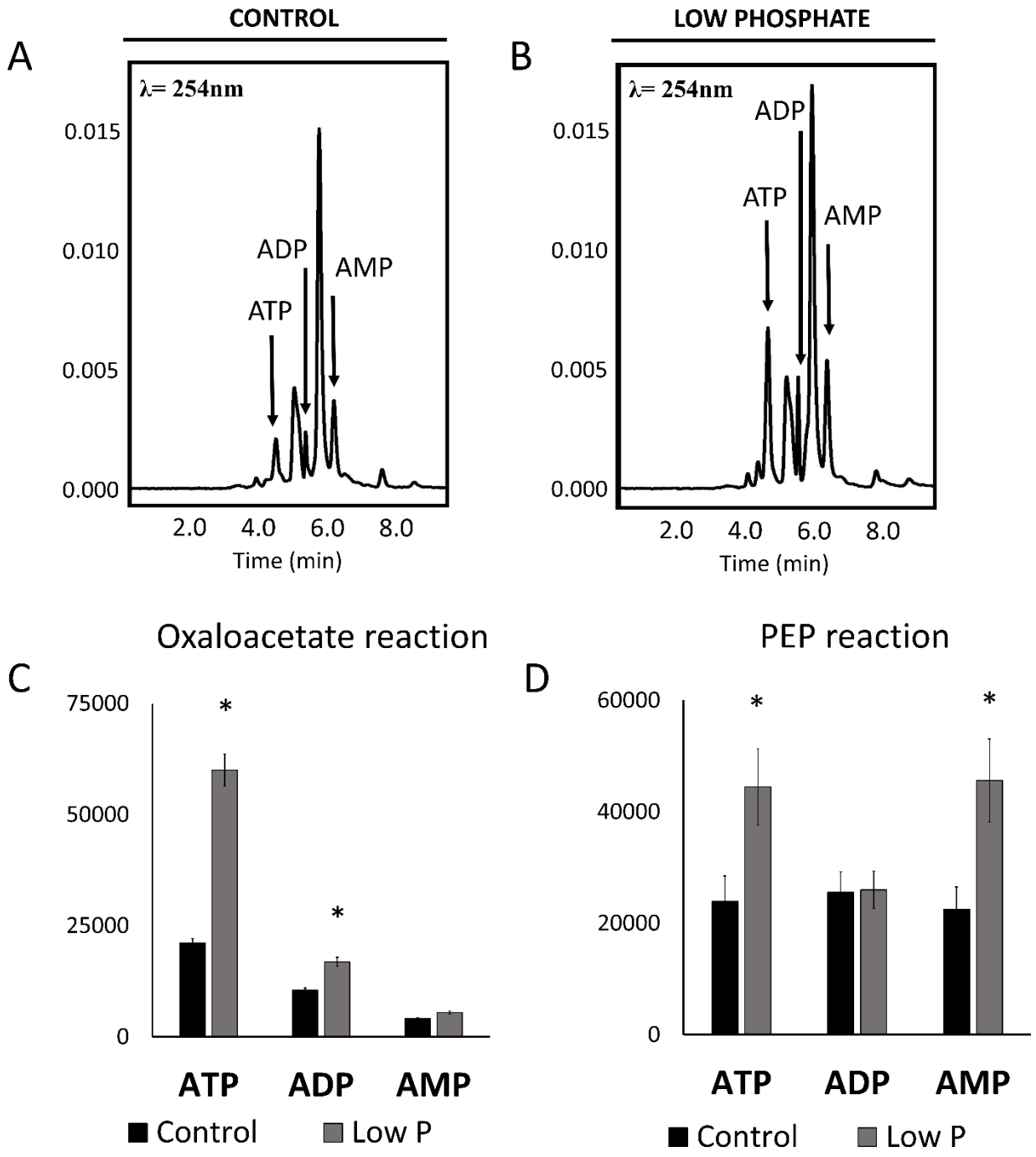

Figure 5.3A-D. Oxaloacetate, PEP, and isocitrate metabolism lead to ATP production in low Pi conditions. A. HPLC chromatogram of *P. fluorescens* cell free extracts incubated with 2 mM oxaloacetate, 0.2 mM AMP and 0.2 mM PPi. Reactions were allowed to take place for 24 hours before they were analyzed by HPLC. Detection was performed at 254 nm for both control conditions as well as low Pi conditions. Peaks corresponding to ATP, ADP and AMP are shown.

B. Quantification of nucleotides resulting from oxaloacetate degradation. Quantification was performed using the area under the curve of the corresponding HPLC peaks over three distinct experiments. An increase in ATP and ADP is observed. B. Quantification of nucleotides from a similar experiment, but using PEP as the substrate. An increase in ATP and AMP is observed. n= 3, *= $p<0.05$.

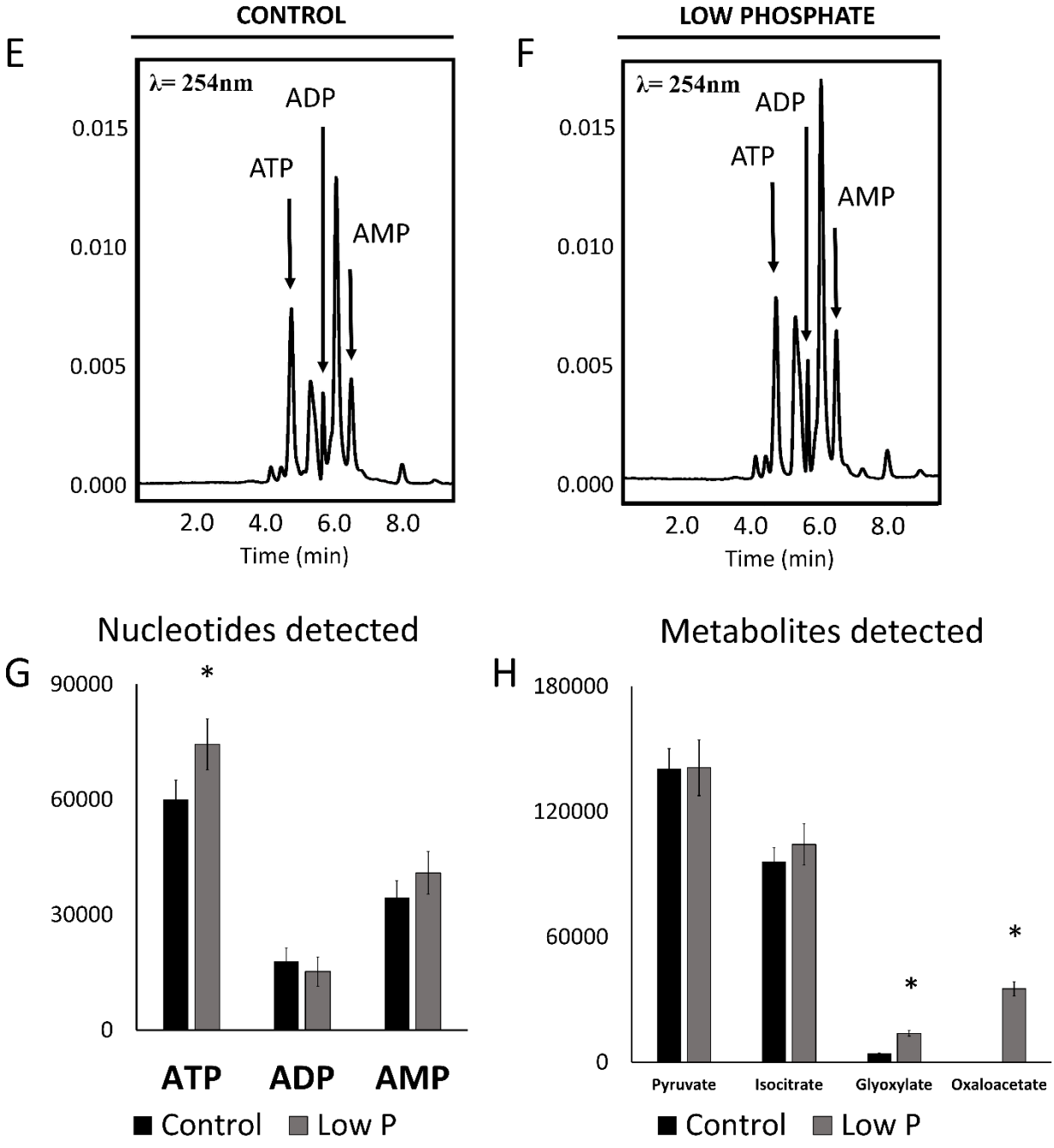

Figure 5.3 E-H Oxaloacetate, PEP, and isocitrate metabolism lead to ATP production in low Pi conditions. HPLC chromatogram of control (E) and low Pi (F) P. fluorescens cell free extracts incubated with 2 mM isocitrate, 0.2 mM AMP and 0.2 mM PPi. Reactions were allowed to take place for 24 hours before they were analyzed by HPLC. Detection was performed at 254 nm for both conditions. Peaks corresponding to ATP, ADP and AMP are shown G. Quantification of nucleotides obtained from isocitrate metabolism. Quantification was performed using the area under the curve of the corresponding peaks of three distinct experiments at 210 nm. Enhanced production of glyoxylate and oxaloacetate is observed in the stressed condition. H. Quantification of nucleotides resulting from isocitrate degradation. HPLC peaks over three experiments at 254 nm were utilized. An increase in ATP is observed. n = 3, *= $p<0.05$.

Gene expression profiling in *P. fluorescens* grown under low phosphate conditions

The targeted proteomics approach showed that a range of enzymes that are more active under phosphate starvation. A gene expression profiling strategy using qRT-PCR was used in order to verify if select genes of interest showed higher gene expression (Figure 5.4). This very specific and robust approach is ideal to confirm the BN-PAGE activity data as well as to probe gene expression of some genes whose proteins are not amenable to the formazan precipitation technique. The phosphate starvation inducible protein (PsiF) was targeted as a control to confirm that the phosphate starvation mechanisms are indeed activated in *P. fluorescens* in the stress medium. This gene was upregulated 10-fold, indicating that phosphate stress being felt by the microbe. Some enzymes identified by BN-PAGE such as ICL, PEPS were found to be upregulated at the transcript level. The enzyme malate synthase (MS) is upregulated over 400-fold. This enzyme acts just downstream of isocitrate lyase in the glyoxylate shunt. This is a clear indication of the metabolic flow going towards malate and oxaloacetate in the low phosphate grown bacteria, as the substrate of this enzyme is glyoxylate, which is produced from isocitrate by ICL. Pyruvate carboxylase (PC) and pyruvate kinase (PK) are also upregulated. This shows that pyruvate is a core metabolite in this system and can provide ready access to oxaloacetate and PEP. The latter can yield ATP upon interaction with PK. Interestingly, some enzymes that can interact with succinate, the other product of ICL, are also significantly upregulated. The enzyme succinate semialdehyde dehydrogenase (SSADH), that converts succinate to succinate semialdehyde is upregulated 15-fold. This indicates that the resulting

succinate from ICL is channelled toward α-ketoglutarate. In fact, α-ketoglutarate decarboxylase, which transforms succinate semialdehyde to KG is upregulated as well with a 3-fold increase (figure 5.4). The enzyme succinyl-CoA synthetase (SCS), which been shown to be implicated in ATP production by substrate level phosphorylation (17) is upregulated and is an important substrate for SLP. Interestingly, ATP generated by this enzyme also generates of succinate, making this an efficient strategy to produce energy in environments where Pi is not readily available. Thus, this targeted metabolomic, proteomic, and transcriptomic analyses provide an intriguing snapshot of the metabolic networks contributing to ATP homeostasis in Pi-stressed *P. fluorescens.*

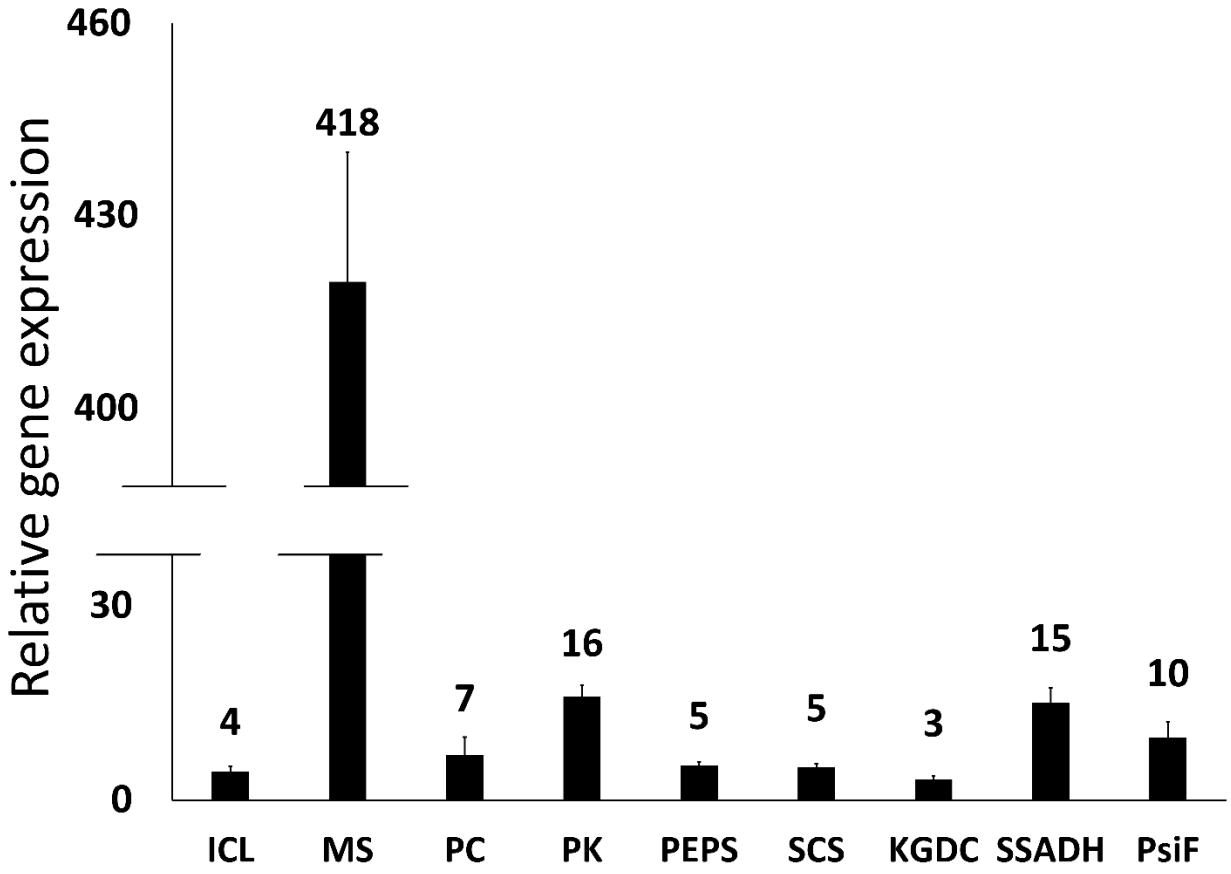

Figure 5.4. Gene expression profiling in P. fluorescens cells subject to Pi starvation. Gene expression probing was done by qRT-PCR. The experiments were performed using the primer pairs from Table 5.1. Relative expression of mRNA transcripts in cells that reached the late exponential phase of growth was determined using the ΔΔCt method. ICL = isocitrate lyase, MS

= malate synthase, PC = pyruvate carboxylase, PK = pyruvate kinase, PEPS = phosphoenol pyruvate synthase, SCS = succinate-CoA synthetase, KGDC = α-ketoglutarate decarboxylase, SSADH = succinate semialdehyde dehydrogenase, PsiF = Phosphate starvation inducible protein. n = 4, $p<0.05$ for all genes tested.

CONCLUSIONS

Taken together, the foregoing data demonstrate the ability of this microbe to survive in a Pi-deficient environment by reconfiguring its metabolism in an effort to produce ATP by SLP. KG generated from glutamine enters a modified TCA cycle is responsible for the synthesis isocitrate. The latter provides the precursors resulting in the generation of PEP and succinyl-CoA, the high-energy metabolites readily transformed into ATP. The cycling of pyruvate, oxaloacetate, succinate and KG orchestrated by the enzymes ICL, MS, PPDK,PEPS, PK, KGDC, SSADH and SCS fuel this ATP-generating network during Pi stress (figure 5.5). Thus, components of the glycolytic, TCA and glyoxylate cycles work in tandem to fulfill the energy need of the Pi-stressed microbe. This adaptive characteristic of *P. fluorescens* to proliferate despite the scarcity of an essential nutrient like Pi makes it an ideal candidate to ameliorate biological activity in alkaline and metal-polluted ecosystems. Emerging bioremediation technologies to treat pollution and biofertilizers dedicated to promote plant growth can serve as effective and environment-friendly strategies to decontaminate polluted areas and re-green nutrient-poor environments (147-149). And this study reveals the metabolic plasticity of *P. fluorescens*, an attribute pivotal in combatting environmental pollution.

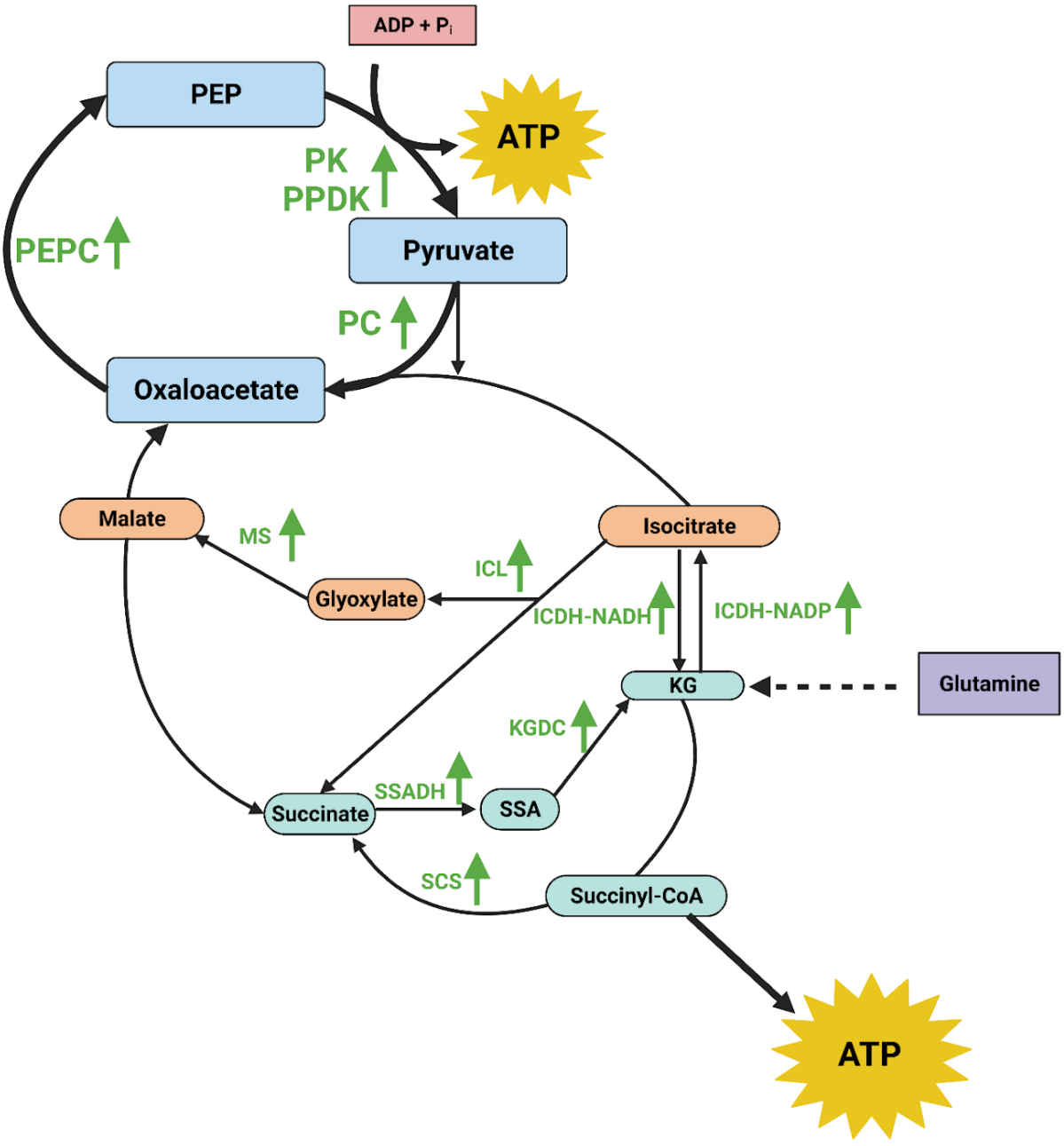
ADP + Pi
PEP
ATP
PK
PPDK
PEPC
Pyruvate
PC
Oxaloacetate
Malate
MS
Isocitrate
ICL
Glyoxylate
ICDH-NADH
ICDH-NADP
KG
Glutamine
KGDC
SSADH
SSA
Succinate
SCS
Succinyl-CoA
ATP

Figure 5.5. Schematic representation of the metabolic adaptation performed by *P. fluorescens* in response to phosphate starvation. Glutamine is converted to KG. KG is transformed into isocitrate by isocitrate dehydrogenase, reverse reaction using NADH (ICDH-NADH). The isocitrate from this reaction is metabolized into succinate and glyoxylate by ICL. The resulting metabolites can progress through the TCA cycle to generate malate and oxaloacetate. Oxaloacetate is converted to PEP by PEPC. The PEP produced can be the fuel for ATP production by the enzymes PEPS and PPDK using a substrate level phosphorylation mechanism. Also, succinate can be transformed into succinyl-CoA by Succinate-CoA synthetase, which can also lead to ATP production by substrate level phosphorylation.

Table 5.1: List of primers used for the qRT-PCR analysis

Gene Name	Symbol	Genome ID (gene location)	Forward Primer [5' to 3']	Reverse Primer [5' to 3']
Phosphate starvation inducible protein	**PsiF**	NZ_LT907842.1 (935251 – 935550)	CGTTGTTGATGATGGGCCTG	TCAGCATTGCAGGTGGTCAT
Malate synthase G	**MS**	NZ_LT907842.1 (6156675 – 6158852)	TGGCCTACAAAGCCTTCCTG	TCGTCATCGACGTTTTGGGT
Pyruvate carboxylase	**PC**	NC_007492.2 (6316963– 6318771)	CCCACGGGTCTTCTTTCAGG	ACAAAGTCGGCTACTGGTCG
Pyruvate kinase II	**PK**	NZ_LT907842.1 (5463846 – 5465297)	CGTCGTACCAAAATCGTCGC	GGAGAAGTTCAGACGGGCAA
Phosphoenolpyruvate synthase	**PEPS**	NZ_LT907842.1 (5086234 – 5088609)	CCTGGAATTCTTCGACGGCT	GTGAGCGATGATCCCCGAAT
Succinate-CoA ligase	**SCS**	NZ_LT907842.1 (2374857 – 2376071)	GGTTCGCAGCAAAGAAGACG	TTGGCCATTGGCATCAGTCT
Succinate semialdehyde dehydrogenase	**SSADH**	NC_007492.2 (225316 – 226758)	GTCGTCAGCTGATGTCGGAA	GTCGAACACGATGAATGGCG
Isocitrate lyase	**ICL**	NZ_LT907842.1 (6193725 – 6195050)	CCCACGGGTCTTCTTTCAGG	ACAAAGTCGGCTACTGGTCG

Housekeeping Gene: Chaperonin 60 (Cpn60)	**N/A**	NZ_LT907842.1 (5505175 – 5506821)	GCGACATGATCGAAATGGGC	GCCAGTCGAGCCTTCTTTCT
Housekeeping Gene: DNA-directed RNA polymerase subunit alpha (rpoA)	**N/A**	NZ_LT907842.1 (6028685 – 6029686)	TCCTGTTGTCCTCAATGCCC	TGCAGCTTGATAGCCAGACC

Authorship statement

Félix Legendre: Experimentation, analysis and writing. Alex MacLean: Experimentation (qPCR experiments) and writing (review and editing). Sujeenthar Tharmalingam: Analysis (qRT-PCR experiments). Vasu D. Appanna: Supervision, conceptualization, analysis, writing (review and editing) and funding acquisition.

Declaration of competing interest

The authors declare that they have no known competing financial interests or personal relationships that could have appeared to influence the work reported in this paper.

Acknowledgements

This study has been funded by the Northern Ontario Heritage Fund. Félix Legendre is a recipient of an Alexander Graham-Bell Canada Graduate Scholarship — Doctoral (CGS D) from the Natural Sciences and Engineering Research Council of Canada (NSERC). Sujeenthar Tharmalingam is supported by funding from Bruce Power and the Northern Ontario School of Medicine.

6 Conclusions and perspectives

The objectives of the thesis were to determine how glutamine was utilized in microbial systems under stress conditions as well as to characterize the biochemical pathways involved in those stress response machineries. Glutamine being a versatile source of carbon for bacteria, the *P. fluorescens* cultures that only had glutamine as a source of carbon were able to grow in an environment that lacked sulfur as well as in a media that had a low amount of phosphate. The physiological observations such as the bacterial growth and the metabolite profile in *P. fluorescens* under abiotic stress coupled with the targeted proteomics strategy permitted the identification of active and inactive enzymes, which ultimately makes mapping the molecular networks possible. The utilization of a gene expression probing methods like qPCR in this study was crucial to allow to confirm that the enzymes that were affected by the stress had their expression levels modulated as well in order to respond to the stress. Both under sulfur starvation and phosphate deficiency conditions, the gene expression profile correlated very well with the enzymatic activity of the corresponding enzyme. Taken together, the data obtained lead to the identification of different molecular pathways that were favored under those conditions regarding energy generation and oxidative stress defense.

Sulfur is such an important element for the cell that *P. fluorescens* growing well in a culture media that had no amount of added sulfur was striking. The balance and interplay between free sulfhydryl groups and disulfide bonds of proteins is crucial to maintain the cell in a healthy reductive state, as many enzymes are dependent on those free sulfhydryl groups to assert their functions. The oxidative environment does not seem to be too much of a detriment to *P. fluorescens* under the conditions used for this study. The enzyme superoxide dismutase and catalase are still very well active even under sulfur starvation and the microbe reaches a good biomass at the stationary phase of growth. Under this oxidative environment, it was not surprising to find that the oxidative phosphorylation and TCA cycle pathways were ineffective, as those pathways generate free radicals, which contribute to the oxidative burden imposed on the cell. The findings concerning the response to sulfur starvation using glutamine as the starting nutrient were two-fold: the cell shifts its metabolism to produce NADPH, an antioxidant and the cell generates the ROS scavenging ketoacid, KG.

The production of the antioxidant NADPH is possible through different means under sulfur starvation. As the starting nutrient is glutamine, glutamate dehydrogenase and isocitrate dehydrogenase are two enzymes that can lead to NADPH production as glutamine is broken down into metabolites that can enter the TCA cycle and be further metabolized. In fact, the cytoplasmic forms of isocitrate dehydrogenase and glutamate dehydrogenase were geared toward the utilization of $NADP^+$ and the concordant production of NADPH. Malic enzyme was identified as another enzyme that was upregulated to produce NADPH. Conversely, enzymes producing NADH were found to have lower activity. The enzyme NAD^+ kinase has been found to be a key player in maintaining NADPH homeostasis as it allows the cell to use up its large NAD^+ pool resulting from NADH-forming reactions to be inhibited. This produces $NADP^+$ which is critical for the aforementioned enzymes. This key finding reveals how microbial systems can combat oxidative stress caused by sulfur starvation by maintaining a healthy amount of NADPH in the cell. Those results corroborate previous studies in which citrate was used as a source of carbon and in which hydrogen peroxide was utilized to inflict oxidative stress in the cells. This NADPH production strategy although it's a core part of glutamine utilization under stress conditions seems to be a mechanism that is evolutionary conserved and that can happen from various starting nutrients.

The second component of the stress response to sulfur starvation using glutamine as a carbon source characterized in this study is the production of KG. Glutamine having a very linear and straightforward way to KG is one of the reasons it is considered a good carbon source. This is also one of the reasons cancer cells are fond of glutamine (150). Seeing increased production of KG knowing its antioxidant properties is expected. However, the molecular mechanism underlying enrichment of KG under oxidative stress or sulfur starvation was unknown. The molecular pathway characterized in this study represents a novel, neat and efficient way to generate the ROS scavenger KG and constitutes a significant finding.

The stress response to phosphate starvation in *P. fluorescens* was studied with the aim of uncovering an alternative mechanism to generate ATP. This was done under the premise that since phosphate levels are very low, it will be difficult to generate ATP through the traditional means of TCA cycle and oxidative phosphorylation. The current study revealed that a substrate

level phosphorylation mechanism is activated upon phosphate starvation. Similar mechanisms have been characterized in microbial systems exposed to metal and oxidative stress (17,117).

Future perspectives of this study are multiple. First, under sulfur starvation, a mechanism to combat ROS was identified. It is very clear that the TCA cycle and oxidative phosphorylation do not function normally under sulfur starvation and since the organism can reach stationary phase with a significant biomass, it is expected that there is a way to produce energy. Previous studies have found some substrate level phosphorylation mechanisms in conditions where oxidative stress was present (17). Since sulfur starvation provokes an oxidative environment, something similar would be expected, but it is not impossible that a novel mechanism could be found.

For phosphate starvation, this study identified an interesting, novel biochemical route to generate ATP. While this mechanism is efficient, it is very plausible that there are more complex mechanisms involved in ATP generation when starting from glutamine. The effect of glutamine synthetase could be one. This enzyme would break down glutamine and ADP into glutamate and ATP (15), generating a molecule of ATP immediately upon the conversion of glutamine to glutamate, the first step of its metabolism. Alternatively, there could be other enzymes and metabolites involved that are not directly linked to the TCA cycle. The enzyme 5-oxoprolinase could be an interesting candidate since it converts glutamate, phosphate and ADP into pyroglutamate (or 5-oxoproline), H_2O and ATP.

Industrial applications of this study are numerous. Abiotic stress is often used with bacteria culturing technique in order to generate value added products. KG is a very sought-after chemical product. Its industrial value is very interesting because it is a popular nutritional supplement. It is pretty prevalent in bodybuilding since KG can help the body to build muscle mass by increasing the amount of creatine and phosphocreatine that the body can produce. Similarly, it can help with treatment of burns as well as wound healing. Also, KG supplementation is common in farm animals (123). More recently, KG nanoparticles have been shown to have potential to treat cyanide poisoning (124). KG is also a precursor to other value-added products, notably ethylene. Considering that the *P. fluorescens* model characterized in this thesis was able to produce a great quantity of KG, it could be used as a bioreactor to generate KG while being a very cheap and environmentally friendly process.

P. fluorescens grown under a lack of phosphate also has potential to generate value-added products such as pyruvate and PEP. PEP is expensive to produce and it is commonly used in science laboratories. This is a possible application of the plasticity of *P. fluorescens'* metabolism demonstrated in this thesis. Also, since the bacteria can grow in an environment with low phosphate, it becomes an interesting option as a bioremediation bacterium for environmental pollution. Heavy metal pollution in the environment can lead to a low amount of phosphate. Alkaline soils can also cause a lack of phosphate in the environment. Bacteria can be used as biofertilizers to aid with plant growth and to decontaminate the environment. Considering that numerous studies have shown that *P. fluorescens* can survive under metal stress and the fact that it can help promote plant growth, this makes it a prime candidate to act as such a biofertilizer. The versatility of this organism's metabolism demonstrated in this study suggest that it could thrive in very harsh environments.

Taken together, the results of this thesis indicate that glutamine can be used as a nutrient by *P. fluorescens* under stress conditions. Under both sulfur and phosphate starvation, the bacteria can thrive with glutamine as the sole source of carbon and nitrogen. Novel molecular pathways governing antioxidative defense response and energy production were identified. Further analysis is required concerning the possibility of this microbe being utilized as a biofertilizer or in the industrial production of value-added products. *P. fluorescens* could definitely be human's friend in the future, with climate change and alarming environmental issues that mankind is currently facing. The need for green technologies will always increase and more research will be needed in order to develop biotechnologies to limit negative impact on the environment. The results presented here not only describe the biochemistry of glutamine under stress conditions, but also establish the basis for future industrial applications using *P. fluorescens* (Figure 6.1).

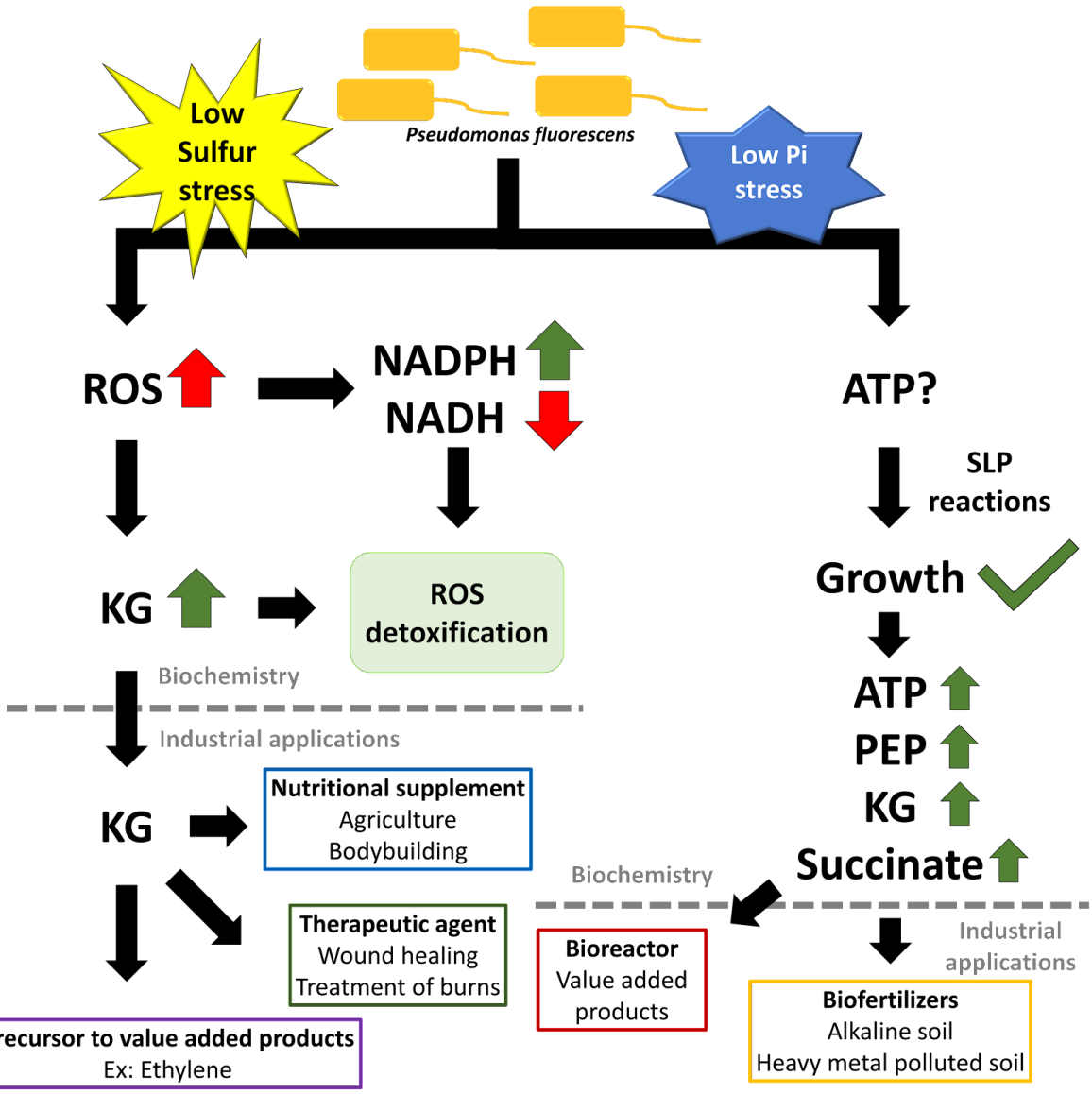

Figure 6.1. Summary of the main findings of the thesis and future perspectives. Under sulfur deficiency, *P. fluorescens* adapts its metabolism to generate more NADPH and less NADH. The antioxidant ketoacid KG is also produced in high amount. This leads to ROS detoxification and cell growth. Industrial applications include using KG as a nutritional supplement for agriculture purposes or bodybuilding, as a therapeutic agent to treat wounds and as a precursor to value added products such as ethylene. Phosphate deficiency triggers SLP reactions aimed at producing ATP. PEP, KG and succinate are enriched in those conditions. *P. fluorescens* can be used as a bioreactor to generate value-added products and as a biofertilizers to help plant growth in alkaline and heavy metal polluted soils.

References

1. Voet, D., Voet, J.G., 2010. Biochemistry. 4th Edition, Wiley, Hoboken.

2. Alhasawi, A.A., Thomas, S.C., Tharmalingam, S., Legendre, F., Appanna, V.D., 2019. Isocitrate Lyase and Succinate Semialdehyde Dehydrogenase Mediate the Synthesis of α-Ketoglutarate in Pseudomonas fluorescens. Front Microbiol 10, 1929. https://doi.org/10.3389/fmicb.2019.01929

3. Thomas, S.C., Alhasawi, A., Auger, C., Omri, A., Appanna, V.D., 2016. The role of formate in combatting oxidative stress. Antonie van Leeuwenhoek 109, 263–271. https://doi.org/10.1007/s10482-015-0629-6

4. Auger, C., Appanna, V.D., 2015. A novel ATP-generating machinery to counter nitrosative stress is mediated by substrate-level phosphorylation. Biochim Biophys Acta 1850, 43–50. https://doi.org/10.1016/j.bbagen.2014.09.028

5. Nolfi-Donegan, D., Braganza, A., Shiva, S., 2020. Mitochondrial electron transport chain: Oxidative phosphorylation, oxidant production, and methods of measurement. Redox Biology 37, 101674. https://doi.org/10.1016/j.redox.2020.101674

6. Becerra, M.C., Páez, P.L., Laróvere, L.E., Albesa, I., 2006. Lipids and DNA oxidation in Staphylococcus aureus as a consequence of oxidative stress generated by ciprofloxacin. Mol Cell Biochem 285, 29–34. https://doi.org/10.1007/s11010-005-9051-0

7. Zhao, X., Drlica, K., 2014. Reactive oxygen species and the bacterial response to lethal stress. Current Opinion in Microbiology, Antimicrobials 21, 1–6. https://doi.org/10.1016/j.mib.2014.06.008

8. Pompella, A., Visvikis, A., Paolicchi, A., Tata, V.D., Casini, A.F., 2003. The changing faces of glutathione, a cellular protagonist. Biochemical Pharmacology, Apoptosis - from Signalling Pathways to Therapeutic Tools 66, 1499–1503. https://doi.org/10.1016/S0006-2952(03)00504-5

9. White, A.R., Cappai, R., 2003. Neurotoxicity from glutathione depletion is dependent on extracellular trace copper. J Neurosci Res 71, 889–897. https://doi.org/10.1002/jnr.10537

10. Varma, S.D., Hegde, K.R., Kovtun, S., 2006. Oxidative Damage to Lens in Culture: Reversibility by Pyruvate and Ethyl Pyruvate. OPH 220, 52–57. https://doi.org/10.1159/000089275

11. Alhasawi, A., Costanzi, J., Auger, C., Appanna, N.D., Appanna, V.D., 2015. Metabolic reconfigurations aimed at the detoxification of a multi-metal stress in Pseudomonas fluorescens: Implications for the bioremediation of metal pollutants. Journal of Biotechnology 200, 38–43. https://doi.org/10.1016/j.jbiotec.2015.01.029

12. Legendre, F., MacLean, A., Appanna, V.P., Appanna, V.D., 2020. Biochemical pathways to α-ketoglutarate, a multi-faceted metabolite. World J Microbiol Biotechnol 36, 123. https://doi.org/10.1007/s11274-020-02900-8

13. Velvizhi, S., Dakshayani, K.B., Subramanian, P., 2002. Effects of α-ketoglutarate on antioxidants and lipid peroxidation products in rats treated with ammonium acetate. Nutrition 18, 747–750. https://doi.org/10.1016/S0899-9007(02)00825-0

14. Bignucolo, A., Appanna, V.P., Thomas, S.C., Auger, C., Han, S., Omri, A., Appanna, V.D., 2013. Hydrogen peroxide stress provokes a metabolic reprogramming in Pseudomonas fluorescens: Enhanced production of pyruvate. Journal of Biotechnology 167, 309–315. https://doi.org/10.1016/j.jbiotec.2013.07.002

15. Aldarini, N., Alhasawi, A.A., Thomas, S.C., Appanna, V.D., 2017. The role of glutamine synthetase in energy production and glutamine metabolism during oxidative stress. Antonie Van Leeuwenhoek 110, 629–639. https://doi.org/10.1007/s10482-017-0829-3

16. Lemire, J., Milandu, Y., Auger, C., Bignucolo, A., Appanna, V.P., Appanna, V.D., 2010. Histidine is a source of the antioxidant, alpha-ketoglutarate, in Pseudomonas fluorescens challenged by oxidative stress. FEMS Microbiol Lett 309, 170–177. https://doi.org/10.1111/j.1574-6968.2010.02034.x

17. Singh, R., Lemire, J., Mailloux, R.J., Chénier, D., Hamel, R., Appanna, V.D., 2009. An ATP and oxalate generating variant tricarboxylic acid cycle counters aluminum toxicity in Pseudomonas fluorescens. PLoS One 4, e7344. https://doi.org/10.1371/journal.pone.0007344

18. Bériault, R., Hamel, R., Chenier, D., Mailloux, R.J., Joly, H., Appanna, V.D., 2007. The overexpression of NADPH-producing enzymes counters the oxidative stress evoked by gallium, an iron mimetic. Biometals 20, 165–176. https://doi.org/10.1007/s10534-006-9024-0

19. Singh, R., Mailloux, R.J., Puiseux-Dao, S., Appanna, V.D., 2007. Oxidative stress evokes a metabolic adaptation that favors increased NADPH synthesis and decreased NADH production in Pseudomonas fluorescens. J Bacteriol 189, 6665–6675. https://doi.org/10.1128/JB.00555-07

20. Auger, C., Lemire, J., Cecchini, D., Bignucolo, A., Appanna, V.D., 2011. The metabolic reprogramming evoked by nitrosative stress triggers the anaerobic utilization of citrate in Pseudomonas fluorescens. PLoS ONE 6, e28469.

21. Aliu, E., Kanungo, S., Arnold, G.L., 2018. Amino acid disorders. Ann Transl Med 6, 471. https://doi.org/10.21037/atm.2018.12.12

22. D'Andrea, G., 2000. Classifying amino acids as gluco(glyco)genic, ketogenic, or both. Biochemical Education 28, 27–28. https://doi.org/10.1111/j.1539-3429.2000.tb00007.x

23. Cruzat, V., Macedo Rogero, M., Noel Keane, K., Curi, R., Newsholme, P., 2018. Glutamine: Metabolism and Immune Function, Supplementation and Clinical Translation. Nutrients 10, E1564. https://doi.org/10.3390/nu10111564

24. Roth, E., 2008. Nonnutritive effects of glutamine. J Nutr 138, 2025S-2031S. https://doi.org/10.1093/jn/138.10.2025S

25. Zhang, J., Pavlova, N.N., Thompson, C.B., 2017. Cancer cell metabolism: the essential role of the nonessential amino acid, glutamine. EMBO J 36, 1302–1315. https://doi.org/10.15252/embj.201696151

26. Feehily, C., Karatzas, K. a. G., 2013. Role of glutamate metabolism in bacterial responses towards acid and other stresses. J Appl Microbiol 114, 11–24. https://doi.org/10.1111/j.1365-2672.2012.05434.x

27. Corpas, F.J., Barroso, J.B., Sandalio, L.M., Palma, J.M., Lupiáñez, J.A., del Río, L.A., 1999. Peroxisomal NADP-Dependent Isocitrate Dehydrogenase. Characterization and Activity Regulation during Natural Senescence. Plant Physiol 121, 921–928. https://doi.org/10.1104/pp.121.3.921

28. Dumaswala, U.J., Zhuo, L., Mahajan, S., Nair, P.N., Shertzer, H.G., Dibello, P., Jacobsen, D.W., 2001. Glutathione protects chemokine-scavenging and antioxidative defense functions in human RBCs. Am J Physiol Cell Physiol 280, C867-873. https://doi.org/10.1152/ajpcell.2001.280.4.C867

29. Liu, S., He, L., Yao, K., 2018. The Antioxidative Function of Alpha-Ketoglutarate and Its Applications. Biomed Res Int 2018. https://doi.org/10.1155/2018/3408467

30. Mailloux, R.J., Singh, R., Brewer, G., Auger, C., Lemire, J., Appanna, V.D., 2009. Alpha-ketoglutarate dehydrogenase and glutamate dehydrogenase work in tandem to modulate the antioxidant alpha-ketoglutarate during oxidative stress in Pseudomonas fluorescens. J Bacteriol 191, 3804–3810. https://doi.org/10.1128/JB.00046-09

31. Bayliak, M.M., Shmihel, H.V., Lylyk, M.P., Vytvytska, O.M., Storey, J.M., Storey, K.B., Lushchak, V.I., 2015. Alpha-ketoglutarate attenuates toxic effects of sodium nitroprusside and hydrogen peroxide in Drosophila melanogaster. Environmental Toxicology and Pharmacology 40, 650–659. https://doi.org/10.1016/j.etap.2015.08.016

32. Guo, S., Duan, R., Wang, L., Hou, Y., Tan, L., Cheng, Q., Liao, M., Ding, B., 2017. Dietary α-ketoglutarate supplementation improves hepatic and intestinal energy status and anti-oxidative capacity of Cherry Valley ducks. Anim. Sci. J. 88, 1753–1762. https://doi.org/10.1111/asj.12824

33. Mailloux, R.J., Bériault, R., Lemire, J., Singh, R., Chénier, D.R., Hamel, R.D., Appanna, V.D., 2007. The tricarboxylic acid cycle, an ancient metabolic network with a novel twist. PLoS One 2, e690. https://doi.org/10.1371/journal.pone.0000690

34. Cory, J.G., Cory, A.H., 2006. Critical Roles of Glutamine as Nitrogen Donors in Purine and Pyrimidine Nucleotide Synthesis: Asparaginase Treatment in Childhood Acute Lymphoblastic Leukemia. In Vivo 20, 587–589.

35. Forchhammer, K., 2007. Glutamine signalling in bacteria. Front Biosci 12, 358. https://doi.org/10.2741/2069

36. Walsh, N.P., Blannin, A.K., Robson, P.J., Gleeson, M., 1998. Glutamine, Exercise and Immune Function. Sports Medicine 26, 177–191. https://doi.org/10.2165/00007256-199826030-00004

37. Petroff, O.A.C., 2002. GABA and glutamate in the human brain. Neuroscientist 8, 562–573. https://doi.org/10.1177/1073858402238515

38. Shelp, B.J., Bown, A.W., McLean, M.D., 1999. Metabolism and functions of gamma-aminobutyric acid. Trends Plant Sci 4, 446–452. https://doi.org/10.1016/s1360-1385(99)01486-7

39. Capitani, G., De Biase, D., Aurizi, C., Gut, H., Bossa, F., Grütter, M.G., 2003. Crystal structure and functional analysis of Escherichia coli glutamate decarboxylase. EMBO J 22, 4027–4037. https://doi.org/10.1093/emboj/cdg403

40. Bönnighausen, J., Gebhard, D., Kröger, C., Hadeler, B., Tumforde, T., Lieberei, R., Bergemann, J., Schäfer, W., Bormann, J., 2015. Disruption of the GABA shunt affects mitochondrial respiration and virulence in the cereal pathogen Fusarium graminearum. Mol Microbiol 98, 1115–1132. https://doi.org/10.1111/mmi.13203

41. Brambilla, G., Parodi, S., Cavanna, M., Caraceni, C.E., Baldini, L., 1970. The immunodepressive activity of Escherichia coli L-asparaginase in some transplantation systems. Cancer Res 30, 2665–2670.

42. Chakrabarty, A.K., Friedman, H., 1970. L-asparaginase-induced immunosuppression: effects on antibody-forming cells and serum titers. Science 167, 869–870. https://doi.org/10.1126/science.167.3919.869

43. Cairns, B.R., 2001. Emerging roles for chromatin remodeling in cancer biology. Trends in Cell Biology 11, S15–S21. https://doi.org/10.1016/S0962-8924(01)82074-2

44. Laurenti, G., Tennant, D.A., 2016. Isocitrate dehydrogenase (IDH), succinate dehydrogenase (SDH), fumarate hydratase (FH): three players for one phenotype in cancer? Biochemical Society Transactions 44, 1111–1116. https://doi.org/10.1042/BST20160099

45. Mullen, A.R., Wheaton, W.W., Jin, E.S., Chen, P.-H., Sullivan, L.B., Cheng, T., Yang, Y., Linehan, W.M., Chandel, N.S., DeBerardinis, R.J., 2012. Reductive carboxylation supports growth in tumour cells with defective mitochondria. Nature 481, 385–388. https://doi.org/10.1038/nature10642

46. Zaidi, N., Swinnen, J.V., Smans, K., 2012. ATP-Citrate Lyase: A Key Player in Cancer Metabolism. Cancer Research 72, 3709–3714. https://doi.org/10.1158/0008-5472.CAN-11-4112

47. Dang, L., Jin, S., Su, S.M., 2010. IDH mutations in glioma and acute myeloid leukemia. Trends in Molecular Medicine 16, 387–397. https://doi.org/10.1016/j.molmed.2010.07.002

48. Dang, L., White, D.W., Gross, S., Bennett, B.D., Bittinger, M.A., Driggers, E.M., Fantin, V.R., Jang, H.G., Jin, S., Keenan, M.C., Marks, K.M., Prins, R.M., Ward, P.S., Yen, K.E., Liau, L.M., Rabinowitz, J.D., Cantley, L.C., Thompson, C.B., Vander Heiden, M.G., Su, S.M., 2009. Cancer-associated IDH1 mutations produce 2-hydroxyglutarate. Nature 462, 739–744. https://doi.org/10.1038/nature08617

49. Zhang, L., Li, J., Zong, L., Chen, X., Chen, K., Jiang, Z., Nan, L., Li, X., Li, W., Shan, T., Ma, Q., Ma, Z., 2016. Reactive Oxygen Species and Targeted Therapy for Pancreatic Cancer. Oxidative Medicine and Cellular Longevity 2016, e1616781. https://doi.org/10.1155/2016/1616781

50. Le, A., Lane, A.N., Hamaker, M., Bose, S., Gouw, A., Barbi, J., Tsukamoto, T., Rojas, C.J., Slusher, B.S., Zhang, H., Zimmerman, L.J., Liebler, D.C., Slebos, R.J.C., Lorkiewicz, P.K., Higashi, R.M., Fan, T.W.M., Dang, C.V., 2012. Glucose-Independent Glutamine Metabolism via TCA Cycling for Proliferation and Survival in B Cells. Cell Metabolism 15, 110–121. https://doi.org/10.1016/j.cmet.2011.12.009

51. Azevedo Neto, A.D. de, Prisco, J.T., Enéas-Filho, J., Lacerda, C.F. de, Silva, J.V., Costa, P.H.A. da, Gomes-Filho, E., 2004. Effects of salt stress on plant growth, stomatal response and solute accumulation of different maize genotypes. Braz. J. Plant Physiol. 16, 31–38. https://doi.org/10.1590/S1677-04202004000100005

52. Lu, C., Vonshak, A., 2002. Effects of salinity stress on photosystem II function in cyanobacterial Spirulina platensis cells. Physiol Plant 114, 405–413. https://doi.org/10.1034/j.1399-3054.2002.1140310.x

53. Coles, C.J., Holm, R.H., Kurtz, D.M., Orme-Johnson, W.H., Rawlings, J., Singer, T.P., Wong, G.B., 1979. Characterization of the iron-sulfur centers in succinate dehydrogenase. Proc Natl Acad Sci U S A 76, 3805–3808. https://doi.org/10.1073/pnas.76.8.3805

54. Fee, J.A., Findling, K.L., Yoshida, T., Hille, R., Tarr, G.E., Hearshen, D.O., Dunham, W.R., Day, E.P., Kent, T.A., Münck, E., 1984. Purification and characterization of the Rieske iron-sulfur protein from Thermus thermophilus. Evidence for a [2Fe-2S] cluster having non-cysteine ligands. Journal of Biological Chemistry 259, 124–133. https://doi.org/10.1016/S0021-9258(17)43630-1

55. Martin, D.R., Matyushov, D.V., 2017. Electron-transfer chain in respiratory complex I. Sci Rep 7, 5495. https://doi.org/10.1038/s41598-017-05779-y

56. Read, A.D., Bentley, R.ET., Archer, S.L., Dunham-Snary, K.J., 2021. Mitochondrial iron–sulfur clusters: Structure, function, and an emerging role in vascular biology. Redox Biology 47, 102164. https://doi.org/10.1016/j.redox.2021.102164

57. Robbins, A.H., Stout, C.D., 1989. Structure of activated aconitase: formation of the [4Fe-4S] cluster in the crystal. Proceedings of the National Academy of Sciences 86, 3639–3643. https://doi.org/10.1073/pnas.86.10.3639

58. Flint, D., Allen, R.M., 1996. Iron−Sulfur Proteins with Nonredox Functions. https://doi.org/10.1021/CR950041R

59. Beinert, H., Kennedy, M.C., 1989. Engineering of protein bound iron-sulfur clusters, in: Christen, P., Hofmann, E. (Eds.), EJB Reviews 1989, EJB Reviews. Springer, Berlin, Heidelberg, pp. 163–173. https://doi.org/10.1007/978-3-642-75189-9_11

60. Johnson, D.C., Dean, D.R., Smith, A.D., Johnson, M.K., 2005. Structure, Function, and Formation of Biological Iron-Sulfur Clusters. Annual Review of Biochemistry 74, 247–281. https://doi.org/10.1146/annurev.biochem.74.082803.133518

61. Lill, R., 2009. Function and biogenesis of iron–sulphur proteins. Nature 460, 831–838. https://doi.org/10.1038/nature08301

62. Balk, J., Pilon, M., 2011. Ancient and essential: the assembly of iron–sulfur clusters in plants. Trends in Plant Science 16, 218–226. https://doi.org/10.1016/j.tplants.2010.12.006

63. Maio, N., Rouault, T.A., 2015. Iron–sulfur cluster biogenesis in mammalian cells: New insights into the molecular mechanisms of cluster delivery. Biochimica et Biophysica Acta (BBA) - Molecular Cell Research, SI: Fe/S proteins 1853, 1493–1512. https://doi.org/10.1016/j.bbamcr.2014.09.009

64. Kertesz, M.A., 2000. Riding the sulfur cycle – metabolism of sulfonates and sulfate esters in Gram-negative bacteria. FEMS Microbiology Reviews 24, 135–175. https://doi.org/10.1016/S0168-6445(99)00033-9

65. Sievert, S.M., Hügler, M., Taylor, C.D., Wirsen, C.O., 2008. Sulfur Oxidation at Deep-Sea Hydrothermal Vents, in: Dahl, C., Friedrich, C.G. (Eds.), Microbial Sulfur Metabolism. Springer, Berlin, Heidelberg, pp. 238–258.

66. Beller, H.R., Chain, P.S.G., Letain, T.E., Chakicherla, A., Larimer, F.W., Richardson, P.M., Coleman, M.A., Wood, A.P., Kelly, D.P., 2006. The genome sequence of the obligately chemolithoautotrophic, facultatively anaerobic bacterium Thiobacillus denitrificans. J Bacteriol 188, 1473–1488. https://doi.org/10.1128/JB.188.4.1473-1488.2006

67. Ohtsuka, H., Shimasaki, T., Aiba, H., 2021. Response to sulfur in Schizosaccharomyces pombe. FEMS Yeast Research 21, foab041. https://doi.org/10.1093/femsyr/foab041

68. Scherer, H.W., 2001. Sulphur in crop production — invited paper. European Journal of Agronomy 14, 81–111. https://doi.org/10.1016/S1161-0301(00)00082-4

69. Kutz, A., Müller, A., Hennig, P., Kaiser, W.M., Piotrowski, M., Weiler, E.W., 2002. A role for nitrilase 3 in the regulation of root morphology in sulphur-starving Arabidopsis thaliana. Plant J 30, 95–106. https://doi.org/10.1046/j.1365-313x.2002.01271.x

70. Maruyama-Nakashita, A., 2008. Transcriptional regulation of genes involved in sulfur assimilation in plants: Understanding from the analysis of high-affinity sulfate transporters. Plant Biotechnology 25, 323–328.

71. Kertesz, M.A., 2001. Bacterial transporters for sulfate and organosulfur compounds. Research in Microbiology 152, 279–290. https://doi.org/10.1016/S0923-2508(01)01199-8

72. van der Ploeg, J.R., Eichhorn, E., Leisinger, T., 2001. Sulfonate-sulfur metabolism and its regulation in Escherichia coli. Archives of Microbiology 176, 1–8. https://doi.org/10.1007/s002030100298

73. Scott, C., Hilton, M.E., Coppin, C.W., Russell, R.J., Oakeshott, J.G., Sutherland, T.D., 2007. A global response to sulfur starvation in Pseudomonas putida and its relationship to the expression of low-sulfur-content proteins. FEMS Microbiol Lett 267, 184–193. https://doi.org/10.1111/j.1574-6968.2006.00575.x

74. Sekowska, A., Kung, H.F., Danchin, A., 2000. Sulfur metabolism in Escherichia coli and related bacteria: facts and fiction. J. Mol. Microbiol. Biotechnol. 2, 145–177.

75. Takeda, E., Ikeda, S., Nakahashi, O., 2012. [Lack of phosphorus intake and nutrition]. Clin Calcium 22, 1487–1491. https://doi.org/CliCa121014871491

76. Babior, B.M., 1999. NADPH oxidase: an update. Blood 93, 1464–1476.

77. Trentini, D.B., Suskiewicz, M.J., Heuck, A., Kurzbauer, R., Deszcz, L., Mechtler, K., Clausen, T., 2016. Arginine phosphorylation marks proteins for degradation by a Clp protease. Nature 539, 48–53. https://doi.org/10.1038/nature20122

78. Thingstad, T.F., Krom, M.D., Mantoura, R.F.C., Flaten, G.A.F., Groom, S., Herut, B., Kress, N., Law, C.S., Pasternak, A., Pitta, P., Psarra, S., Rassoulzadegan, F., Tanaka, T., Tselepides, A., Wassmann, P., Woodward, E.M.S., Riser, C.W., Zodiatis, G., Zohary, T., 2005. Nature of Phosphorus Limitation in the Ultraoligotrophic Eastern Mediterranean. Science. https://doi.org/10.1126/science.1112632

79. Hopkins, B., Ellsworth, J., 2005. Phosphorus availability with alkaline/calcareous soil. Western Nutrient Management Conference.

80. Romano, S., Schulz-Vogt, H.N., González, J.M., Bondarev, V., 2015. Phosphate Limitation Induces Drastic Physiological Changes, Virulence-Related Gene Expression, and Secondary Metabolite Production in Pseudovibrio sp. Strain FO-BEG1. Appl Environ Microbiol 81, 3518–3528. https://doi.org/10.1128/AEM.04167-14

81. Hsieh, Y.-J., Wanner, B.L., 2010. Global regulation by the seven-component Pi signaling system. Curr Opin Microbiol 13, 198–203. https://doi.org/10.1016/j.mib.2010.01.014

82. Rhodes, M.E.Y. 1959, n.d. The Characterization of Pseudomonas fluorescens. Microbiology 21, 221–263. https://doi.org/10.1099/00221287-21-1-221

83. Upadhyay, A., Srivastava, S., 2010b. Evaluation of multiple plant growth promoting traits of an isolate of Pseudomonas fluorescens strain Psd. Indian J Exp Biol 48, 601–609.

84. Kalita, P.J., Ram, R.M., 2019. Industrial Applications of Pseudomonas fluorescens: A Patent Survey, in: Singh, H.B., Keswani, C., Singh, S.P. (Eds.), Intellectual Property Issues in Microbiology. Springer, Singapore, pp. 383–402. https://doi.org/10.1007/978-981-13-7466-1_21

85. Hu, J., Cai, W., Wang, C., Du, X., Lin, J., Cai, J., 2018. Purification and characterization of alkaline lipase production by Pseudomonas aeruginosa HFE733 and application for biodegradation in food wastewater treatment. Biotechnology & Biotechnological Equipment 32, 583–590. https://doi.org/10.1080/13102818.2018.1446764

86. Barathi, S., Vasudevan, N., 2001. Utilization of petroleum hydrocarbons by Pseudomonas fluorescens isolated from a petroleum-contaminated soil. Environment International, 87.

Environmental Geochemistry in the Tropics and Subtropics 26, 413–416. https://doi.org/10.1016/S0160-4120(01)00021-6

87. Middaugh, J., Hamel, R., Jean-Baptiste, G., Beriault, R., Chenier, D., Appanna, V.D., 2005. Aluminum triggers decreased aconitase activity via Fe-S cluster disruption and the overexpression of isocitrate dehydrogenase and isocitrate lyase: a metabolic network mediating cellular survival. J Biol Chem 280, 3159–3165. https://doi.org/10.1074/jbc.M411979200

88. Jordan, P.A., Tang, Y., Bradbury, A.J., Thomson, A.J., Guest, J.R., 1999. Biochemical and spectroscopic characterization of Escherichia coli aconitases (AcnA and AcnB). Biochemical Journal 344, 739–746. https://doi.org/10.1042/bj3440739

89. Tseng, C.-P., Yu, C.-C., Lin, H.-H., Chang, C.-Y., Kuo, J.-T., 2001. Oxygen- and Growth Rate-Dependent Regulation ofEscherichia coli Fumarase (FumA, FumB, and FumC) Activity. Journal of Bacteriology 183, 461–467. https://doi.org/10.1128/JB.183.2.461-467.2001

90. Cheng, V.W.T., Ma, E., Zhao, Z., Rothery, R.A., Weiner, J.H., 2006. The Iron-Sulfur Clusters in Escherichia coli Succinate Dehydrogenase Direct Electron Flow. J. Biol. Chem. 281, 27662–27668. https://doi.org/10.1074/jbc.M604900200

91. Forman, H.J., Zhang, H., Rinna, A., 2009. Glutathione: Overview of its protective roles, measurement, and biosynthesis. Molecular Aspects of Medicine, Glutathione in Health and Disease 30, 1–12. https://doi.org/10.1016/j.mam.2008.08.006

92. Groitl, B., Jakob, U., 2014. Thiol-based redox switches. Biochimica et Biophysica Acta (BBA) - Proteins and Proteomics, Thiol-Based Redox Processes 1844, 1335–1343. https://doi.org/10.1016/j.bbapap.2014.03.007

93. Kobayashi, K., 2017. Sensing Mechanisms in the Redox-Regulated, [2Fe–2S] Cluster-Containing, Bacterial Transcriptional Factor SoxR. Acc. Chem. Res. 50, 1672–1678. https://doi.org/10.1021/acs.accounts.7b00137

94. Auger, C., Han, S., Appanna, V.P., Thomas, S.C., Ulibarri, G., Appanna, V.D., 2013. Metabolic reengineering invoked by microbial systems to decontaminate aluminum: Implications

for bioremediation technologies. Biotechnology Advances 31, 266–273. https://doi.org/10.1016/j.biotechadv.2012.11.008

95. Anderson, S., Appanna, V.D., Huang, J., Viswanatha, T., 1992. A novel role for calcite in calcium homeostasis. FEBS Letters 308, 94–96. https://doi.org/10.1016/0014-5793(92)81059-U

96. Bradford, M.M., 1976. A rapid and sensitive method for the quantitation of microgram quantities of protein utilizing the principle of protein-dye binding. Analytical Biochemistry 72, 248–254. https://doi.org/10.1016/0003-2697(76)90527-3

97. Han, S., Auger, C., Appanna, V.P., Lemire, J., Castonguay, Z., Akbarov, E., Appanna, V.D., 2012. A blue native polyacrylamide gel electrophoretic technology to probe the functional proteomics mediating nitrogen homeostasis in Pseudomonas fluorescens. Journal of Microbiological Methods 90, 206–210. https://doi.org/10.1016/j.mimet.2012.05.006

98. Lemire, J., Kumar, P., Mailloux, R., Cossar, K., Appanna, V.D., 2008. Metabolic adaptation and oxaloacetate homeostasis in P. fluorescens exposed to aluminum toxicity. Journal of Basic Microbiology 48, 252–259. https://doi.org/10.1002/jobm.200800007

99. Alhasawi, A.A., Appanna, V.D., 2016. Manganese orchestrates a metabolic shift leading to the increased bioconversion of glycerol into α-ketoglutarate. https://doi.org/10.3934/bioeng.2017.1.12

100. Munoz, D., Doumenq, P., Guiliano, M., Jacquot, F., Scherrer, P., Mille, G., 1997. New approach to study of spilled crude oils using high resolution GC-MS (SIM) and metastable reaction monitoring GC-MS-MS. Talanta 45, 1–12. https://doi.org/10.1016/S0039-9140(96)02054-1

101. Beyer, W.F., Fridovich, I., 1987. Assaying for superoxide dismutase activity: Some large consequences of minor changes in conditions. Analytical Biochemistry 161, 559–566. https://doi.org/10.1016/0003-2697(87)90489-1

102. Boyne, A.F., Ellman, G.L., 1972. A methodology for analysis of tissue sulfhydryl components. Analytical Biochemistry 46, 639–653. https://doi.org/10.1016/0003-2697(72)90335-1

103. Livak, K.J., Schmittgen, T.D., 2001. Analysis of Relative Gene Expression Data Using Real-Time Quantitative PCR and the 2−ΔΔCT Method. Methods 25, 402–408. https://doi.org/10.1006/meth.2001.1262

104. Singh, R., Beriault, R., Middaugh, J., Hamel, R., Chenier, D., Appanna, V.D., Kalyuzhnyi, S., 2005. Aluminum-tolerant Pseudomonas fluorescens: ROS toxicity and enhanced NADPH production. Extremophiles 9, 367–373. https://doi.org/10.1007/s00792-005-0450-7

105. Hamel, R., Levasseur, R., Appanna, V.D., 1999. Oxalic acid production and aluminum tolerance in Pseudomonas fluorescens. Journal of Inorganic Biochemistry 76, 99–104. https://doi.org/10.1016/S0162-0134(99)00120-8

106. Hamel, R., Appanna, V.D., 2003. Aluminum detoxification in Pseudomonas fluorescens is mediated by oxalate and phosphatidylethanolamine. Biochimica et Biophysica Acta (BBA) - General Subjects 1619, 70–76. https://doi.org/10.1016/S0304-4165(02)00444-0

107. Finkel, T., Holbrook, N.J., 2000. Oxidants, oxidative stress and the biology of ageing. Nature 408, 239–247. https://doi.org/10.1038/35041687

108. Green, J., Paget, M.S., 2004. Bacterial redox sensors. Nat Rev Microbiol 2, 954–966. https://doi.org/10.1038/nrmicro1022

109. Ferguson, G.D., Bridge, W.J., 2019. The glutathione system and the related thiol network in Caenorhabditis elegans. Redox Biol 24, 101171. https://doi.org/10.1016/j.redox.2019.101171

110. Tong, W.-H., Rouault, T.A., 2007. Metabolic regulation of citrate and iron by aconitases: role of iron-sulfur cluster biogenesis. Biometals 20, 549–564. https://doi.org/10.1007/s10534-006-9047-6

111. Hirst, J., 2009. Towards the molecular mechanism of respiratory complex I. Biochemical Journal 425, 327–339. https://doi.org/10.1042/BJ20091382

112. Chenier, D., Beriault, R., Mailloux, R., Baquie, M., Abramia, G., Lemire, J., Appanna, V., 2008. Involvement of fumarase C and NADH oxidase in metabolic adaptation of Pseudomonas 113. fluorescens cells evoked by aluminum and gallium toxicity. Appl Environ Microbiol 74, 3977–3984. https://doi.org/10.1128/AEM.02702-07

114. Py, B., Barras, F., 2010. Building Fe–S proteins: bacterial strategies. Nat Rev Microbiol 8, 436–446. https://doi.org/10.1038/nrmicro2356

115. Legendre, Félix, Tharmalingam, S., Bley, A.M., MacLean, A., Appanna, V.D., 2020. Metabolic adaptation and NADPH homeostasis evoked by a sulfur-deficient environment in Pseudomonas fluorescens. Antonie Van Leeuwenhoek 113, 605–616. https://doi.org/10.1007/s10482-019-01372-7

116. Lemire, J.; Mailloux, R.; Darwich, R.; Auger, C.; Appanna, V.D. Disruption of L-carnitine metabolism by aluminum toxicity and oxidative stress promotes dyslipidemia in human astrocytic and hepatic cells. Toxicol. Lett. 2011, 203, 219–226.

117. Jarrett, S.G., Boulton, M.E., 2005. Antioxidant up-regulation and increased nuclear DNA protection play key roles in adaptation to oxidative stress in epithelial cells. Free Radical Biology and Medicine 38, 1382–1391. https://doi.org/10.1016/j.freeradbiomed.2005.02.003

118. Alhasawi, A., Auger, C., Appanna, V. p., Chahma, M., Appanna, V. d., 2014. Zinc toxicity and ATP production in Pseudomonas fluorescens. Journal of Applied Microbiology 117, 65–73. https://doi.org/10.1111/jam.12497

119. Mesquita, C.S., Oliveira, R., Bento, F., Geraldo, D., Rodrigues, J.V., Marcos, J.C., 2014. Simplified 2,4-dinitrophenylhydrazine spectrophotometric assay for quantification of carbonyls in oxidized proteins. Anal Biochem 458, 69–71. https://doi.org/10.1016/j.ab.2014.04.034

120. Auger, C., Appanna, V., Castonguay, Z., Han, S., Appanna, V.D., 2012. A facile electrophoretic technique to monitor phosphoenolpyruvate-dependent kinases. Electrophoresis 33, 1095–1101. https://doi.org/10.1002/elps.201100517

121. Auger, C., Appanna, N.D., Alhasawi, A., Appanna, V.D., 2015. Deciphering metabolic networks by blue native polyacrylamide gel electrophoresis: A functional proteomic exploration. EuPA Open Proteomics 7, 64–72. https://doi.org/10.1016/j.euprot.2015.05.003

122. Appanna, V.P., Alhasawi, A.A., Auger, C., Thomas, S.C., Appanna, V.D., 2016. Phospho-transfer networks and ATP homeostasis in response to an ineffective electron transport chain in Pseudomonas fluorescens. Archives of Biochemistry and Biophysics 606, 26–33. https://doi.org/10.1016/j.abb.2016.07.011

123. Coudray-Lucas, C., Le Bever, H., Cynober, L., De Bandt, J.P., Carsin, H., 2000. Ornithine alpha-ketoglutarate improves wound healing in severe burn patients: a prospective randomized double-blind trial versus isonitrogenous controls. Crit Care Med 28, 1772–1776. https://doi.org/10.1097/00003246-200006000-00012

124. Wang, L., Hou, Y., Yi, D., Li, Y., Ding, B., Zhu, H., Liu, J., Xiao, H., Wu, G., 2015. Dietary supplementation with glutamate precursor α-ketoglutarate attenuates lipopolysaccharide-induced liver injury in young pigs. Amino Acids 47, 1309–1318. https://doi.org/10.1007/s00726-015-1966-5

125. Sultana, S., Talegaonkar, S., Nishad, D.K., Mittal, G., Ahmad, F.J., Bhatnagar, A., 2018. Alpha ketoglutarate nanoparticles: A potentially effective treatment for cyanide poisoning. Eur J Pharm Biopharm 126, 221–232. https://doi.org/10.1016/j.ejpb.2017.06.017

126. Lemire, J., Alhasawi, A., Appanna, V.P., Tharmalingam, S., Appanna, V.D., 2017. Metabolic defence against oxidative stress: the road less travelled so far. J Appl Microbiol 123, 798–809. https://doi.org/10.1111/jam.13509

127. Mills, E., O'Neill, L.A.J., 2014. Succinate: a metabolic signal in inflammation. Trends Cell Biol 24, 313–320. https://doi.org/10.1016/j.tcb.2013.11.008

128. Hamel, R., Appanna, V.D., Viswanatha, T., Puiseux-Dao, S., 2004. Overexpression of isocitrate lyase is an important strategy in the survival of Pseudomonas fluorescens exposed to aluminum. Biochem Biophys Res Commun 317, 1189–1194. https://doi.org/10.1016/j.bbrc.2004.03.157

129. Mailloux, R.J., Hamel, R., Appanna, V.D., 2006. Aluminum toxicity elicits a dysfunctional TCA cycle and succinate accumulation in hepatocytes. J Biochem Mol Toxicol 20, 198–208. https://doi.org/10.1002/jbt.20137

130. MacLean, A., Bley, A.M., Appanna, V.P., Appanna, V.D., 2020. Metabolic manipulation by Pseudomonas fluorescens: a powerful stratagem against oxidative and metal stress. J Med Microbiol 69, 339–346. https://doi.org/10.1099/jmm.0.001139

131. Ravasz, D., Kacso, G., Fodor, V., Horvath, K., Adam-Vizi, V., Chinopoulos, C., 2017. Catabolism of GABA, succinic semialdehyde or gamma-hydroxybutyrate through the GABA shunt impair mitochondrial substrate-level phosphorylation. Neurochem Int 109, 41–53. https://doi.org/10.1016/j.neuint.2017.03.008

132. Zhang, S., Qian, X., Chang, S., Dismukes, G.C., Bryant, D.A., 2016. Natural and Synthetic Variants of the Tricarboxylic Acid Cycle in Cyanobacteria: Introduction of the GABA Shunt into Synechococcus sp. PCC 7002. Frontiers in Microbiology 7, 1972. https://doi.org/10.3389/fmicb.2016.01972

133. Müller, W., Schröder, H.C., Wang, X., 2019. The phosphoanhydride bond: One cornerstone of life. The Biochemist 41, 22–27. https://doi.org/10.1042/BIO04104022

134. Strahl, H., Errington, J., 2017. Bacterial Membranes: Structure, Domains, and Function. Annu Rev Microbiol 71, 519–538. https://doi.org/10.1146/annurev-micro-102215-095630

135. Ardito, F., Giuliani, M., Perrone, D., Troiano, G., Muzio, L.L., 2017. The crucial role of protein phosphorylation in cell signaling and its use as targeted therapy (Review). Int J Mol Med 40, 271–280. https://doi.org/10.3892/ijmm.2017.3036

136. Máthé, P., Máthé-Gáspár, G., Szili-Kovács, T., Sipter, E., Anton, A., 2007. Changes in the Parts of the Rhizosphere Phosphorus Cycle Influencing by Heavy Metal Contamination. Cereal Research Communications 35, 761–764. https://doi.org/10.1556/CRC.35.2007.2.149

137. Kelliher, J.L., Radin, J.N., Kehl-Fie, T.E., 2018. PhoPR Contributes to Staphylococcus aureus Growth during Phosphate Starvation and Pathogenesis in an Environment-Specific Manner. Infect Immun 86, e00371-18. https://doi.org/10.1128/IAI.00371-18

138. Stankeviciute, G., Guan, Z., Goldfine, H., Klein, E.A., 2019. Caulobacter crescentus Adapts to Phosphate Starvation by Synthesizing Anionic Glycoglycerolipids and a Novel Glycosphingolipid. mBio 10, e00107-19. https://doi.org/10.1128/mBio.00107-19

139. Bosak, T., Schubotz, F., de Santiago-Torio, A., Kuehl, J.V., Carlson, H.K., Watson, N., Daye, M., Summons, R.E., Arkin, A.P., Deutschbauer, A.M., 2016. System-Wide Adaptations of Desulfovibrio alaskensis G20 to Phosphate-Limited Conditions. PLoS One 11, e0168719. https://doi.org/10.1371/journal.pone.0168719

140. Alvarez-Martin, P., Fernández, M., O'Connell-Motherway, M., O'Connell, K.J., Sauvageot, N., Fitzgerald, G.F., MacSharry, J., Zomer, A., van Sinderen, D., 2012. A Conserved Two-Component Signal Transduction System Controls the Response to Phosphate Starvation in Bifidobacterium breve UCC2003. Appl Environ Microbiol 78, 5258–5269. https://doi.org/10.1128/AEM.00804-12

141. Pfaff, J., Denton, A.K., Usadel, B., Pfaff, C., 2020. Phosphate starvation causes different stress responses in the lipid metabolism of tomato leaves and roots. Biochimica et Biophysica Acta (BBA) - Molecular and Cell Biology of Lipids 1865, 158763. https://doi.org/10.1016/j.bbalip.2020.158763

142. Schubotz, F., 2019. Membrane Homeostasis upon Nutrient (C, N, P) Limitation, in: Geiger, O. (Ed.), Biogenesis of Fatty Acids, Lipids and Membranes, Handbook of Hydrocarbon and Lipid Microbiology. Springer International Publishing, Cham, pp. 823–847. https://doi.org/10.1007/978-3-319-50430-8_59

143. VanBogelen, R.A., Olson, E.R., Wanner, B.L., Neidhardt, F.C., 1996. Global analysis of proteins synthesized during phosphorus restriction in Escherichia coli. Journal of Bacteriology. https://doi.org/10.1128/jb.178.15.4344-4366.1996

144. Duruibe, J., C, O., Egwurugwu, J., 2007. Heavy Metal Pollution and Human Biotoxic Effects. Int. J. Phys. Sci. 2, 112–118.

145. Al-Aoukaty, A., Appanna, V.D., Falter, H., 1992. Gallium toxicity and adaptation in Pseudomonas fluorescens. FEMS Microbiology Letters 92, 265–272. https://doi.org/10.1111/j.1574-6968.1992.tb05272.x

146. Alhasawi, A., Appanna, V., 2015. Aspartate metabolism and pyruvate homeostasis triggered by oxidative stress in Pseudomonas fluorescens: a functional metabolomic study. Metabolomics DOI 10.1007/s11306-015-0841-4. https://doi.org/10.1007/s11306-015-0841-4

147. Ahn, S., Jung, J., Jang, I.-A., Madsen, E.L., Park, W., 2016. Role of Glyoxylate Shunt in Oxidative Stress Response. Journal of Biological Chemistry 291, 11928–11938. https://doi.org/10.1074/jbc.M115.708149

148. Kapahi, M., Sachdeva, S., 2019. Bioremediation Options for Heavy Metal Pollution. J Health Pollut 9, 191203. https://doi.org/10.5696/2156-9614-9.24.191203

149. Ojuederie, O.B., Babalola, O.O., 2017. Microbial and Plant-Assisted Bioremediation of Heavy Metal Polluted Environments: A Review. Int J Environ Res Public Health 14, 1504. https://doi.org/10.3390/ijerph14121504

150. Kumar, S., Diksha, Sindhu, S.S., Kumar, R., 2022. Biofertilizers: An ecofriendly technology for nutrient recycling and environmental sustainability. Curr Res Microb Sci 3, 100094. https://doi.org/10.1016/j.crmicr.2021.100094

151. Li, T., Le, A., 2018. Glutamine Metabolism in Cancer, in: Le, A. (Ed.), The Heterogeneity of Cancer Metabolism, Advances in Experimental Medicine and Biology. Springer International Publishing, Cham, pp. 13–32. https://doi.org/10.1007/978-3-319-77736-8_2